A Machine Design for Launching Curling Stones and an Initial Evaluation of its Efficacy

A Thesis Submitted to the
College of Graduate and Postdoctoral Studies
In Partial Fulfillment of the Requirements
For the Degree of Master of Science
In the Department of Mechanical Engineering
University of Saskatchewan
Saskatoon

By

Amirhossein Ravanbod

PERMISSION TO USE

In presenting this thesis/dissertation in partial fulfillment of the requirements for a Postgraduate degree from the University of Saskatchewan, I agree that the Libraries of this University may make it freely available for inspection. I further agree that permission for copying of this thesis/dissertation in any manner, in whole or in part, for scholarly purposes may be granted by the professor or professors who supervised my thesis/dissertation work or, in their absence, by the Head of the Department or the Dean of the College in which my thesis work was done. It is understood that any copying or publication or use of this thesis/dissertation or parts thereof for financial gain shall not be allowed without my written permission. It is also understood that due recognition shall be given to me and to the University of Saskatchewan in any scholarly use which may be made of any material in my thesis/dissertation.

Requests for permission to copy or to make other uses of materials in this thesis/dissertation in whole or part should be addressed to:

Head of the Mechanical Engineering
3B48 Engineering Building
57 Campus Drive
Saskatoon, SK S7N 5A9 Canada

OR

Dean
College of Graduate and Postdoctoral Studies
University of Saskatchewan
116 Thorvaldson Building, 110 Science Place
Saskatoon, Saskatchewan S7N 5C9 Canada

ABSTRACT

The goal of this thesis was to design, prototype, and test a device to launch curling stones at preset linear and rotational velocities, and at preset angles to the long axis of the curling ice sheet. This device will help sports scientists, physicists, and engineers investigate curling stone behavior, which can help inform several ongoing debates regarding the reason for this behavior. Moreover, this device will help curlers practice different sweeping techniques and help ice technicians calibrate the ice surface.

After initial research and design, a prototype was fabricated and tested, including validation and experimental tests. Validation tests illustrated that the prototype is able to consistently launch the curling stones at preset linear and rotational velocities. The consistency of linear launching speeds met respective constraints and objectives of the project. However, the consistency of the curling stone's rotational launch speed imparted by the prototype was not sufficient. Some recommendations were expressed to remedy this issue.

Experimental tests were also performed using the prototype. These tests show that the stone's lateral distance travelled is independent of the curling stone's rotational speed while it has a rotational motion, but it has a strong relationship with the stone's linear speed i.e. the curling stone's lateral displacement increases with its linear speed. Another investigation was done on the curling stone's longitudinal distance travelled. Results showed that the curling stone travels less far longitudinally in subsequent throws after conditioning of the ice i.e. the curling stone's longitudinal distance travelled decreases after each throw. Furthermore, the effect of changes in the curling stone's weight on its longitudinal distance travelled was investigated in additional tests. The data collected in this test was confounded.

DEDICATION

I dedicate my thesis to my family and my friends. A special feeling of gratitude to my loving parents, Hajie Yad and Ali Ravanbod. Without their endless love and encouragement, I would never have been able to complete my graduate studies. This thesis is also dedicated to my siblings, Reza, Roya, Maria, and Elham who were there for me throughout this process and gave me lots of support. I love you all and I appreciate everything that you have done for me.

I would like to dedicate my thesis to my friends who were there for me when I needed someone to talk to: Zohre Gheisary, Mehrdad Dadgar, and Hamed Alizade.

ACKNOWLEDGEMENTS

I would like to express my appreciation and thanks to the following people without their support the completion of this project would never have occurred.

I would like to express my deepest appreciation to my supervisor, Dr. Sean Maw, who gave me continuous support, encouragement, and suggestions. His patience with me was wonderful. I am also very grateful to Mr. Eugene Hritzuk, a former World Senior men's champion skip. He not only helped me with partial funding and consulting on this project, but also prepared the facilities to test the prototype of the Rock Launcher. I would like to extend my deepest gratitude to my committee, Drs. Jim Bugg and Joel Lanovaz, who were more than generous with their experience and precious time. Their assistance and consultations on the designing stage and the analyzing data of my project has helped me to accomplish my project.

TABLE OF CONTENTS

LIST OF FIGURES

LIST OF TABLES

GLOSSARY OF TERMS AND ACRONYMS

Backlash in mechanical engineering is the play between adjacent movable parts (as in a series of gears).

Backline is the line across the ice at the back of the house.

BTS: Brower Timing System

Curl is the distance that the rock moves laterally while travelling down the ice sheet.

Hack bases are plastic blocks that replaced the hacks during ice scraping to protect hacks from any damage.

Hacks are the footholds at each end of the ice from which the stone is delivered.

Hog line is a line 10 meters from the hack at each end of the ice.

Pebbles result from small droplets of water being sprayed onto the ice surface and freezing.

Peel shot is a takeout shot that removes a stone from play, and the delivered stone also rolls out of play.

PRL: Prototype of the Rock Launcher

PWM: Pulse Width Modulation

Rock and **Stone** are terms used to refer to the curling stone, which is made of granite (mass is 17-20 kg).

SCAMPER is an acronym, and each letter stands for one thinking technique; Substitute, Combine, Adapt, Modify, Put to another use, Eliminate, Reverse.

Sheet (or Ice Sheet) is the specific playing surface upon which a curling game is played.

Stone's running band is a ring-shaped area beneath the curling stone, which is the only part of the stone in touch with the ice.

In **Sweeping,** curlers use a broom to sweep the ice in front of a moving stone.

Take out is removal of a stone from the playing area by hitting it with another stone.

Weight is the amount of force applied to the stone during delivery.

1. INTRODUCTION

Curling is a winter sport, played on ice, where two teams take turns sliding stones made of granite towards a target known as the House. Curling stones (also called rocks) are made of a special type of granite and weigh almost 20 kg each. Curlers use brooms to sweep in front of the curling stone while it is travelling down the ice (Ohman, 2004). The actual effects of sweeping on curling ice are still unclear, however one theory suggests that sweeping causes the ice to melt briefly, creating a thin film of liquid water that acts as a lubricant between the stone and the ice. This lubrication reduces the friction between the stone and the ice surface, allowing the stone to maintain its momentum longer (Shegelski et al., 1996). Sweeping makes the stone curl less and move in a straighter line. Curling ice is not like hockey ice. It is "pebbled". Pebbles are the result of small droplets of water being sprayed onto the ice surface and freezing. These pebbles cause the stone to "roar" while moving down the ice. This is why the sport is also called the Roaring Game. Also, these pebbles lead to unusual deviations in a stone's trajectory, and this has been attracting scientists' attention.

In 1924, Harrington, at the University of Saskatchewan, started to investigate and explain the reason behind the curl (lateral motion) of the curling stone, which is different from a stone's lateral motion in a non-pebbled environment (Harrington, 1924). One of the common examples of a non-pebbled environment is a spinning drinking glass slid along a smooth tabletop. If a drinking glass, which is pushed down a table, rotates around its center of mass clockwise, its trajectory will deviate to the left side. On the contrary, a curling stone, when it is travelling down the pebbled ice and rotating clockwise, deviates to the right side. Up to now, many scientists have tried to explain this behavior of the curling stone and they have proposed as many as seven different theories to describe this matter. However, these proposed explanations fail to comprehensively describe the behavior of the stone quantitatively or qualitatively.

There are several reasons for this lack of success. One of them is that the thermodynamic effect of the stone on the ice is partially unknown since this influence is not durable i.e. it disappears quickly. The methodology of their studies is another contributing factor. They often used a human curler to throw the stone while they were recording data, which can generate or

increase the chance of inconsistency. It is difficult to release the rock at specific rotational and longitudinal velocities. Even top athletes, as seen during competitions, sometimes miss the weight that they ought to put on the stone. The weight of a shot is a term that curlers use to compare the linear velocity of the rock i.e. this term explains how hard a rock is thrown ("Curling Tips - Garrison Golf and Curling Club," 2016). Therefore, a machine that would be able to launch a stone at specific longitudinal and rotational velocities at a specific angle to the centerline of the ice would be useful for scientific studies.

1.1. Background and Motivation

Studying the physics of curling is not the only reason to design such a machine though. Based on an interview with Lawrence Kucheran (2019), the ice technician at the highly competitive Saskatoon Nutana Curling club, curling clubs do not match stones before games and players have to warm up before each game to figure out which curling stones will have more curling motion and which ones will have more longitudinal displacement. A machine could therefore help curlers to match curling stones. If stones thrown down the same path with the same weight and rotation travel the same distance (within a foot or two) with the same amount of curl, then the stones are sufficiently matched (Tschirhart, 2020). Also, the ice technicians would be able to calibrate the ice faster and with better accuracy using such a machine. Ice calibration means testing the condition of the ice sheets of the curling rink to ensure that they have similar qualities to make sure that the curlers can play fairly. In addition, and perhaps most importantly, such a machine could help curlers to compare and improve their sweeping techniques. With this device, curlers would be able to launch curling stones with consistency at controlled velocities and specific directions, and this would allow curlers to compare the effectiveness of different sweeping techniques. The benefits of having this device would not only be for curlers though.

As noted in the Introduction, there have been controversies among sport scientists since the investigation of curling stone behavior started almost a century ago. A group of sport scientists recently tried to explain that the rotational motion affects the stone's travelling distance (Maeno, 2014; Maeno, 2016). Meanwhile, some other research shows that the stone's rotational motion does not influence the stone's travelling distance (Jensen & Shegelski, 2004; Penner, 2001). A rock launching machine could be utilized to investigate the effects of the curling stone's rotational motion on its behavior.

The difference in travelling distance is a factor that curlers need to understand, and that is why stone matching is important before each competition. Before a match, curlers typically release the stones a few times to distinguish the stones in terms of their travelling distance under identical linear and rotational speeds. In each curling ice sheet, 16 stones are using for curling which can have slightly different masses. Most of the theories introduced to explain a curling stone's unusual behavior are based on the friction between the running band and the ice surface. One contributing factor to the friction between the pebbles and the running band is the curling stone's weight. Investigating the effects of curling stone mass changes will lead to a better understanding of a stone's behavior and the friction between the curling stone and ice.

1.2. Objectives

The design objectives of this project are to design, build, prototype, and test a machine to speed up a curling stone from rest to preset rotational and linear velocities, and to release the stone before the hog line at a preset angle to the long axis of the ice sheet. This machine will help sports scientists, physicists, and engineers to evaluate the theories that try to explain the behavior of curling stones, will allow curlers and coaches to improve their sweeping techniques and match curling stones, and will help ice technicians to calibrate the ice.

The research objectives are to investigate the relationship between the curling stone's lateral and longitudinal distance travelled based on the linear and rotational launch speeds and to examine how changes in stone weight influence the stone's longitudinal distance travelled. The first investigation would show how the lateral and longitudinal distances travelled by curling stones change under different linear and rotational speeds. The second experiment would illustrate the effect of a small change in a stone's weight, which is one of the contributing factors to the friction between the stone and ice, on its longitudinal distance travelled.

1.3. Thesis Outline

The remainder of this thesis is organized as follows. Chapter 2 provides a literature review and examines prior works.

Chapter 3 presents the problem definition for this design, including problem statement, value proposition, scope, functions, objectives, and constraints. Chapter 3 also discusses the stakeholders of this project.

Chapter 4 addresses the conceptual solutions that were considered, and introduces the best concept based on the evaluation of the options. This chapter also derives the equations of motion

describing the system dynamics and details the modelling of the mechanical structure and the electrical circuits. At the end of Chapter 4, prototype construction and its assembly will be described.

Chapter 5 describes the performance of the prototype. It shows some collected data and discusses the results of the validation tests.

Chapter 6 reports on the collected data and discusses the results of the experiments focused on relationships between lateral and longitudinal distances travelled, dependent on initial linear and rotational velocities, and on the effects of minor differences in stone masses.

Chapter 7 concludes this thesis with conclusions, a summary of prototype performance, and recommendations for future work.

2. PRIOR WORKS

In this chapter, a literature review is presented, and models of existing "curling machines" are described.

2.1. Literature Review

From 1924 up to now, different theories have been proposed to explain the curl of the curling stone. Most of these theories are based on the asymmetry of the frictional force exerted on the running band of the stone. The running band is a ring-shaped area beneath the curling stone which is the only part of the stone in contact with the ice. The running band is very important in explaining the behavior of the rock on the ice. Another essential parameter is the ice surface. As noted earlier, the ice surface of the curling rink has bumps on it i.e. pebbles. Their average sizes are 1–2 mm in height and 3–10 mm in diameter, and their "population density" ranges from 2×10^4 to $5 \times 10^4\ m^{-2}$. The purpose of pebbling is to decrease the friction between the stone and the ice by diminishing the contact area (Maeno, 2014). It also makes the stone's motion more predictable. On a non-pebbled surface, the lateral motion of the stone is exaggerated and unpredictable (for the magnitude and direction of the lateral motion), making it difficult to play stones all the way through to the other end of the sheet (Ohman, 2004).

Different theories have different approaches to describe how and why the distribution of the friction is different on the running band. Harrington (1924) was the first to express that the lateral displacement of the rock requires that the friction on the one side (left/right) of the running band must be larger than the other side (right/left, respectively). This difference arises because the relative velocity of the band to the ice surface of one side of the running band exceeds the relative velocity on the other side due to the rotation of the stone. Macaulay and Smith (1930) some years later, unaware of the work of Harrington (1924), proposed that the lateral displacement of the rock requires higher friction on the trailing half of the rock compared to the leading half. The water-layer model proposed by Shegelski et al. (1996) assumed that the friction at the rear half of the running band is greater than the front half because the water layer produced by frictional heating is transported to the front half by some unknown mechanism. Denny (2002) proposed that small ice particles can be collected by the running band and the accumulation of these particles causes

lower friction on one side (left/right) of the running band with respect to the stone's direction of rotation. In this idea, dry friction is responsible for the lateral motion of the stone because the friction is between ice and ice. However, this idea has not been developed further.

The evaporation-abrasion model of Maeno (2009) suggested that the friction at the trailing half of the running band is larger due to an evaporation-abrasion mechanism. Another model to explain the unusual behavior of the stone is the scratch-guiding model. Nyberg et al. (2013) assumed that scratches formed on the ice surface by asperities of the leading half of the running band can guide the rear half, leading to the lateral displacement of the stone. However, there is no experimental evidence in support of this model, and Shegelski and Lozowski (2019) showed that the scratches on the ice surface could not cause the observed lateral motion of the stone. The pivot-slide model by Shegelski and Lozowski (2016, 2018) proposed that the stone sticks and pivots at a point with the lowest velocity relative to the ice, but experimental evidence has not been obtained to show that ice can allow pivoting of the heavy stone at a point even for a short time.

Independent of the ongoing controversy on different theories, some researchers try to investigate the effects of the curling stone's rotational motion on its trajectory. Maeno (2016) showed in Figure 2.1 (his Figure 10.14) that the curl distance (lateral displacement) linearly decreases with rotational speed. The linear speed of the stone in his experiment was within the range of typical curling and the stone's rotational speed is presented in Figure 2.1. This figure's different graph markers correspond to different curlers, rotation direction, and release positions on the same ice sheet. On the other hand, Jensen and Shegelski (2004) illustrated that with a rotational speed in the range of 0 to 5 total rotations of the curling stone (around 0 to 72 degrees/second) the lateral displacement (curl) of the stone is insensitive to the rotational speed of the curling stone (Figure 2.2; their Figure 7). The stone's linear speed in the Jensen and Shegelski (2004) experiment was within the range of typical curling. Based on observation and review of the literature, a curling stone needs roughly 25 seconds to travel its trajectory down the ice and stop at the house in a typical draw shot. So, the stone's total number of turns can be converted to degrees per second by multiplying it by 14.4 °/s.

Shegelski and Lozowski (2018) derived a model to explain the behavior of the curling stone. In this model, the total curl distance is independent of the stone's initial angular speed of rotation. However, they noted that the variation of curl distance with angular speed during actual curling play is around 2% (Shegelski & Lozowski, 2018). Denny (2002) also derived a model that

is called a snowplow, showing that the curl is insensitive to the rotational motion. In both of these models, the linear speed of the curling stone was within the range of typical curling. Penner (2001) explained that the lateral displacement of the stone increases with the initial angular speed up to approximately one complete rotation. Then, the curl decreases with increasing rotational speed. In his experiment, the stone's linear speed was within the range of typical curling.

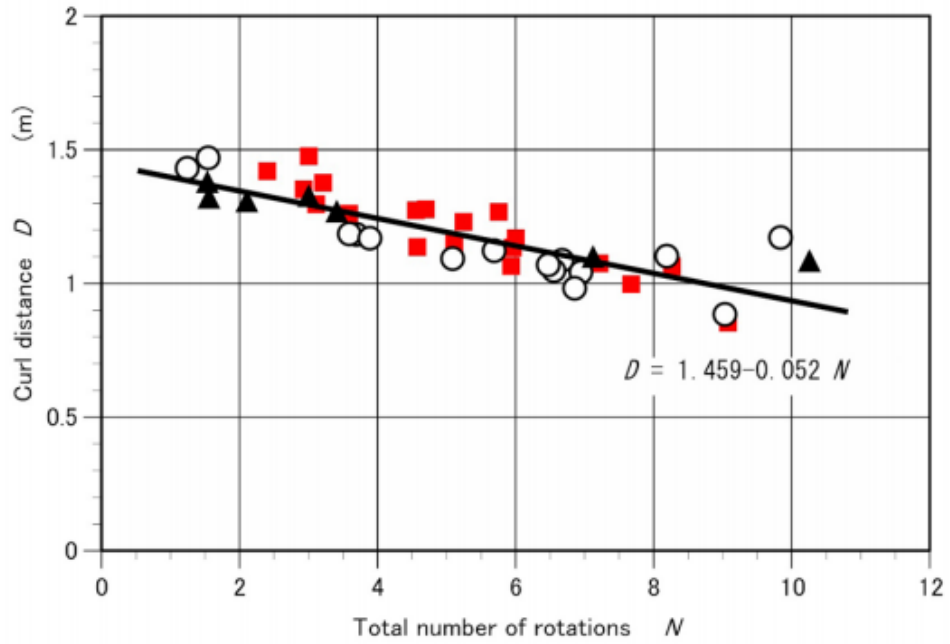

Figure 2.1: Curl distance obtained by a high-precision measurement. Different markers correspond to different curlers, rotation direction, and release position on the same ice sheet. From "The Engineering Approach to Winter Sports" by N. Maeno, 2016, Curling, 327–347.

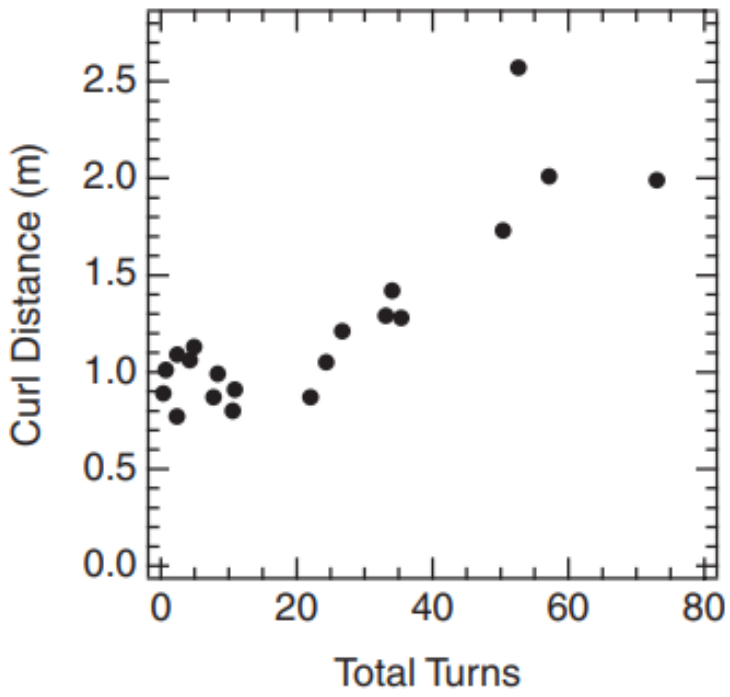

Figure 2.2: Measured curl distances plotted against the number of turns for a curling rock on pebbled ice. The curling rock release velocities were generally decreased for shots with larger numbers of turns such that the curling-rock trajectory finished close to the legal target area of the rink (i.e. roughly fixed trajectory length). From "The motion of curling rocks: Experimental investigation and semi-phenomenological description", by Jensen, E. T., & Shegelski, M. R., 2004, Canadian Journal of Physics, 82(10).

As discussed earlier in this section, some theories are based on the asymmetric friction of the right and left side of the curling stone while some others are based on the asymmetric friction of the lead and rear side of the curling stone. The friction between the curling stone and ice was always an important factor in theories introduced to explain the behavior of the curling stone. One of the contributing parameters in friction between the curling stone and ice is the mass of the curling stone. Based on the model of ice pebble-stone friction of Lozowski (Lozowski et al., 2015), the mass of the curling stone is a contributing factor to the shear stress of the water layer between the curling stone and pebbles. Although the curling stone's mass can be an important factor in the friction between the curling stone and ice, few papers investigate the effects of changing a curling stone's mass on its behavior. Based on the literature, the mass of a curling stone varies between 17 and 20 kg (Lozowski et al., 2015)

2.2. Existing Models

In this section, the prior work that has been done to build robots to help curlers and curling coaches is covered. Three different products have already been developed: SweepTracker, Rock Thrower, and Curly. These robots' strengths and weaknesses will be discussed in the following sub-sections.

2.2.1. SweepTracker

SweepTracker was developed in Ontario, Canada (Figure 2.3). It has four legs, a monitor, and two arms. The two arms hold, push, and rotate a curling stone. One wheel on each arm rotates the curling stone. The Ontario designers named their device SweepTracker as it is designed to qualitatively evaluate the effects of sweeping on the behavior of the curling stone. Also, it is able to measure the friction between the ice and the stone while it is pushing the stone down the ice. Although they have not published any papers on the robot, they published online results of the effects of the sweeping on the friction between the ice and the stone.

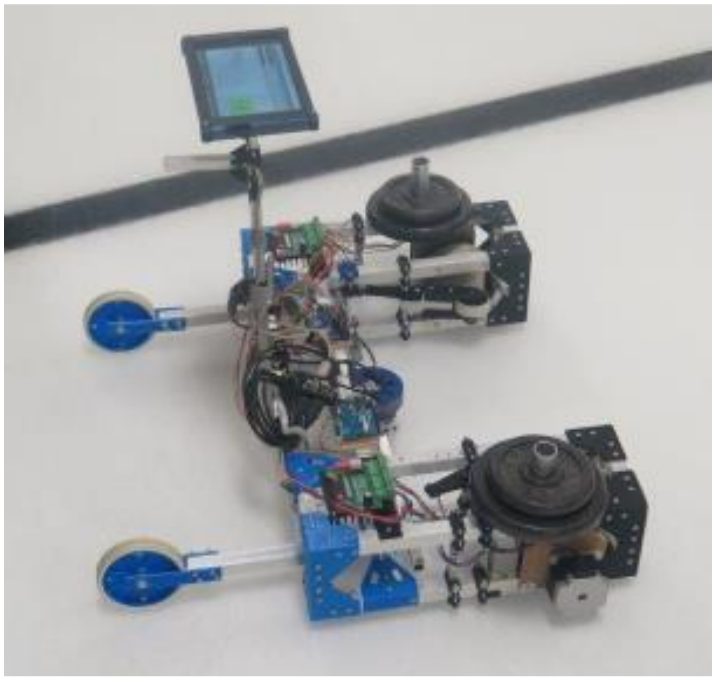

Figure 2.3: The SweepTracker robot (Super User,2021).

Based on the published video clips of this robot, it releases the stone somewhere after the hog line, which is not the case for curlers in typical curling. In actual play, curlers must release the stone somewhere before the hog line. The hog line is presented in Figure 2.4. SweepTracker can, however, be used for matching curling stones. The price for rock matching services provided by

this robot for four ice sheets is roughly $500 for a club in the Greater Toronto Area, and this price increases significantly according to the distance from Toronto (Park, 2014). It is a compact robot, and it can be considered a portable device which can be transferred to other curling clubs without major effort. However, operating SweepTracker is a complex task that no one except a member of its design group can do. So, a customer needs to pay the wages of its operator as well as the cost of travelling for using this device somewhere outside of the Greater Toronto Area. These points make this robot an expensive option for curling clubs.

Also, considering its motion and the weight located on its front wheels (Figure 2.3), presumably to increase the friction between the wheels and the ice surface, its wheels would probably change the ice while moving on the ice to launch the curling stone. Lahayne et al. (2016) explain that the friction between the rubber and the ice depends on the pressure between them, the relative velocity of them, and the temperature. The rubber (wheels) can smooth the ice by shear-induced plastic flow (Lahayne et al., 2016) as per their Figure 8. Consequently, this makes SweepTracker a sub-optimal option for ice calibration and repetitive training exercises.

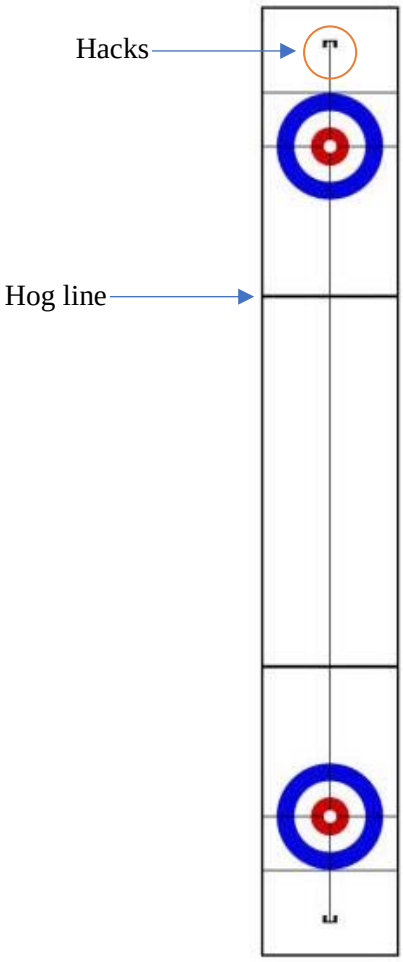

Figure 2.4: The layout of a curling sheet.

2.2.2. Rock Thrower

The Rock Thrower is a machine that was developed in Manitoba, Canada. To collect information on this device, the author had a conversation with Chris and Lorne Hamblin (curling coaches) who developed the idea of the Rock Thrower, and some video clips published by Mitch Rosset were examined. Mitch Rosset is a Senior Digital Broadcast Journalist working at Global News.

The EASCAN™ company, with the cooperation of the Hamblins, fabricated this machine. It took 18 months and $40,000 to build the Rock Thrower. This machine is a 3.6-meter-long apparatus which has four legs attached to the hacks and to the side walls. Also, it is connected to its control center which is attached to the wall of the building beside the ice sheet (Figures 2.5 and 2.6). Therefore, this device is not portable. The owners said the purpose of building this machine was to teach curlers to judge rocks and to help improve their sweeping techniques. Mitch Rosset

reported that “Every shot the machine sends down the ice is nearly 100% accurate” (Rosset, 2017). However, they have not published any scientific reports to illustrate this claim. The Rock Thrower is capable of throwing a variety of shots, including peel shots. A peel is a takeout shot that removes a stone from play and the delivered stone also rolls out of play. This shot is thrown with much more weight than a normal shot (“Curling Terminology,” 2020). Although it appears that this device is well designed, the cost makes it unaffordable for most curling clubs and curling teams.

Figure 2.5: The Rock Thrower (Rosset, 2017).

Figure 2.6: Chris Hamblin uses a touch screen computer to tell the Morris Curling Club’s rock-throwing machine what kind of shot to deliver (Rosset, 2017).

2.2.3. Curly

Curly was designed by a South Korean team of about 60 researchers from eight different institutions including Korea University and the Ulsan National Institute of Science and Technology. This machine uses AI to throw a curling stone. This robot, which can act both as a skip and as a thrower, competes against curlers on an actual curling ice sheet (Figure 2.7). Curly has three main parts: an AI-based curling strategy and simulation engine, the thrower robot, and the skip robot. This AI Curling Robot System uses a vision system and the AI to recognize the best shot. Curly uses special tools like strategy-oriented software and a curling simulator that was meant to help the robot adjust its strategy based on the environment. The thrower part will receive the calculated information based on the AI simulation and will then throw the rock. The thrower part of Curly has two arms to hold and rotate the stone in the desired direction as shown in Figure 2.8 (Won et al, 2018).

Curly runs over the ice surface with the curling stone and releases the stone near the hog line. This robot promises a revolution in the teaching of curling; however, like SweepTracker, the motion of its wheels over the ice surface may cause unintentional changes on the ice surface which makes this robot a less than ideal choice for ice calibration (recall that the effects of rubber wheels on ice are discussed in the last paragraph of section 2.1.1. SweepTracker). Also, the purpose of designing and building this robot is to make an AI robot that can compete with human teams. It is not designed to help ice technicians calibrate the ice or help curlers enhance their sweeping techniques. Moreover, based on its cutting-edge technology, its cost is probably beyond the affordability of any curling club.

Figure 2.7: Curly during the match against a human team. Curly has a long arm which is equipped with a camera to record the positions of the stones and to send this information to its control center (Ruptly, 2018).

Figure 2.8: Curly's arms are holding a curling stone (Ruptly, 2018).

3. DESIGN PROBLEM DEFINITION

3.1. Problem Statement

In order to study curling dynamics and sweeping, to calibrate curling ice, and to match curling stones quickly and with minimal effort, curling clubs, curling researchers, and ice technicians require a device to throw a curling stone from rest to a preset linear speed and rotational velocity and to release the curling stone at a specific angle to the long axis (centerline) of the ice sheet before the hog line. This device will be referred to as the Rock Launcher in this thesis.

3.2. Value Proposition

This device will provide curling clubs with quick and accurate ice calibration and stone matching, will facilitate curling research for sports scientists, physicists, and engineers, and will help curlers to compare and improve their sweeping techniques, all at a lower cost relative to SweepTracker and Rock Thrower.

3.3. Scope

This project will develop a product for curlers, curling clubs, and sports scientists, physicists, and engineers who are working on the behavior of the curling stone. The product will accelerate a curling stone from stationary and release it before the hog line at a preset rotational velocity and a linear speed at a preset angle to the centerline of the ice sheet. This device will not measure the trajectory and final position of the launched curling stone nor the friction between the rock and the ice surface. It will not determine the quality of the curling ice or of the curling stone; neither will it measure the effectiveness of the sweeping. This project will conclude with a demonstration of a prototype of the device as it assists in carrying out an experimental study.

3.4. Functions

The device must accelerate a curling stone. It will accelerate the stone from rest to a preset linear speed and a preset rotational velocity and release it before the hog line at a preset angle to the centerline of the ice sheet. In typical curling, the exact position of the release is not a crucial parameter as long as it occurs before the hog line.

3.5. Design Objectives and Constraints

In this section, the objectives and the constraints of the design will be discussed and later a Pairwise Comparison Chart will be presented.

3.5.1. List of Design Objectives

The lower the manufacturing cost, the better. The manufacturing costs include the costs of material plus the costs to convert the material into the final product. The goal is to design this device so that the final product is affordable for curling clubs. Better affordability means that more clubs can purchase and use the device, and that more devices can be sold. For this purpose, materials with lower costs will be used as long as this will not change the functionality of the device.

The lower the knowledge required for operating this device, the better. Devices requiring less procedural knowledge will require less training and will likely reduce errors in operation while enhancing affinity. The easier the solution is to use, the more likely and more easily the device will be adopted into curling clubs. In other words, it will be more accessible if the device requires less specialized knowledge or tools during operation.

The faster the device can perform a task, the better. This objective can be divided into two parts. The first part is the set-up time of the device, and the second part is the time that the device needs to throw a curling stone. The faster the device can be set up to launch curling stones, and to throw the curling stones, the more ice sheets can be calibrated, the more stones can be matched, and the more training can be performed.

The more portable the device, the better. The portability is a function of the weight and the bulkiness of the device. The more straightforward it is to move the device from one ice sheet to another or from one rink to another, the greater the value and use of the device.

The finer the output increment that can be set for launch speeds and angles, the better. The finer the output increments the device can be set to, to release a curling stone, the greater the sensitivity of experiments that can be performed. This device has three variables to be set before each shot: a linear speed, a rotational velocity, and an angle to the centerline.

The more consistent the release of a curling stone, the better. The more consistent an output is, responding to the same input, the clearer and more repeatable experiments will be that can be performed. The standard deviation of the output will be used to measure the consistency of

the outputs of the device. The standard deviation will be measured for the three variables (linear and rotational speeds and releasing angle to the centerline of the ice sheet).

The less time and expense that the device requires for maintenance, the better. The less frequent, the less expensive, and the less knowledge required for the maintenance of the device, the more affordable it will be for customers.

3.5.2. List of Design Constraints

- ICE CONDITION:

Since one of the applications of the Rock Launcher is to calibrate the curling ice, it must be designed in a way that it will not damage the ice. Damaging the ice includes changing the ice condition, scratching the ice surface, melting the ice, and breaking or cracking the pebbles or the ice.

- SIZE:

The final design has to fit in a section of the curling ice sheet from the hacks to the hog line and within the width of an ice sheet. This area at hand on the ice sheet is 41.62 m^2 (see Appendix A.4.). Also, the final product has to be able to be transported by a typical sedan. This factor increases the portability of the device.

- ENVIRONMENTAL CONSTRAINTS:

The final design must be able to perform its tasks in the environment of a curling rink (temperature between -4.5°C and +5°C and from 50% to 55% of humidity) (Ohman, 2004). To deal with safety margins on these values, the device must operate within a range of -10°C and +10°C and 40% to 90% humidity. This means that the device must be able to continue the stone launching without any loss in performance in this environment. Also, since this device may be left out in closed places during summer or winter, it must tolerate temperatures between -40°C to +40°C while it is off.

- LAUNCH SPEED CONSTRAINTS:

The device must be able to launch the stone with a linear speed up to 3 m/s and with a rotational velocity up to 2.09 rad/s (the stone does 3 complete rotations in 9 seconds at its maximum rotational speed) (Hritzuk, 2019). Also, the linear and rotational velocities must be independent of each other i.e. the operator must be able to set them separately.

- ## RELEASE ANGLE:

This angle is the angle between the centerline of the ice sheet and the direction in which the stone is released. The range of this angle must be ±3 degrees to the centerline of the ice sheet (see Appendix A.6.).

- ## MINIMUM NUMBER OF OUTPUT INCREMENTS:

After interviewing curlers and coaches, it became clear that there is a range of opinions regarding the necessary minimum number of output increments for each variable. Based on a rule of thumb and adopting these decisions as provisional constraints, it was decided to have ten magnitude settings for each variable.

- ## SOUND CONSTRAINT:

The final design must not produce sounds exceeding 70 dB while it is working since loud sounds may disturb curlers on the other ice sheets. This sound level is the volume of loud talking (Ovchinnikov & Ivanov, 2011).

- ## CONSISTENCY:

Consistency describes how repeatable the outputs of the device are given the same input commands. Maeno used 0.5 m/s and 0.1 rad/s as the intervals for the curling stone's linear and rotational speed values in his tests (Maeno, 2013). Also, Penner and Nyberg reported values of the stone's linear and rotational speed with one decimal point in their tests (Penner, 2001; Nyberg et al., 2013) In their tests, the unit of linear speed is m/s and the unit of rotational speed is rad/s. Therefore, to be conservative and to satisfy scientists' demand, 0.1 m/s was selected as the maximum standard deviation for the curling stone's linear speed, and 1°/s was selected as the maximum standard deviation for its rotational speed.

- ## RINK COMPATIBILITY:

Since this device is designed based on the collected information and dimensions of the Granite and Nutana curling rinks in Saskatoon, the device must be usable at these clubs. However, it does not mean that it can be only used in these curling clubs. It must be usable in curling clubs which have the same dimensions of hacks as the Granite and Nutana curling clubs in Saskatoon.

- STONE CONDITION:

The final design must not change any quality of a thrown stone other than its linear and angular velocities.

- MANUFACTURING COST:

The manufacturing of the final design must not cost more than $12,000. Note that all reported costs in this document are in Canadian dollars. This price is based on the information collected from potential customers and primary estimation of the total cost of the final design.

- RATE OF ROCK LAUNCHING:

Based on observations during a competition, each cycle of throwing a curling stone takes up to one minute. Therefore, in order to be similar to the actual game, this device must be able to launch a curling stone at least once per minute. This factor will help curling coaches and curlers to simulate the actual game and also, it helps the sport scientists to see how the ice conditions change by the time in an actual game.

- MAINTENANCE COSTS:

The maintenance cost is an estimate of the annual repair and consumable costs for the device. The maintenance costs must not exceed $600 per year. The detail of this cost is explained in Appendix A.5.

3.5.3. Accuracy

Accuracy can be defined as the closeness of the measured values to the target value. The main focus of this project is the consistency of the output of the device under each setting of the rotational and linear velocities combined with the minimum number of output increments and the maximum values of the rotational and linear velocities. The combination of these parameters (the consistency, the minimum number of increments, and the maximum values of the rotational and linear velocities) makes the accuracy less important for this project. Since the user benefits from a range of settings (output increments) from zero to the maximum value, they can simply go up or down on the settings to achieve desired velocities without considering the accuracy of a specific output.

3.5.4. Ranking of Objectives

A Pairwise Comparison Chart (PCC) was used to rank the objectives. The PCC is found below in Table 3.1.

Table 2.1: Pairwise Comparison Chart.

Objectives	Mfg. Cost	Knowledge	Set up / Launch Time	Portability	Minimum Output Increments	Consistency	Maintenance Cost	Total	Rank
Mfg. Cost	**	1	1	1	1	1	1	6	1
Knowledge	0	**	0	0	0	0	1	1	7
Set up / Launch Time	0	1	**	0	0	0	0	1	6
Portability	0	1	1	**	0	0	0	2	5
Minimum Output Increments	0	1	1	1	**	0	0	3	4
Consistency	0	1	1	1	1	**	0	4	3
Maintenance Cost	0	0	1	1	1	1	**	4	2

The objectives in Table 3.1 are scored based on the information that the curlers and coaches provided in interviews and based on the points which were discussed in the “List of Design Objectives” and the “List of Design Constraints” sections. The final ranking is calculated based on the total scores of each objective.

This chart shows that the manufacturing cost is the most important factor and after that the maintenance cost is the second most important factor in this design. Overall, since the similar existing models are expensive and not affordable for the curling clubs, efforts will be made to reduce the final cost of the device as much as possible, as long as it will not spoil the functionality of the device and will not prevent the constraints from being satisfied. Furthermore, the consistency and the minimum output increments of the final design are discussed comprehensively in the objectives section, as well as in the constraints section. Although they are important factors, since there are sufficient constraints on these factors, they can be accepted as the third and fourth objectives in the ranking list. Finally, the portability, set up time, and knowledge are the fifth, sixth, and seventh objectives in the ranking list, respectively.

3.7. Stakeholders

Curling clubs, Curling Canada, the International Olympic Committee, the World Curling Federation, ice technicians, curlers, and scientists, physicists, and engineers who are working on

curling, are all groups that have interest in or may be directly impacted by a solution to the proposed problem.

Curling Clubs. This device will provide curling clubs with quicker (more frequent) ice calibration and stone matching. The curling clubs can be considered as a primary stakeholder.

Curling Canada. If the Rock Launcher is developed and used here in Canada, it may give Canadian curlers an advantage in training and in international competition, which would influence high performance funding for Curling Canada.

The International Olympic Committee. Fair play is one of the significant issues during competitions in Olympic Games. By using this device, the condition of the surface of the ice sheet can be verified to be similar.

The World Curling Federation. This device may help the Curling Federation to define a standard condition for the surface of the ice sheet and maintain this condition during competitions.

Ice technicians. Ice technicians are responsible for preparing the ice before each game or tournament and for checking the condition of the ice. The solution to this problem specifically would help the ice technicians to check the condition of the ice surface after preparation with higher consistency and speed.

Curlers. This device will launch curling stones with consistency at preset speeds and directions. Therefore, it will help curlers to compare the effectiveness of different sweeping techniques.

Scientists. As far as it was explained earlier, there is still uncertainty as to why the curling stone behavior on the pebbled ice surface is different from curling in a flat ice or dry environment. This device will facilitate the research on curling.

4. CONCEPTUAL SOLUTIONS AND MODELLING

In this Chapter, conceptual solutions for the problem defined in Chapter 3 are described. After the best solution is selected, a model of that solution is presented using CAD software. Finally, a prototype of the selected solution is designed and described.

4.1. Conceptual Solutions and Selection of Best Concept

This section focusses on the comparison of alternative conceptual solutions and the selection of the best concept based on the constraints and the objectives.

4.1.1. Alternative Conceptual Solutions

Several ideation techniques were utilized to generate possible solutions. The ideation started with brainstorming and then continued with SCAMPER and analogy. Utilizing different techniques lead to a broader range of alternatives. From the ideation, 13 alternative conceptual solutions were developed. During the first iteration of the evaluation process, these conceptual solutions were passed through the constraints' filters to ensure that each of these concepts could meet the requirements described in Chapter 3. This assessment reduced the number of conceptual solutions to three. These three were assessed in a second iteration. Below are descriptions of each of the 13 initial alternative solutions. Also, a code name was given to each solution for reference.

- OFF THE SHELF LINEAR ACTUATOR (OTS LINEAR ACTUATOR)

The idea of this conceptual solution is to use a linear actuator to push a curling stone from stationary to a preset linear velocity. At the same time, another motor produces the rotational motion of the stone. In this mechanism, the stone must be accelerated to the desired speed in a relatively short distance since most of the OTS linear actuators have short arms (actuator shafts) (Figure 4.1).

Figure 4.1: Linear actuator (Moog Inc, 2021).

- SLIDER-CRANK

The slider-crank mechanism is a well-known mechanism that is famous for converting rotational motion into linear motion and was used in traditional trains. This mechanism consists of two links which relate to different types of joints (Figure 4.2). In this concept, two motors are required; one as an actuator for the slider-crank mechanism and the other one to rotate the curling stone.

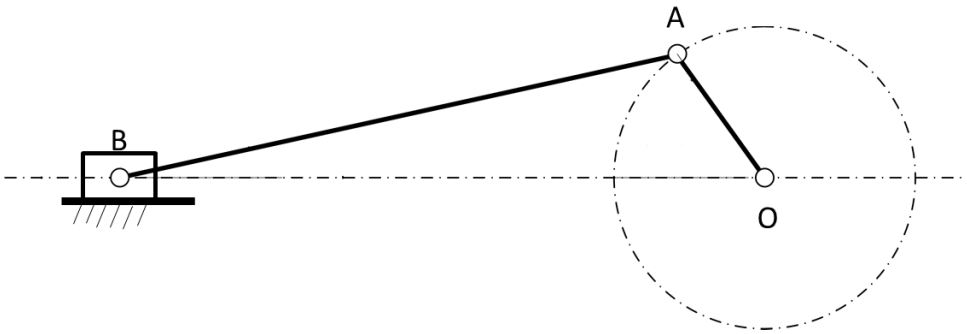

Figure 4.2: Slider crank mechanism.

- RAMPS

This idea involves using ramps of different sizes (height and length) to accelerate the stone to a preset linear velocity. These ramps are similar to playground slides. On each side of the ramp, a rubber strip will be mounted to rotate the curling stone around the instantaneous center of rotation i.e. where the stone grips the one strip while it is sliding down the ramp. These rubber strips

increase the friction on one side of the curling stone and consequently, the curling stone rotates around the instantaneous center of rotation while sliding down the ramp (Figure 4.3).

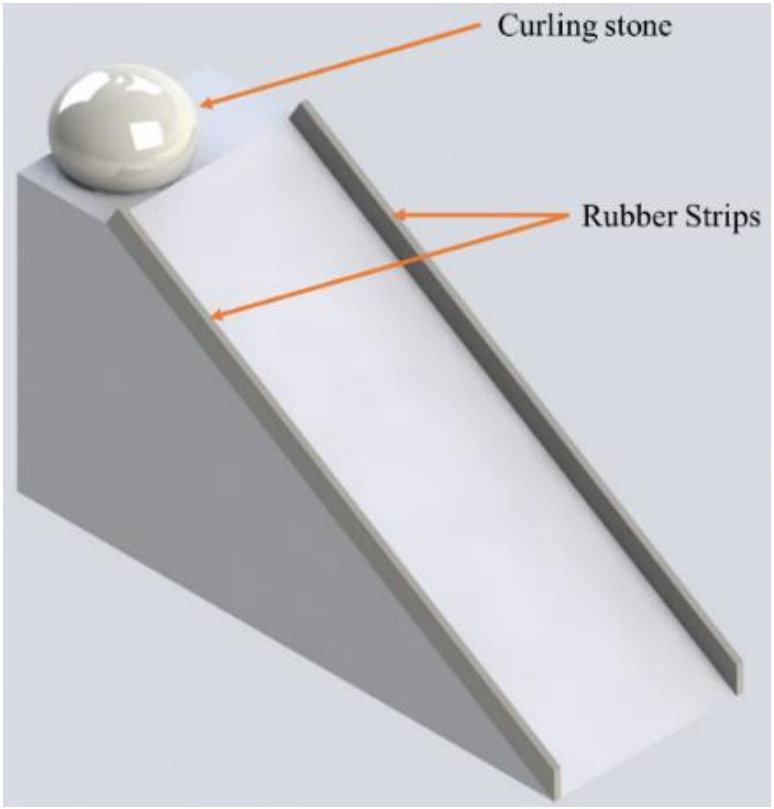

Figure 4.3: Ramps mechanism.

- PENDULUM

A pendulum can be used to punch the curling stone to give it enough momentum to reach the desired velocity. The spot on the circumference of the curling stone the pendulum hits will define the direction of its rotational motion and its rotational speed. If the pendulum hits through the CoG (Center of Gravity) of the stone, the direction of the stone's linear motion can be determined but the stone will not rotate.

- ONE CHAIN AND TWO MOTORS

In this idea, one motor is connected through a sprocket to a chain. This chain carries a cradle-shaped part which transmits the motion to the curling stone. A long beam supports the cradle-shaped part. Another motor is mounted on the cradle-shaped part and is responsible for rotating the curling stone to a preset angular speed. This mechanism can be found in Figure 4.4.

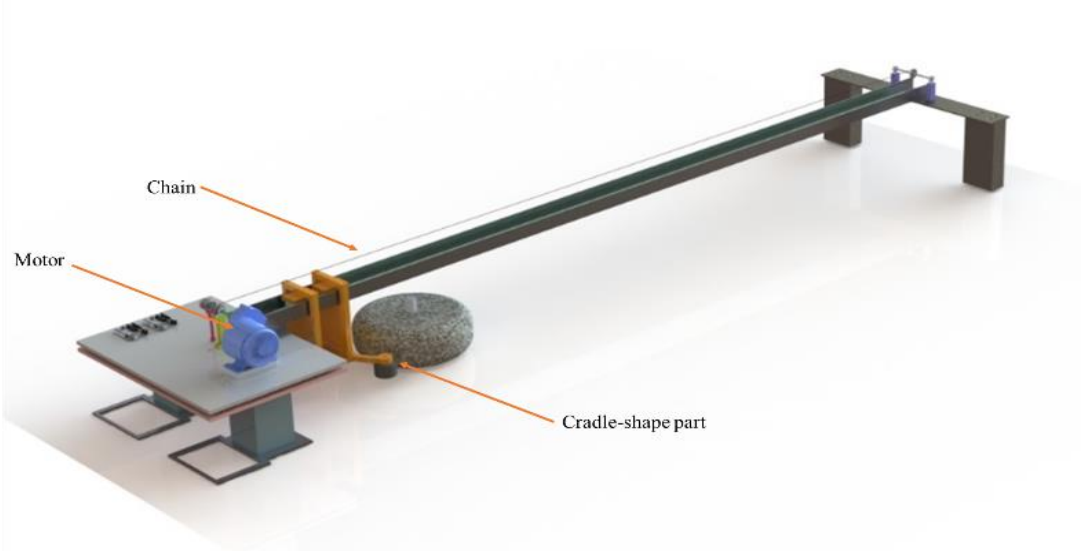

Figure 4.4: The chain and two motors mechanism.

- BALL SCREW

Implementing a screw to convert the rotational motion of a motor to a linear motion is the basis of this idea. The ball screw mechanism is typically used in 3D printers and it is known as a precise mechanism for positioning with very little backlash (Figure 4.5). Backlash in mechanical engineering is "the play between adjacent movable parts (as in a series of gears)" ("Merriam-Webster Dictionary," 2021). In addition, another motor will be utilized to rotate the curling stone.

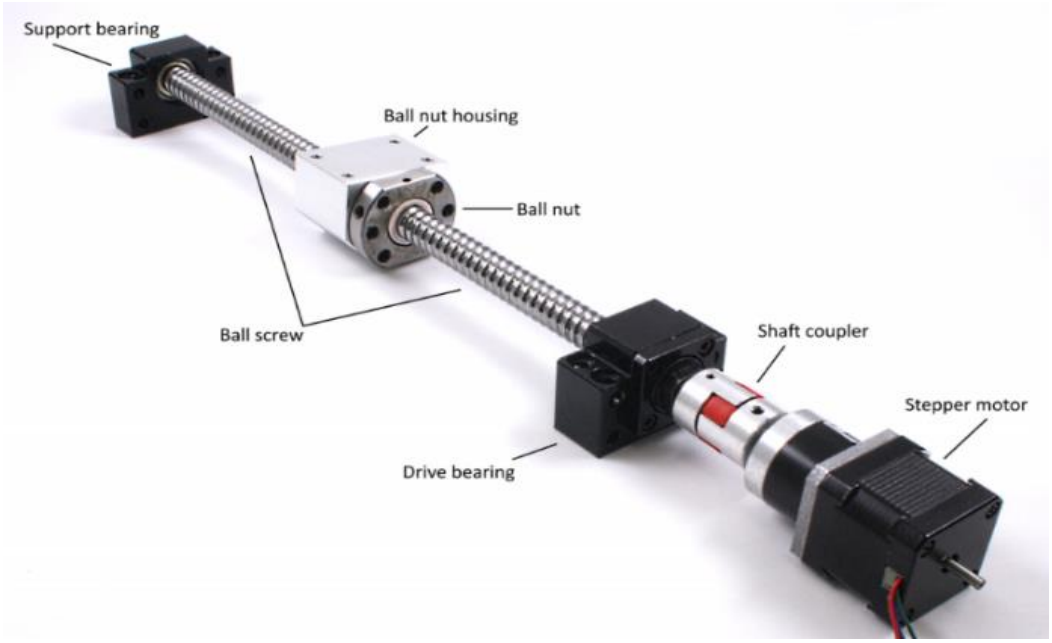

Figure 4.5: Ball screw mechanism ("Linear Motion Primer - Phidgets Legacy Support," 2020).

- SPRINGS

A compressed spring can produce the force needed to accelerate a curling stone. Springs with different sizes can be utilized for different velocities. Also, the spot on the stone's circumference that the spring exerts the force to the curling stone will determine its rotational direction and the speed of its rotational motion. If the spring exerts the force through the CoG of the stone, the direction of the stone's linear motion can be determined but the stone will not rotate.

- RACK AND PINION GEAR

A rack and pinion gear connected to a rotational actuator can provide the linear motion to a curling stone along with another motor to produce the rotational motion of the curling stone. The motor rotating the pinion gear is mounted on the cradle-shaped part and it travels down the ice with the stone to the release point (Figure 4.6).

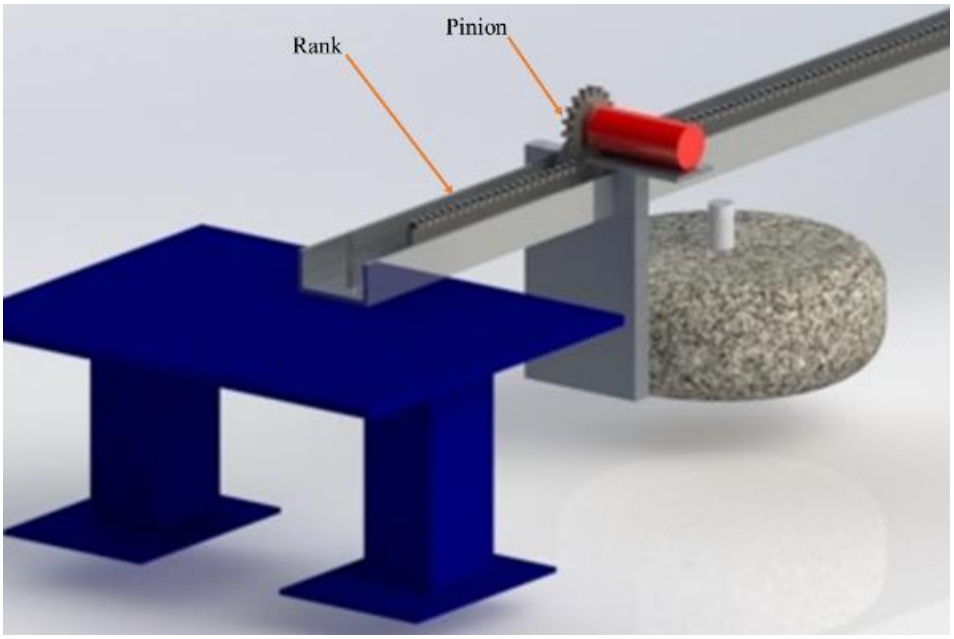

Figure 4.6: Rack and pinion mechanism.

- TWO WHEELS

Figure 4.7 displays this mechanism. As this figure shows, two wheels can be used to give a curling stone both linear and rotational velocities. This mechanism, a "Jugs soccer machine™", is currently used for launching soccer balls and footballs. To produce rotational motion on the curling stone, one wheel rotates with a different velocity compared to the other wheel.

Figure 4.7: Jugs soccer machine ("Soccer MachineTM," 2018).

- FOUR PULLEYS AND TWO BELTS

This idea is very similar to the idea of two wheels. In this mechanism, a curling stone is held in the middle of two belts each going around two pulleys (Figure 4.8). Once the pulleys rotate, the friction between the belts and the curling stone will accelerate the curling stone linearly and rotationally. The difference between speeds of pulleys determines the rotational velocity of the curling stone.

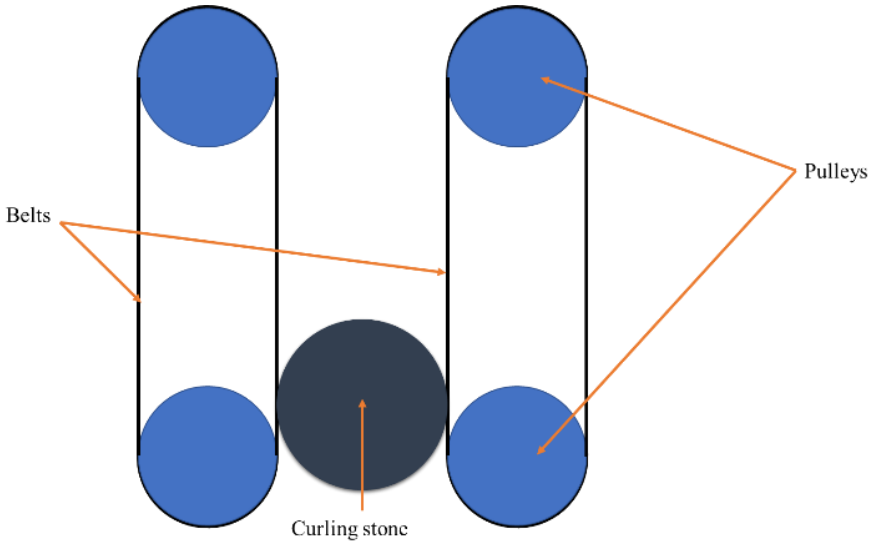

Figure 4.8: Top view of the "four pulleys and two belts" mechanism.

- ELECTROMAGNET

The required force to accelerate a curling stone can be provided by an electromagnetic force. In this mechanism, a temporary electromagnetic field is produced by a coil of wire connected to a DC power supply. Also, a permanent magnet is connected to a curling stone. The force

produced by the temporary magnetic field on the permanent magnetic mounted on the curling stone will accelerate the stone.

- TWO PULLEYS AND ONE BELT

This mechanism consists of two pulleys and a belt attached to the pulleys. Once the pulleys rotate, the belt coils around the pulleys and the stone will be launched. The difference in the speeds of pulleys determines the rotational velocity of the curling stone. Figure 4.9 displays this mechanism.

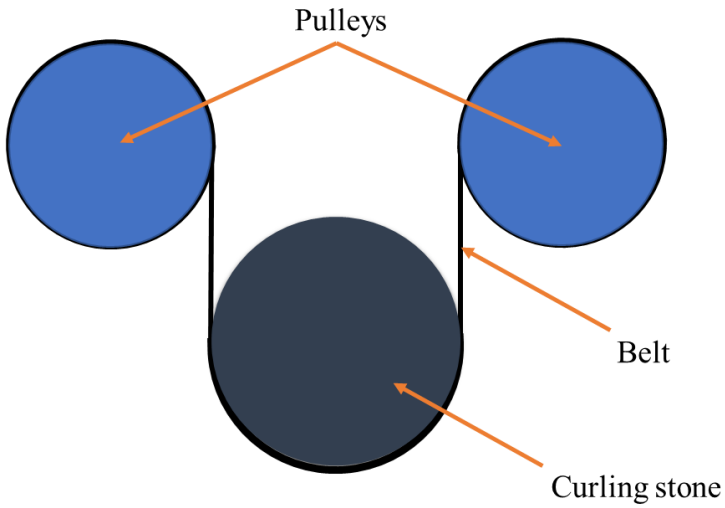

Figure 4.9: Top view of the "two pulleys and a belt" mechanism.

- PNEUMATIC JET

The idea of the pneumatic jet alternative was to use compressed air to push the stone. The spot on the curling stone's circumference which the nozzle blows at determines the direction of the stone's rotation and the magnitude of its rotational velocity. If the pneumatic jet blows through the CoG of the stone, the direction of the stone's linear motion can be determined but the stone will not rotate.

4.1.2. Data Gathering and First Iteration of Evaluation

For the first iteration of evaluation, a chart was utilized to evaluate the conceptual solutions described in the previous section based on their abilities to meet the constraints. Table 4.1 shows a summary of the constraint(s) which the intended mechanism is not able to satisfy. In the following paragraphs, it is discussed why a concept cannot satisfy one or more constraints.

Table 4.1: Constraints filters mechanisms.

Mechanisms	Constraints Not Satisfied		
OTS Linear Actuator	Speed Constraints		
Slider-Crank	Size		
Ramps	Speed Constraints	Minimum Output Increments	Consistency
Pendulum	Speed Constraints		
One Chain and Two Motors	-	-	-
Ball Screw	-	-	-
Springs	Consistency	Speed Constraints	
Rack and Pinion Gear	-	-	-
Two wheels	Consistency	-	-
Four Pulleys and Two Belts	Consistency	-	-
Electromagnet	Stone Condition	Manufacturing Cost	Maintenance Cost
Two Pulleys and One Belt	Speed Constraints		
Pneumatic Jet	Ice Condition	Speed Constraints	Sound Constraints

Based on the information collected online, most of the OTS linear actuators have a short arm and they are designed for low speed and high consistency applications. In this project, the curling stone needs to be accelerated to 3 m/s which makes the OTS linear actuators a poor option. Also, in the speed constraints section ("List of Design Constraints", Section 3.5.2.), it is mentioned that the linear speed and the rotational speed must be able to be set independently. This constraint rejects the ramps, pendulum, springs, two pulleys and one belt, and pneumatic jet options since none of these mechanisms can provide independent linear and rotational velocities to the curling stone. Furthermore, the pneumatic jet will change the condition of the air of the curling rink and consequently, it is not a good option for this project. The temperature of a curling rink varies between -4.5°C to +5°C (Ohman, 2004). This temperature variation will alter a spring's constant. Therefore, the springs option cannot pass the consistency constraint as well.

Although the electromagnetic solution can satisfy the speed constraints, the complexity of using this mechanism to accelerate the stone makes it expensive to manufacture and to maintain. In addition, as discussed in the constraints section, the condition of the curling stone must not be changed except for its linear and rotational velocities. However, for the electromagnetic mechanism, the stone has to be changed to have a permanent magnetic mounted on it.

Another mechanism which is rejected by the constraints is the slider-crank. This mechanism has two arms, a crank (link OA in Figure 4.2) and a coupler (link AB in Figure 4.2). Since the crank link is the component which rotates around one of its ends, it requires sufficient space. Therefore, this mechanism cannot work within the size constraints compared to the other options.

Two wheels, and four pulleys and two belts are two mechanisms working based on the friction between the wheels or belts and the curling stone. Changes in temperature and humidity affect the frictional force between the stone and wheels or belts (Lahayne et al., 2016). The temperature of a curling rink can vary between -4.5°C to +5°C, so these mechanisms might not be as consistent as is required. Consequently, the two wheels mechanism, and four pulleys and two belts mechanism cannot sufficiently satisfy the consistency constraints. Therefore, they are eliminated in this iteration.

After the first round of evaluation, 13 alternative solutions were reduced to three conceptual solutions: rack and pinion, chain and two motors, and ball screw. In the next iteration, the remaining three concepts are evaluated using a weighted decision matrix.

4.1.3. Second Iteration of Evaluation

After the first iteration, three alternative solutions remained: the rack and pinion, the chain and two motors, and the ball screw. A weighted decision matrix was utilized to compare the three remaining options based on their ability to satisfy the objectives (see Table 4.2). Weighted decision matrices or numerical decision matrices are charts in which each objective is weighted based on how important it is. Therefore, in this method, solutions get more priority based on their capability to satisfy the most important objectives (McCahan et al., 2015).

The total weight in the decision matrix is 100%, and the maximum potential score is 100%. Since the manufacturing cost has a high priority in comparing these mechanisms, the metric is divided into six values for the manufacturing cost so that the score can be chosen among 0%, 20%, 40%, 60%, 80%, and 100%. For the rest of the objectives, the score can be chosen among the four values, 0%, 30%, 60%, and 100%.

Ultimately, the best concept selected in this iteration must compete with human curlers since currently, curlers perform tasks like stone matching or throwing the curling stone for scientific purposes. However, because the human curlers are only able to estimate the required speed i.e. they are not consistently accurate in launching a curling stone, human curlers cannot

meet the consistency constraint of the design. Thus, human curlers are filtered out by the constraint of the design even though they would likely excel against some of the other objectives.

Table 4.2: Weighted decision matrix.

Objectives	Weight	Rack and Pinion		Chain and two motors		Ball Screw	
		Rating	Score	Rating	Score	Rating	Score
Manufacturing Cost	30%	40%	12.0%	80%	24.0%	20%	6.0%
Knowledge	5%	30%	1.5%	30%	1.5%	30%	1.5%
Set up / Launch Time	7%	30%	2.1%	30%	2.1%	30%	2.1%
Portability	8%	30%	2.4%	30%	2.4%	30%	2.4%
Minimum Number of Output Increments	10%	100%	10.0%	100%	10.0%	100%	10.0%
Consistency	15%	100%	15.0%	100%	15.0%	100%	15.0%
Maintenance Cost and time	25%	30%	7.5%	60%	15.0%	30%	7.5%
Total	100%		50.5%		70.0%		44.5%
Rank			2		1		3

In Table 4.2, after scoring each concept against each objective, the chain and two motors received the highest percentage compared to other options.

The three mechanisms discussed in this iteration received identical scores for knowledge, set up time, launch time, portability, the minimum number of output increments, and consistency since their mechanical structures are mostly similar. However, their mechanisms that convert the motor's rotational motion to the linear motion are different. Therefore, they have different manufacturing and maintenance costs.

Regarding the manufacturing cost, the chain and two motors received the highest score among other mechanisms. This is because the rack and pinion mechanism and the ball screw mechanism both have long components, the rack (see Figure 4.10) and the screw (see Figure 4.11), which makes these mechanisms expensive to manufacture. The manufacturing cost of these parts is high because they are not off-the-shelf parts. Also, in the rack and pinion mechanism, the motor producing the linear motion of the curling stone is mounted on the part which is responsible for pushing the curling stone (see Figure 4.10). The motor's weight on one side of this part causes a high moment on this part, making the stabilizing of this part more complicated and consequently more expensive to manufacture. Furthermore, designing and manufacturing the screw and the part that pushes the stone in the ball screw mechanism is complicated and expensive, so it received the lowest score (e.g., see Appendix A.16).

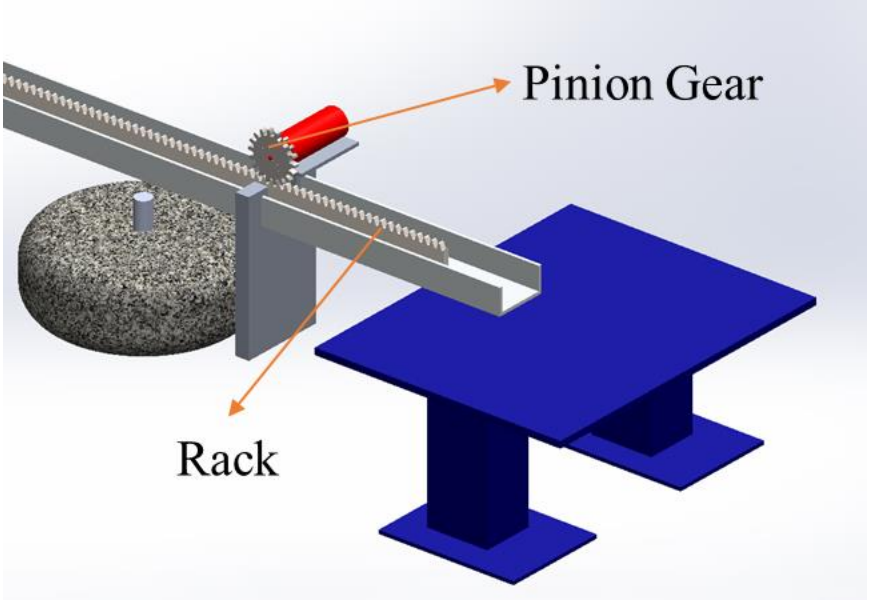

Figure 4.10: Rack and Pinion mechanism. The pinion is attached to the motor's shaft. Once the motor's shaft rotates, the pinion engages with the rack and moves the part that pushes the curling stone. The Red cylinder is the main actuator / motor.

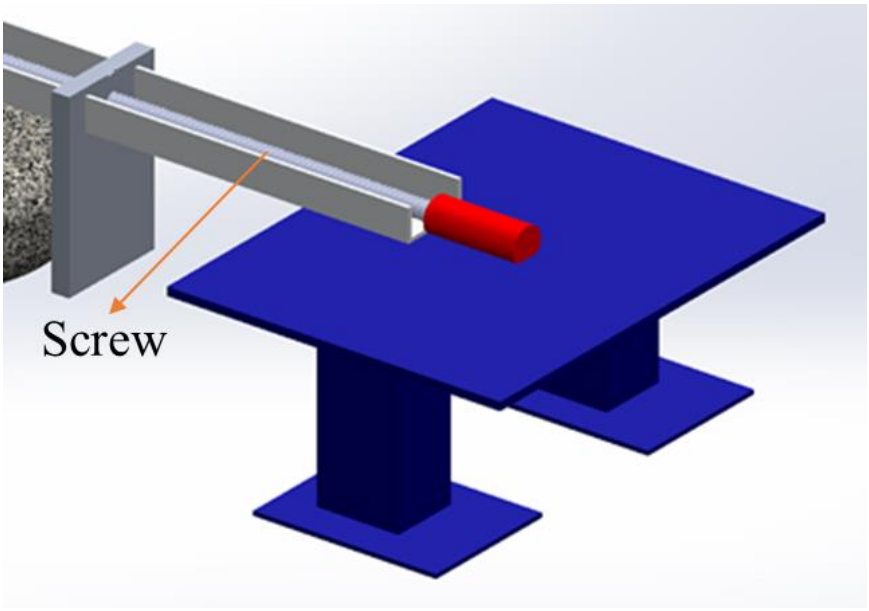

Figure 4.11: Ball screw mechanism. The motor rotates the screw. The part that pushes the curling stone has a threaded hole. The screw rotates inside that threaded hole and moves that part. The Red cylinder is the main actuator / motor.

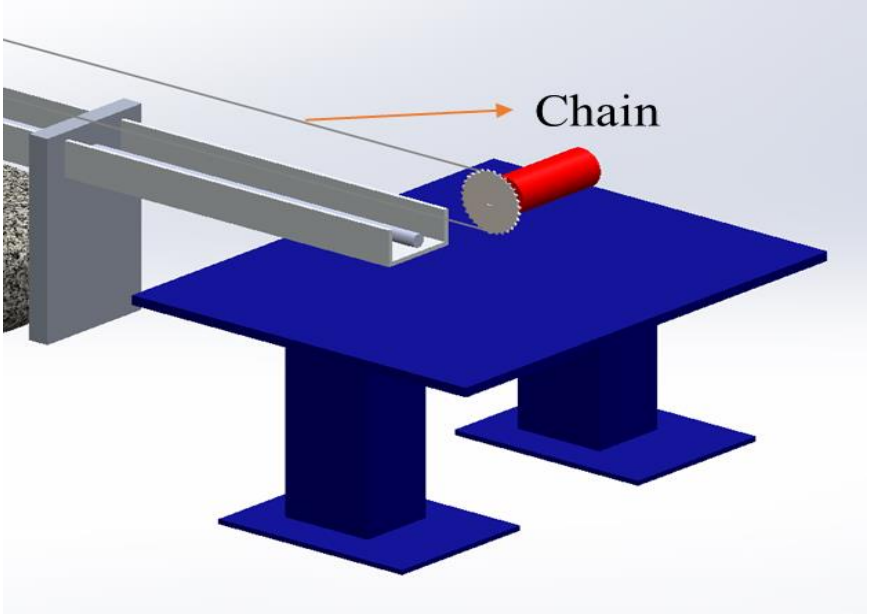

Figure 4.12: Chain and two motors mechanism. The motor rotates the sprocket. The sprocket runs the chain loop and consequently moves the part that pushes the curling stone. The Red cylinder is the main actuator / motor.

In terms of maintenance cost and time, the ball screw mechanism received the lowest score since the screw part, and the part that moves along this screw (the ball bearing), needs more frequent lubrication. Also, since the motor moves with the part that pushes the stone, it is more likely that the motor's wiring needs more frequent maintenance in the rack and pinion mechanism. Therefore, this mechanism received the lowest score compared to the chain and two motors mechanism in maintenance cost and time.

4.2. Configuration Solution for the Chain and Two Motors

The mechanism that received the highest score in the last iteration, the chain and two motors, will be described in the following paragraphs. This mechanism's motion is explained, along with a model of this mechanism using CAD software to show how different parts interact.

This mechanism includes three main parts i.e. two supports and a beam. From now on, the beam will be referred as the "bridge" as it is like a bridge between the two supports. The bridge supports the cradle-shaped part ("cradle mount" in Figure 4.13) that pushes the curling stone from one end and releases it at the other end of the bridge. The required power is provided by a motor mounted on the "main platform". The power is transmitted to the cradle mount through a chain.

This chain loops around a sprocket mounted at each end of the bridge. Also, the “end leg” supports the end of the bridge. Figure 3.13 shows the parts of this mechanism.

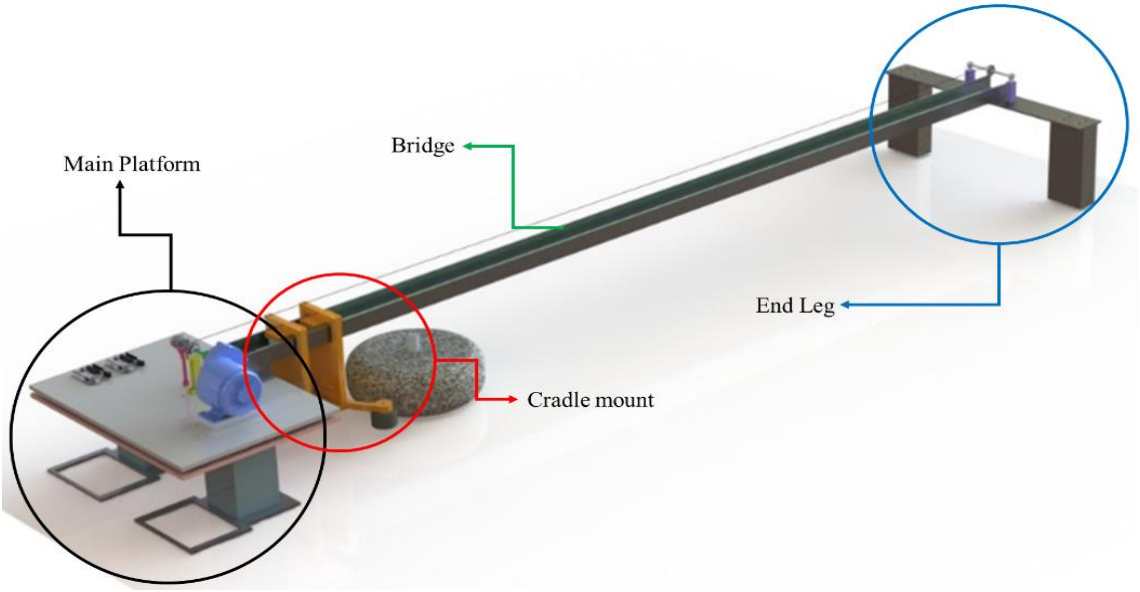

Figure 4.13: The chain and two motors mechanism and its parts.

In this mechanism, aluminum 6061 alloy will be used to fabricate most parts; some other parts which are not under much stress will be fabricated out of plastic (acrylics). The aluminum 6061 alloy and acrylic plastic are not known as brittle materials in the temperature and humidity range of curling clubs. The chance of oxidization of aluminum in this condition is also relatively low.

To prevent the ice from being damaged, each part of the device that is in contact with ice is tipped with rubber. The information collected from ice technicians shows that metals (due to their high heat conductivity) can melt the ice quickly. Therefore, strips of rubber are used to prevent any contact between ice and aluminum. Furthermore, the cradle mount pushes the stone with two wheels. Rubber covers these wheels' circumference to protect the stone from any damage and to increase the traction between the wheels and the curling stone.

This mechanism's electrical components can be divided into two groups, the electrical components of the motor responsible for the linear motion of the stone, and the electrical components of the motor rotating the stone. From now on, the motor pushing the stone down the ice will be referred as the “main motor”, and the motor rotating the curling stone will be referred to as the “rotational motor”.

Regarding the size constraints, most parts of this mechanism are within the required range, or they can be dissembled. The only part that may cause an issue in satisfying this constraint is the bridge. The bridge is a long u-shaped aluminum beam. In order to satisfy the size constraint, a 2.2 m long bridge was selected.

4.2.1. Equations of Motion

The equations of motion of the device are required in order to select the best actuator, control system, and power supply based on the discussed design constraints and objectives. In the following paragraphs, a brief description of the equations of motion are presented. The detailed calculation of the values presented here can be found in Appendix A.1.

4.2.1.1. Linear Motion

The device pushes the curling stone to accelerate it to a preset linear speed. The maximum required linear speed of the curling stone is 3 m/s. The curling stone has a mass of 20 kg, and the available length of the bridge is 2 m. About 10 cm of its actual 2.2 m length is needed at each end for attachment to the main platform and the end leg. Assuming the acceleration is constant, using $s = \frac{1}{2}at^2 + v_0t + s_0$ and considering $v = at$, the acceleration of the stone can be determined. Note that *s* is the displacement (m), which is the length of the bridge here, *a* is acceleration (m/s^2), *v* is velocity (m/s) which is the maximum linear velocity here, *t* is the time of action (s), and v_0 and s_0 are the initial values of speed and displacement. The stone's needed acceleration is equal to 2.25 m/s^2 and the time of action is equal to 1.33 s. Then the force required to produce the desired acceleration can be calculated by $F = ma$ where *F* is the required force (N), and *m* is mass, which is the mass of the curling stone (20 kg) plus the mass of the cradle mount (2.5 kg) plus the mass of chain (0.6 kg). The kinetic frictional force between the stone and the ice is added to the force calculated in the previous step ($F_{\text{kinetic friction}}$ = 4.4 N). The total force is equal to 56.4 N. To linearly accelerate the curling stone, the motor must rotate the sprocket (the sprocket has a 73.5 mm diameter). This sprocket runs a chain loop, and the cradle mount is attached to this chain. Consequently, the cradle mount moves the curling stone. So, the required torque and rotational speed of the sprocket to accelerate the curling stone to the maximum linear speed can be determined by $\tau = Fd$ (τ is the required torque (N·m), *F* is the total force calculated recently (N), and *d* is the radius of the sprocket (m)), and $v = \omega r$ (ω is the rotational velocity (rad/s), and *r* is the radius of the sprocket (m)). The torque and rotational speed required of the sprocket to linearly

move the stone at a constant acceleration to the maximum speed are 2.07 N·m and 81.6 rad/s, respectively. A 1.5 factor of safety is applied on the value of the torque calculated here. Therefore, the motor must provide 3.11 N·m (see Appendix A.1.1. for detailed calculations).

4.2.1.2. Rotational Motion

A motor installed on the cradle mount is responsible for rotating the stone. The maximum required rotational speed of the stone is 2.09 rad/s. A wheel is installed on the motor shaft with a 3.6 cm radius. The rotational motion provided by the motor is transmitted to the curling stone through this wheel. First, the angular acceleration can be determined using $\omega = \dot{\omega}t$ where $\dot{\omega}$ is the angular acceleration (rad/s^2), and t is the time of action (s). The rotational motor has 1.33 seconds to accelerate the stone to the maximum angular speed. Consequently, the angular acceleration is 1.57 rad/s^2. Then, the required torque on the curling stone to rotate it up to the maximum rotational speed can be calculated by $\tau_{rot.} = I\dot{\omega}$ where $\tau_{rot.}$ is the required torque (N·m), and I = 10.96·x 10^{-2} kg·m^2 is the moment of inertia of the curling stone. The calculated rotational torque ($\tau_{rot.}$= 0.172 N·m) plus the torque required to overcome the kinetic friction from the ice (4.40 N kinetic friction multiply by 0.065 m, the radius of the running band, is equal to 0.286 N·m) is equal to the total torque. Therefore, total torque required = 0.458 N·m. With the total torque calculated, the torque on the rotational motor's wheel can be determined using $\tau_{stone}/R = \tau_{wheel}/r$ and the required rotational speed on this wheel can be determined using $\omega_{stone}R = \omega_{wheel}r$ where R = 14.5 cm is the radius of the curling stone (m) and r is the radius of the wheel (m). The torque and rotational speed required of the wheel in order to rotate the curling stone at its maximum rotational speed are 0.114 N·m and 8.42 rad/s, respectively. A 1.5 factor of safety is applied on the value of the torque calculated here. Therefore, the motor must provide 0.171 N·m (see Appendix A.1.2. for detailed calculations).

4.2.2. Mechanical Modelling

In this section, a mechanical model of the chain and two motors mechanism is presented, and each component of this mechanism is discussed.

As mentioned earlier in this Section, the mechanism has three main parts; the main platform, the bridge, and the end leg. The main platform is responsible for supporting all electrical boards as well as the main motor. Figure 4.14 displays the configuration of the main platform. The main platform has two supports which attach to the hacks. In order to fit these supports to the hacks, they are designed with rectangular holes in them. A plate is attached to the top of these

supports using bolts and another identical plate is located on top of it. The top plate has the bridge attached to it, and this plate can be rotated around its center. This makes it possible to rotate the bridge in order to release the stone at a preset angle.

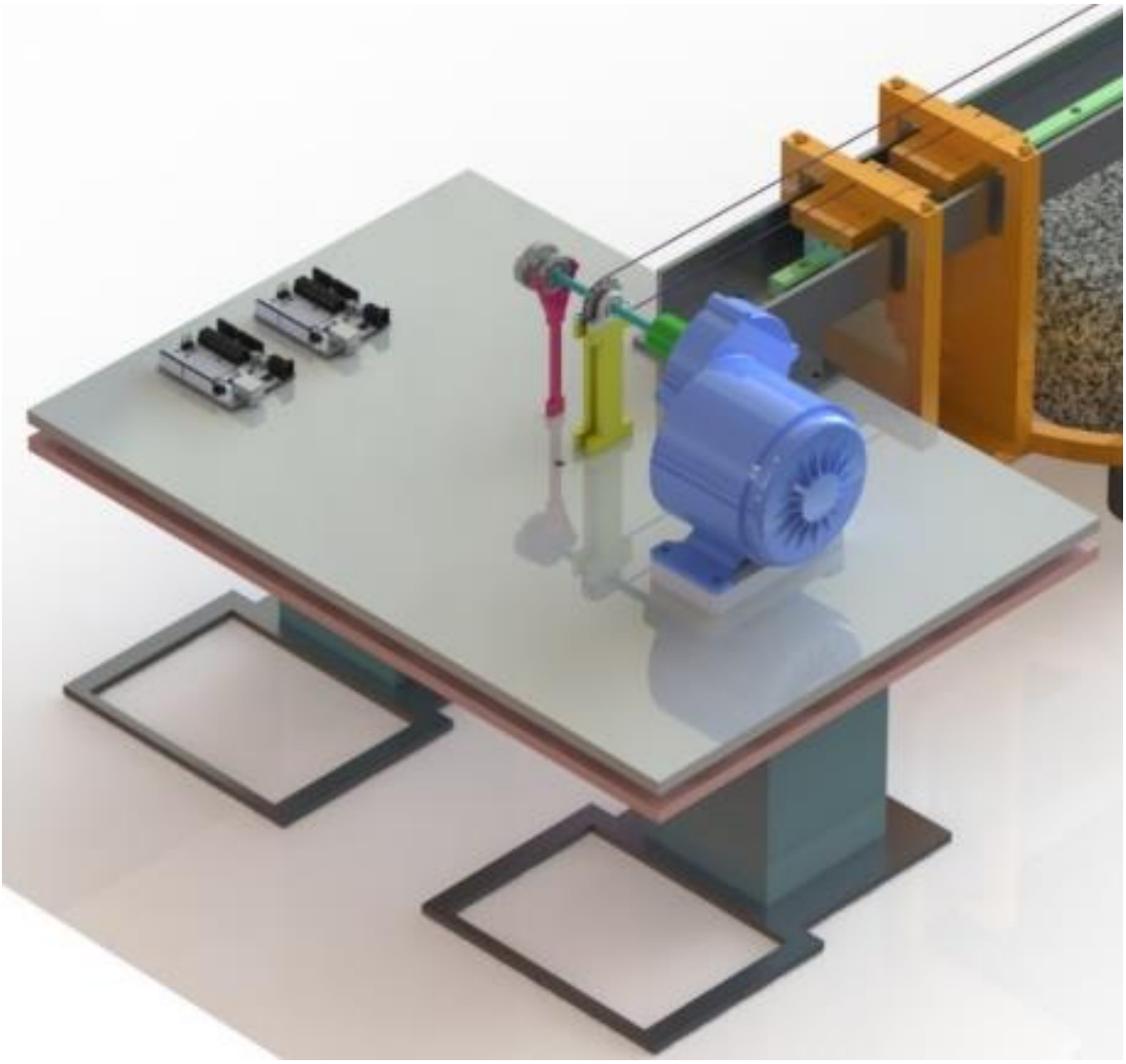

Figure 4.14: The main platform.

The 2.2 m long bridge has four parts, a linear bearing rail, a cradle mount, a chain, and two sprockets. Two linear bearings attach the cradle mount to the rail. The figures below show the bridge and its parts. The cradle mount pushes the stone down the ice and releases it at the end of the bridge. The cradle mount has a c-shaped part which covers 90 degrees of the stone's circumference to support the stone while it is pushed down the ice and the rotational motor located at 45 degrees from the base of cradle (see Figure 4.17).

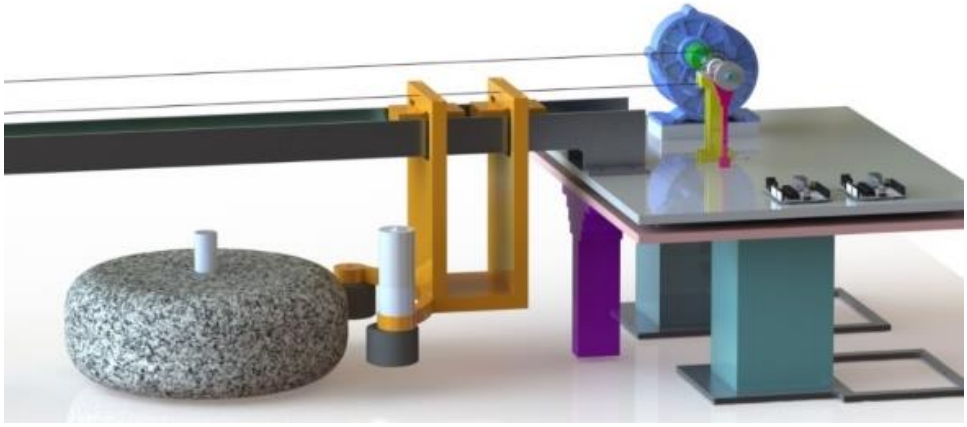

Figure 4.15: The bridge mechanism and its parts.

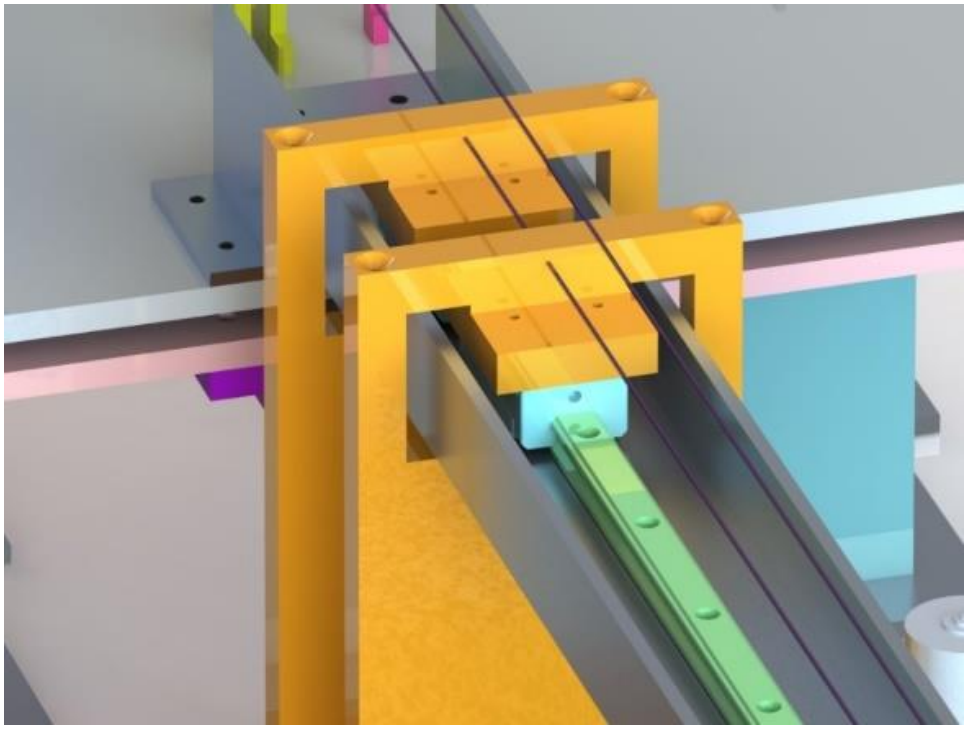

Figure 4.16: The linear bearing (Light blue), the rail (light green).

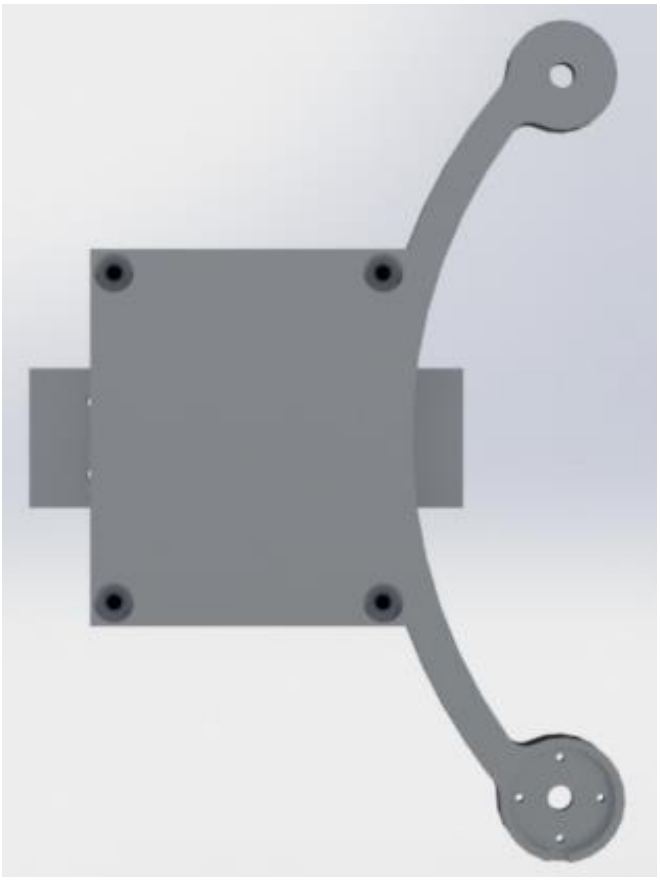

Figure 4.17: The bottom view of the cradle mount.

The end leg is responsible for supporting the end of the bridge. Figure 4.18 shows the end leg. Two supports of the end leg stand on the ice surface. As a result, the bottoms of these supports have to be equipped with rubber strips in order to protect the ice from any damage.

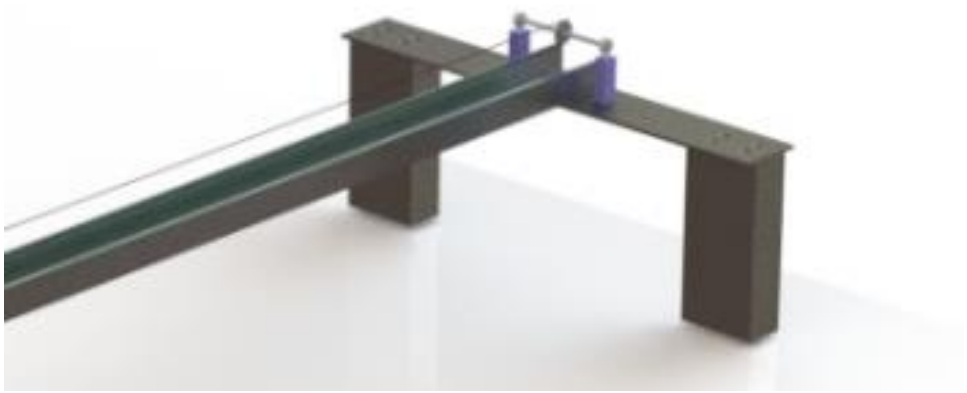

Figure 4.18: The end leg.

4.3. Proof of Concept and Prototype

To validate the design presented in this chapter, two physical models were fabricated. These helped to improve the device's design in order to better satisfy the objectives.

The first model (a proof of concept) was made out of cardboard. This proof of concept was very simple and only had mechanical components. The scale of this model was half of the actual dimensions for the device design. The cardboard proof of concept showed that the system for setting the release direction of the stone with respect to the centerline of the ice was feasible. Figure 4.19 displays this model.

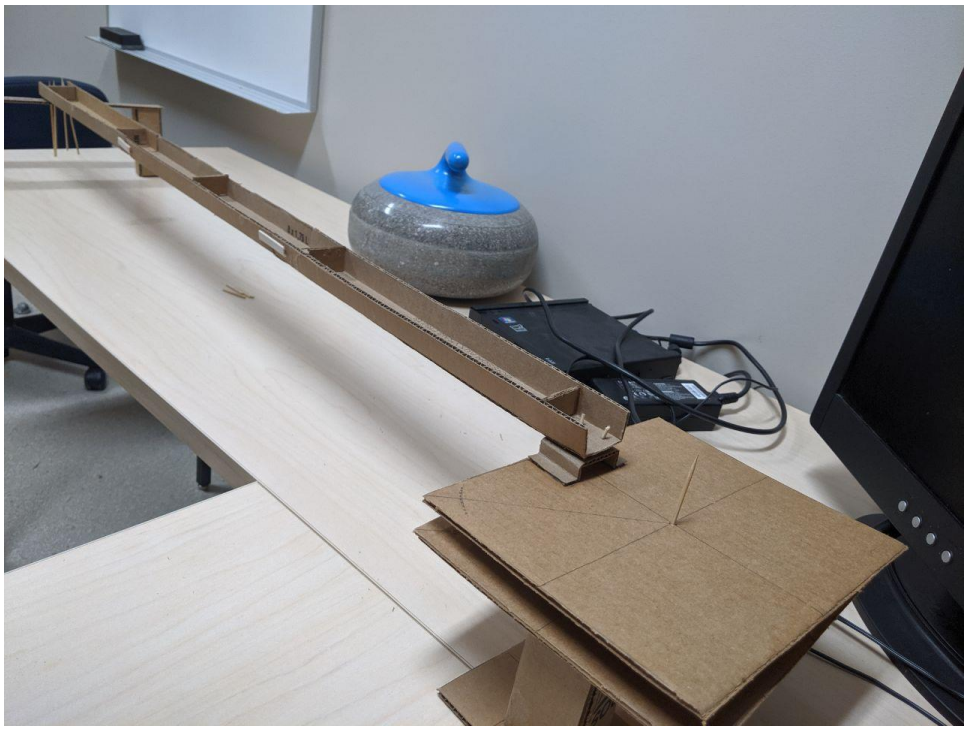

Figure 4.19: The cardboard proof of concept.

The second model (a prototype) was a device with all the necessary mechanical and electrical components to fulfill the functions of the device. The two plates of the main platform were fabricated out of acrylic. The supports (legs) of the main platform (the light green parts in Figure 4.15) were fabricated out of PLA using a 3D printer. The end leg was first fabricated out of acrylic; however, the selected thickness of the acrylic used in the end leg was not sufficient to tolerate the stress applied on it (it bended considerably). So, since wood was more accessible and less expensive, wood was used to fabricate the end leg of this prototype (Figure 4.20). These decisions were made after a stress analysis (presented in Appendix A.13) had been performed on

these parts. Also, the release angles relative to the centerline were set to throw the curling stone to the side edge of the house using this prototype. The maximum angle to the center line was +/- 3°, as per the design constraints.

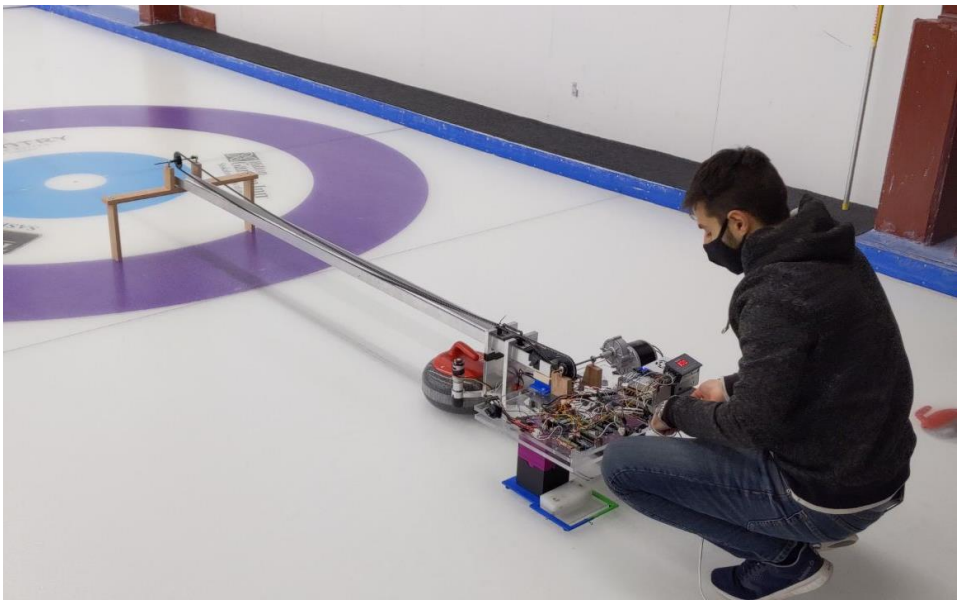

Figure 4.20: The prototype.

A DC motor was utilized for the main motor in the prototype. This motor can provide 50% of the rpm required to reach the stone's maximum linear speed. The rotational motor is also a brushed DC motor. Since the main purpose of prototyping is to show whether the design works and the budget allocated for this prototype was limited, this decision was made. Also, the combination of the rotational motor and the wheel attached to its shaft rotates the curling stone to 50% of the curling stone’s required maximum rotational speed. In this prototype, it was decided to use an off-the-shelf high traction wheel for the rotational motor which has 50% of the diameter of the designed wheel since the designed wheel has to be manufactured i.e. it was not available off-the-shelf, and its manufacturing cost was outside of the budget envelope for this prototype. The wheels that are used in this prototype have a rubber cover to increase the traction between the wheels and the curling stone.

The prototype has two main electrical parts, the electrical components of the main motor and the electrical components of the rotational motor. The control board of the main motor has an Arduino Uno and a motor driver as well as a potentiometer (Figure 4.21). The Arduino Uno is equipped with an Atmega 328P. This 28-pin chipset can be programmed via the Arduino board.

The operating voltage of the Arduino is 7-12V which is supplied by an adapter converter. The Arduino controls a Cytron motor driver using pulse width modulated (PWM) signals. This motor driver can supply the motor with a current up to 20A. The main motor is a 24V and 350W DC motor (MY1016Z3) which can supply 10.1 N·m at 330rpm or 34.5 rad/s ("DC Motor, MY1016Z3 24V, and 350W Gear Reduction Electric Motor for E-Bike Scooter: Amazon.ca: Toys & Games," 2021). The operator uses a potentiometer to control the linear speed. This potentiometer sends signals to the Arduino and the Arduino reads these signals and controls the motor driver accordingly. Also, the operator starts the process of launching the stone with a toggle switch.

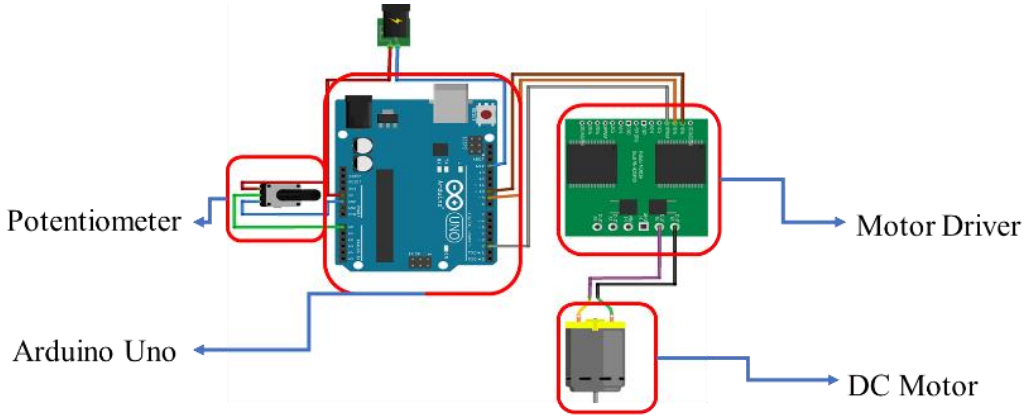

Figure 4.21: A schematic of the control system of the linear motor.

The rotational motor is controlled by an Arduino Uno which is in contact with the main motor's Arduino. The main motor's Arduino controls the starting and stopping time of the rotational motor. The Arduino board sends PWM signals to a single channel H-bridge MOSFET motor driver. This motor driver can supply the motor with 5 to 15V at up to 50A (Figure 4.22). The rotational motor is a brushed DC type which can provide up to 6.76 N·m at 118 RPM or 12.4 rad/s ("12V, 118RPM 958.2oz-in HD Premium Planetary Gearmotor w/ Encoder," 2016). The load on the rotational motor at the maximum speed is 0.171 N·m or 24.2 oz·in. Based on the rotational speed-load graph of the rotational motor (this graph can be found in the spec sheet of this motor presented in Appendix A.8), this motor can rotate at almost 110 rpm which means that it is able to rotate the curling stone up to 83 °/s. The user interface of this control board is a 4-position rotational key and a 3-position toggle switch. The rotational key controls the speed of the rotational motor. It has four positions; stop, low speed, medium speed, and high speed. The toggle switch controls the direction of the rotation and it has three positions: clockwise, zero, and counterclockwise. This prototype has three settings (increments) for the rotational speeds since

evaluating its performance under these three settings is sufficient to validate the design and has less complexity compared to ten settings. Afterwards, once the prototype has passed the tests, it can be simply modified to have a greater number of increments for its rotational speed.

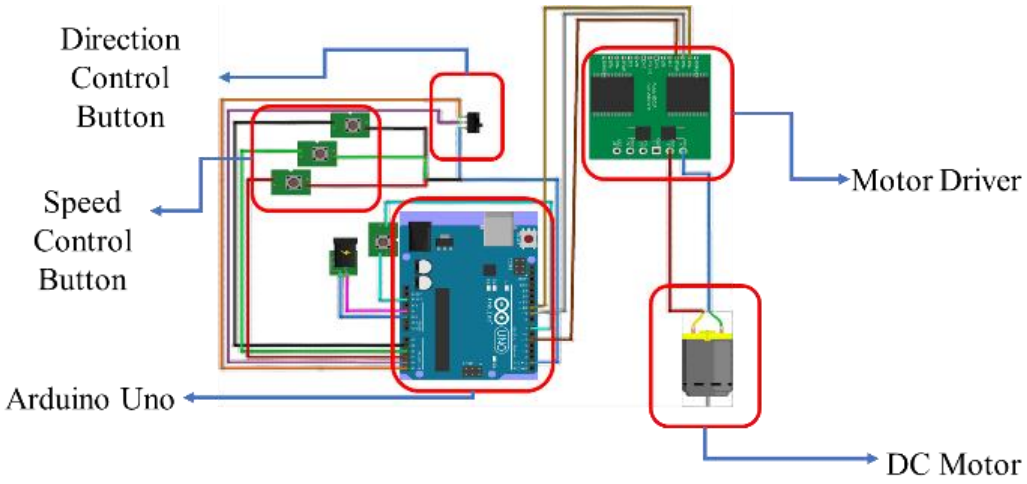

Figure 4.22: A schematic of the control system of the rotational motor.

In summary, in this chapter, alternative concepts and evaluation iterations were discussed. These iterations showed the most successful concept. A configuration design was then presented. Also, the equations of motion of the best mechanism were studied and the mechanical and electrical model of this concept was described. Finally, a proof of concept and a prototype were described. In the following chapter, the results of the validation tests of this prototype, as well as some experiments and their results, are presented.

5. VALIDATION

Once the prototype was fabricated, it was tested to determine whether the key design elements could satisfy the project constraints and objectives. For this purpose, one preliminary test and two validation tests were completed. In this section, these validation tests and their results will be discussed. The validation tests examine the rotational and linear motions of the curling stone at release, as imparted by the PRL.

The PRL also can throw the curling stone at a preset angle to the ice sheet center line. Due to the time restrictions on the ice use during COVID, validation and further study on this function was not covered at this time.

5.1. Preliminary Test

In the preliminary test, the PRL was set up on a curling ice sheet, and a curling stone was launched multiple times. The goal of this test was to check to see if the device would work under the environmental conditions of the curling rink i.e. would the Rock Launcher throw a stone? Another purpose of this test was to investigate whether the mechanical and electrical components of the PRL would work as expected.

For the first try on the ice, the system was programmed to run the main motor with constant velocities i.e. if the operator wanted to launch the curling stone at a specific velocity (say "*v*"), the system would move the cradle mount at a constant velocity *v* for the whole launching process (this will be referred to as a "constant speed profile"). Generally, the control system of the dc motor is only controlling the input voltage of the motor to produce the desired angular velocity as the output. Once the voltage is set, based on the desired linear velocity, and the motor starts, the motor passes through two states, a transition state and a steady state. The acceleration of the motor occurs in the transition state and then the motor runs at a constant speed in its steady state. The period of the transition state of the dc motor depends on its coil resistance and its inductor. The transition state continues until the speed of the motor settles at the desired speed, and the transient state takes four to five times of the time constant (the time constant of a dc motor is equal to its inductor

divided by its resistance) ("TRANSIENT BEHAVIOUR – CURRENT SURGES (Motors And Drives)," 2021).

Observing the behavior of the stone during launching shows that the stone sticks to the ice when it is left on the ice even for a short period of time e.g. 1 to 2 seconds. An informal experiment on the ice illustrated that the force required to initially move the stone (to overcome the static friction) was approximately 10 times greater than the force required to keep the stone moving on the ice surface (to overcome the kinetic friction; see Appendix A.7 for more detail). Due to this initial stickiness between the stone and the ice, the PRL threw the stone inconsistently. The PRL kicked the stone ahead of the cradle mount as it initiated the stone's movement. This behavior made the engagement between the cradle mount and the stone inconsistent, and subsequently, the rotational motion of the stone was erratic.

To solve this issue, the main motor's Arduino Uno controller was reprogrammed. The Arduino with the new program was able to launch the stone using three different sets of speed profiles. In the first set, the motor starts with a constant relatively low speed, and after 1 second, the speed steps up to the preset linear speed. Figure 5.1 shows examples from this set of speed profiles. Note that 10% speed means the main (linear) motor's speed is 10% of its maximum speed. As such, from here on in, X% speed means X% of the motor's maximum speed. The nominal maximum speed of the main motor is 300 rpm or 1800 °/s which produces a linear speed of 1.26m/s for the curling stone. Therefore, percentages from 1% to 99% can produce linear speeds that can be calculated based on the 100% linear speed. For example, the motor moves the cradle mount for a total of approximately 2 seconds when a setting of 100% (1.26 m/s) is selected as the launching speed (see Figure 5.1) i.e. the motor moves the cradle mount at 10% (0.13 m/s) for 1 second and then steps up the speed to the preset linear speed for another second. So if the preset speed is 50% (0.63 m/s), the motor moves the cradle mount at 10% (0.13 m/s) for 1 second and then steps up the speed to 50% (0.63 m/s) and runs the cradle mount for approximately 3 more seconds to reach the end of the bridge.

It was expected that the bond between the ice and the stone would break in the first stage of this set of speed profiles without damaging the cradle, and in the second stage, the motor would accelerate the stone to the preset linear speed. Again, this acceleration would occur in the transition state of the motor. Once the stone reached the preset linear speed, the motor would run the cradle

mount at this speed until it reached the end of the bridge. Unfortunately, the responses of the stone to this first set of speed profiles were qualitatively similar to the set of constant speed profiles.

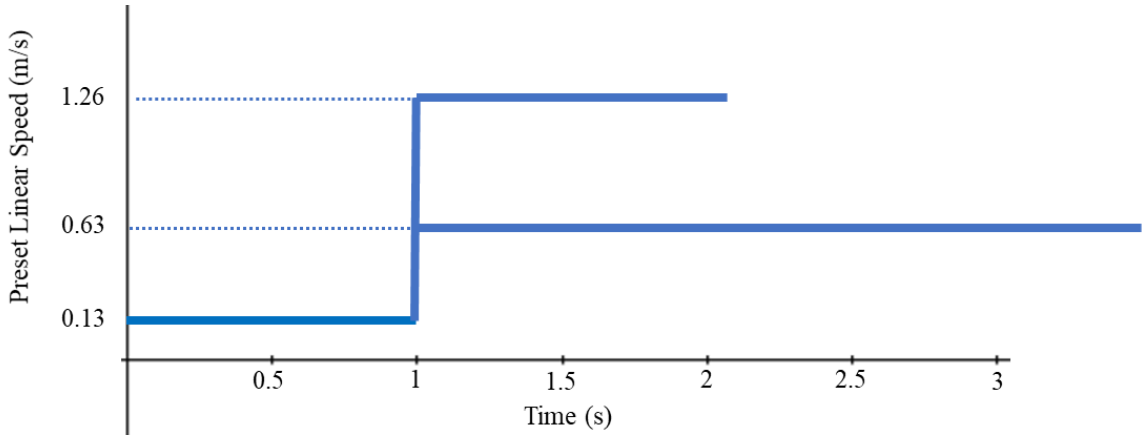

Figure 5.1: Two examples of the first set of speed profiles of the main motor.

The second set of speed profiles increased the speed of the motor at a constant rate. The acceleration of the motor in this profile is related to the preset speed. Figure 5.2 shows examples of this profile. In this profile, the acceleration of the motor when the preset speed is 100% (1.26m/s) is different than when the preset speed is 50% (0.63 m/s). Since only the voltage of the motor can be controlled and the voltage controls the output angular velocity, to create the acceleration the Arduino was programmed to increase the voltage in a constant increment at each time interval for each linear velocity. The voltage increment and the time interval are different for each linear velocity in this set of speed profiles. The programming of this set of profiles has been explained in Appendix A.2.2.2.

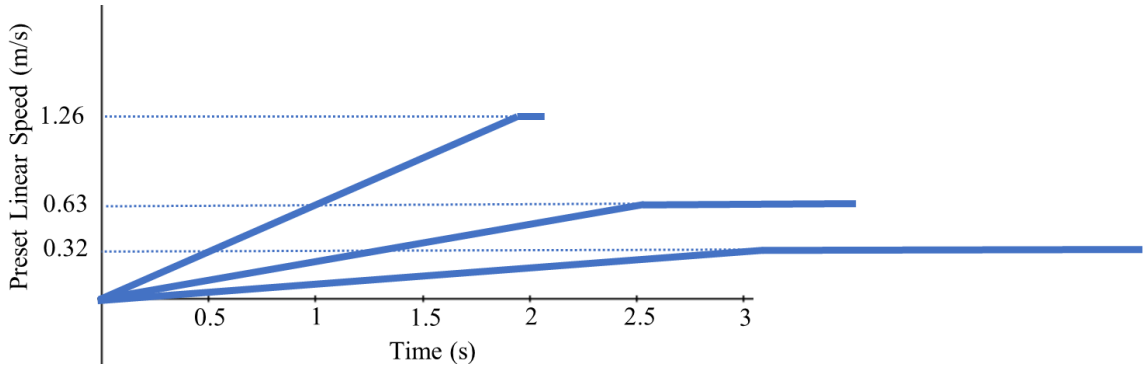

Figure 5.2: Three examples of the second set of speed profiles of the main motor.

Finally, the third set of speed profiles accelerated the stone with the same constant acceleration in all cases i.e. in this set of speed profiles, the angular velocity of the motor is

increased at a constant rate for all linear velocities until the target speeds are reached. Once the speed of the motor reaches the preset speed, the main motor rotates at the target speed. Figure 5.3 shows examples from this set of speed profiles. Based on preliminary tests with these profiles, at low speeds, there was no discernable difference in the performance of the PRL under the second and the third set of speed profiles. However, at high speeds, the performance of the PRL was more consistent with the third set of speed profiles. Therefore, the third set was utilized for the rest of the tests.

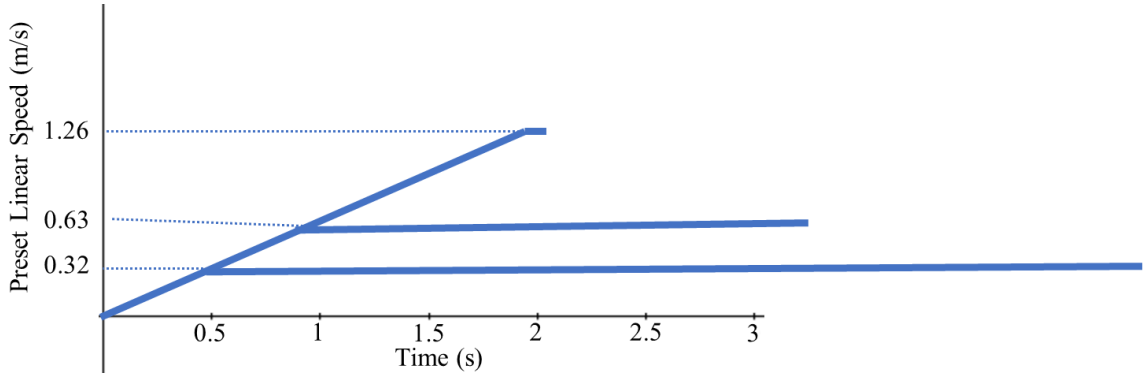

Figure 5.3: Three examples of the third set of speed profiles of the main motor.

5.2. Rotational Validation Test

In the first bank of validation tests, the rotational motion provided by the PRL was studied.

5.2.1. Objective and Hypothesis

This test aimed to validate the consistency of the rotational motion of the curling stone at release. It was anticipated that the standard deviation of the curling stone's rotational speed at release would meet the constraint i.e. it would be less than 1 °/s.

5.2.2. Methodology

To record the stone's rotational motion, an Android software application "RPM Speed and Wow" (Martignano, 2011) was utilized. This software was installed on a smartphone. The precision of this software is 0.1 rpm, or 0.6 °/s. Two sets of data can be recorded using this software; the first set includes the maximum, the average, and the minimum rotational speed, and the second set includes the speed-time graph, which shows the changes in the stone's rotational speed during a 10-seconds recording period. The smartphone was attached to the stone above its center of gravity during this test (see Figure 5.4).

Figure 5.4: The smartphone attached to the stone above stone's center of gravity.

The general procedure for this test had three steps. Before each trial, the running band was brushed off in a consistent manner. Next, the stone was moved into the cradle mount facing down the ice as per a typical throw from the house (the handle of the curling stone was pointing toward the hacks). At this point, the start button of the software displayed on the smartphone was pressed and simultaneously, the start switch of the PRL was turned on. Meanwhile, the main platform of the PRL was held to steady it. To use the PRL, the hacks on the curling ice sheet were replaced with two white plastic blocks. These two blocks are called hack bases or nylon blocks. These blocks replace the hacks during ice scraping to protect hacks from any damage ("Hacks," 2014). The main platforms of the PRL are designed to be installed on these plastic blocks. During the tests, there was a small gap between the leg structure and the plastic blocks attached to the hacks (roughly a 1-2 cm gap). Since the reaction force exerted on the cradle mount by the stone causes the main platform to slide backwards slightly on the ice, and this slide might cause inconsistency in the measurements, the main platform was held in place while launching the curling stone. Once the stone had been launched and had slid down the ice, it stopped. All of the data (the min, the max, the average rotational speed, and the speed-time graph) were recorded from the software on

the smartphone. The recorded graphs were processed using "GetData Graph Digitizer" ("Digitize graphs and plots - GetData Graph Digitizer - graph digitizing software," 2021). This software can extract points from a graph and save them in an Excel sheet. Also, during this set of rotational validation trials, the same stone was used every time, and the same ice sheet was used for launching the stone. This stone had a mass of 18.9 +/- 0.1 kg.

The target rotational speed (for high rotational speed) is the expected rotational speed calculated based on the maximum speed provided by the motor with respect to the required torque. The maximum speed of the rotational motor based on the required torque is 110 rpm or 660 °/s (discussed in Section 4.3). This produces a rotational speed of 83.0 °/s for the curling stone assuming no slipping occurs between the stone and the rotational motor's wheel. Three rotational speeds were determined for this validation testing. The target speeds for low rotational speed (one third of the high rotational speed) and mid rotational speed (two thirds of the high rotational speed) were calculated based on the high rotational speed. Thus, the motor rotated at 33% (27.7 °/s), 66% (55.4 °/s), and 100% (83.0 °/s) of its maximum speed at the low, mid, and high speed settings, respectively. The zero speed was when the motor did not rotate (it was locked) while the wheel attached to the other side of the cradle mount (the idler wheel) was free to rotate.

This rotational validation testing was divided into two parts: the first part was conducted at 0.85 m/s (70%) linear speed, and the second part at 1.04 m/s (85%) linear speed. The purpose of the first part was to refine the process of data collection. Thus, only the data collected in the second part was analyzed in detail. In the second part, the stone was launched 20 times. The trials were divided into five sets of four trials. The order of the four trials in a set was randomized between zero (0 °/s), low (27.7 °/s), mid (55.4 °/s), and high (83.0 °/s) settings. The direction of the rotational motion was set clockwise for the whole test and all throws were at an angle of 0 degrees to the center line. Also, during this test, the curling stone's release point didn't change i.e. the end leg never moved. The collected data in the first set showed evidence of noise that was due to the inconsistency of the procedure. Once the procedure was refined, the remaining sets were problem-free. Thus, the data of the four remaining sets (sets 2 to 5) are analyzed here.

To validate the consistency of the rotational motion that the device provides to the stone, the stone's rotational speed at release i.e. the stone's rotational speed once it leaves the cradle mount, was analyzed. The rotational speed of the stone at release can be extracted from the recorded graph for each trial. Figure 5.5 is an example of the graphs that the Android software

recorded. This graph shows that the software started to record the data a few milliseconds before the cradle mount started moving (the plot starts with zero rotational speed for a few milliseconds). Also, it is speculated that the fluctuation of the rotational speed between 0 and 2 seconds was due to intermittent traction between the rotational motor wheel and the stone. While the stone is travelling down the ice, the number of pebbles underneath the running band changes. The changes in the number of pebbles supporting the running band cause changes in the friction between the stone and the ice (Maeno, 2014). Therefore, the changes in the number of pebbles underneath the running band leads to oscillations in the stone's rotational speed by changing the frictional force between the stone's running band and the ice surface (this will be discussed further in the next chapter).

Based on the time versus linear preset speed plot presented in Figure 5.6, the stone with 85% linear speed leaves the cradle mount 2.6 seconds after the device starts. The relation between the main motor speed and time was obtained by running the device without a curling stone at 10 speed settings and recording the time the cradle mount needed to reach the end of the bridge. The speed settings for plotting this graph were 10-100%, in 10% increments. This graph was then utilized to estimate the time the stone takes to be released at the end of the bridge. The validity of this graph was investigated by timing the device while it was launching a curling stone. The timing was performed using a stopwatch. The investigation showed that the uncertainty of the estimation was approximately 0.2 seconds for 85% speed, which can be considered to be human variability since a stopwatch was used. The estimates of the time that the cradle mount takes to reach the end of the bridge was used to determine the curling stone's rotational speed at release using the graph recorded on the smartphone.

The software's start button was pressed manually, which increases the possibility of noise being introduced through human error. However, since the difference of the stone's rotational speed at release with and without consideration of these errors was roughly 1%, the error of the estimate was neglected and 2.6 seconds was used as the release time of the stone to extract the rotational speed of the stone upon release, from time versus linear preset speed graphs.

Prior to this test, the ice was scraped with 5 passes: 3 passes with a straight blade and 2 passes with an angle blade. The pebble preparation was done in two rounds. In the first one, the pebbles were prepared with a #76 fine pebble head with pebbling water at 56°F, and 46 seconds was the travel time. Travel time is the time that ice technicians travel from one end to another end

of the curling ice sheet while spraying water on the sheet (Hritzuk, 2020). In the second round, the pebbles were prepared with a #74 medium pebble head with pebbling water at 56°F (13.3°C), and 36 seconds was the travel time. The ice temperature was 22.4°F (-5.3°C) and the air humidity was 55%.

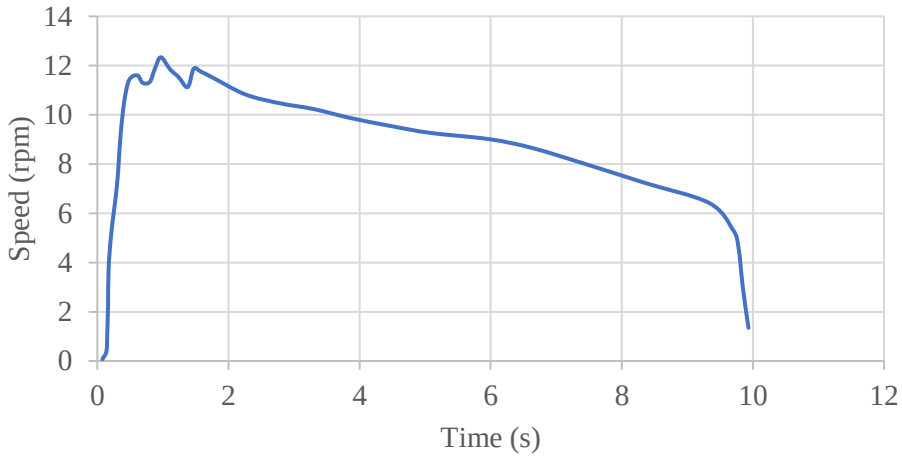

Figure 5.5: Rotational speed of the stone vs time graph for trial no.7 presented here as an example of the recorded graphs by "RPM Speed and Wow". The linear speed in this test is 85% and the corresponding release time is 2.6s.

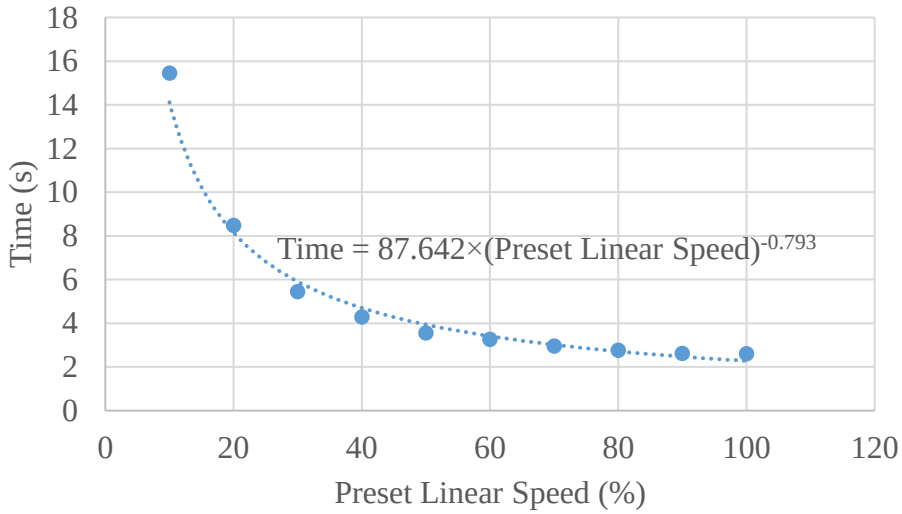

Figure 5.6: Time (s) vs preset linear speed (%) graph. The equation presented in this graph was used to estimate the time that the cradle mount takes to reach the end of the bridge. In this test, the preset linear speed used was 85%. The release time for 85% linear speed is 2.6s.

5.2.3. Results and Discussion

The four good sets of collected data are presented in Figure 5.7. The rotational speed of the stone at release for each selected preset rotational speed varied in a narrow range. For example, the rotational motor's low speed rotated the stone up to an angular speed between 18 and 20 °/s. Each data set's standard deviation and error values (differences between target speed and observed speed) are presented in Table 5.1. The error column represents the difference of the target rotational speed and the average actual rotational speed. The high target speed is the expected high rotational speed calculated based on the maximum speed provided by the motor with respect to the required torque and assuming no slipping occurs between the curling stone and the rotational motor's wheel. Then the other target speeds were calculated based on the high speed. The consistency (or repeatability) of the stone's rotational motion can be evaluated by looking at the standard deviation of the rotational speed at release. The constraint on the rotational speed discussed in Chapter 3 states that the rotational speed's standard deviation must be equal to or less than 1 °/s. The standard deviation at zero speed is less than 1 °/s, so it is acceptable. However, the rest of the rotational speeds at low, mid, and high settings have standard deviations greater than 1°/s (see Table 5.1). Therefore, the PRL could not meet the constraints on the rotational speed of the stone at release. The error percentage of the rotational speed decreases from low (27.7 °/s) speed to high (83.0 °/s) speed. In other words, the difference between the actual and expected rotational speed at higher rotational speeds is lower compared to the low rotational speeds, on a percentage basis.

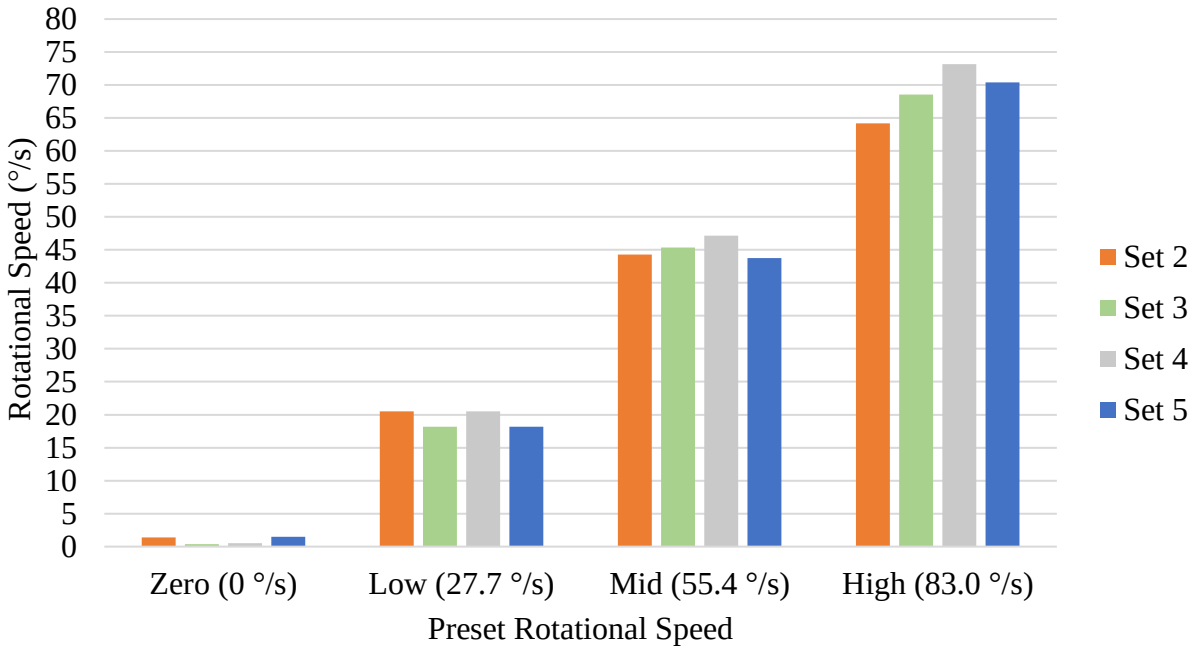

Figure 5.7: The rotational speed of the stone at release vs preset rotational speed. The data collected in the first set was corrupted, so the data of the four remaining sets (sets 2 to 5) are analyzed here. Each set refers to a group of trials of zero, low, mid,

Table 5.1: Analyzed data of the rotational speed of a stone at release. All the data presented in this table are in deg/sec.

Preset Rotational Speed (Target Rotational Speed)	Average	STD	Absolute Error	Error Percentage
Zero (0 °/s)	1.0	0.6	-1.0	-
Low (27.7 °/s)	19.4	1.4	8.3	30%
Mid (55.4 °/s)	43.3	1.5	12.1	22%
High (83.0 °/s)	69.9	3.8	13.1	16%

A curling stone at a higher rotational speed has greater angular momentum. In the equation $L = I\omega$, L is the angular momentum and I and ω are the moment of inertia and the rotational speed, respectively. The higher momentum of a stone with a higher speed causes the stone's motion to be less affected by the changes in the friction between the stone's running band and the ice. While the stone moves on the ice surface, due to the changes in the number of pebbles, the friction between the running band and ice changes (Maeno, 2014). The description discussed in this paragraph explains the lower errors at the higher rotational speeds of the curling stone at release.

Based on previous experiments on curling, the stone with no initial rotational speed might start to rotate at some point and continue to rotate (Shegelski & Lozowski, 2018). This can explain

why the stone at release developed some rotational motion even when the rotational speed setting of the PRL was set as zero.

5.2.4. More Data of Stone's Rotational Speed at Release

In the first scientific experiment (see Section 6.1), more data on rotational motion was gathered that provided more data for validation. The data in this experiment was gathered for low, mid, and high rotational speed, and was collected in three sets. In each set, the stone launched 18 times. The linear speeds of the stone for sets 1, 2, and 3 were 0.38 m/s (30%), 0.76 m/s (60%), and 1.26 m/s (100%), respectively. The procedure for gathering these data is similar to Section 5.1.2.1, except the stone was not launched at zero rotational speed. These data are presented in Tables 5.2 to 5.4. The third set of speed profiles (Figure 5.3) was used to perform this test.

Table 5.2: Analyzed data of the rotational speed of the stone at release for 30% linear speed. All the data presented in this table are in deg/sec.

Preset Rotational Speed (Target Rotational Speed)	Average	STD	Absolute Error	Error Percentages
Low (27.7 °/s)	9.3	6.8	18.5	67%
Mid (55.4 °/s)	31.9	6.6	23.5	42%
High (83.0 °/s)	55.9	5.0	27.1	33%

Table 5.3: Analyzed data of the rotational speed of the stone at release for 60% linear speed. All the data presented in this table are in deg/sec.

Preset Rotational Speed (Target Rotational Speed)	Average	STD	Absolute Error	Error Percentages
Low (27.7 °/s)	10.4	4.8	17.3	62%
Mid (55.4 °/s)	35.0	6.2	20.4	37%
High (83.0 °/s)	63.5	3.2	19.5	23%

Table 5.4: Analyzed data of the rotational speed of the stone at release for 100% linear speed. All the data presented in this table are in deg/sec.

Preset Rotational Speed (Target Rotational Speed)	Average	STD	Absolute Error	Error Percentages
Low (27.7 °/s)	11.0	6.0	16.7	60%
Mid (55.4 °/s)	34.3	7.8	21.1	38%
High (83.0 °/s)	65.3	3.4	17.7	21%

The data regarding the stone's rotational speed collected from the first scientific experiment seemed to be corrupted. An investigation of the rotational motor showed that a malfunction of the rotational motor might have caused this issue. Two possible issues might have caused this malfunction. The wheel of the rotational motor is attached to the motor's shaft by a set

screw. Based on the investigation after the experiment, this screw was loosened on the day of the experiment. Consequently, the shaft slipped inside the wheel's hole, so the wheel was not strong enough to rotate the curling stone. Another possibility for this malfunction was a loose wire in the rotational motor circuit. The rotational motor has many wires in its circuit as well as two switches. It is possible that the wire connecting the motor driver to the motor might have been loose, which caused the malfunction. Note that this experiment was actually the last one performed, out of all the experiments performed. There was no evidence of this data corruption in the earlier experiments. However, although these rotational speeds did not meet the specified constraints defined for this project, they can still be referred to as three different speed ranges to analyze them in the experimental section.

5.2.5. Conclusion

The consistency of the curling stone rotational speed at release was examined in this validation test. The PRL is able to launch the curling stone at different rotational speeds. However, the standard deviation of the stone rotational speed at release was not within the defined constraint range (below 1 °/s.).

5.3. Linear Validation Test

In the second bank of validation tests, the linear motion provided by the PRL was studied.

5.3.1. Objective and Hypothesis

This test aimed to validate the consistency of the linear motion of the curling stone at release. It was anticipated that the standard deviation of the curling stone's linear speed at release would meet the constraint i.e. it would be less than 0.1 m/s.

5.3.2. Methodology

The linear motion data were collected in four sets with five trials in each set. The collected data included the stone's linear speed at release, and the longitudinal and lateral distance travelled before stopping. In this bank of tests, the rotational speed was set to zero for all four sets, and the linear speeds were ordered randomly among 0.38 m/s (30%),0.57 m/s (45%),0.76 m/s (60%),1.01m/s (80%), and1.26 m/s (100%) of maximum speed. The third set of speed profiles (Figure 5.3) was used to perform this test. All throws were at an angle of 0 degrees to the center line and during this test the curling stone's release point did not change i.e. the end leg never moved. A Brower Timing System (BTS) was utilized to record the linear speed of the stone

(Brower Timing Systems, 2020). The BTS uses a pair of laser beams. The system shows the time that an object takes to travel between these two laser beams and its accuracy is 0.001 of a second. One laser beam was located on each side of the end legs (see Figure 5.8). The distance between these two laser beams was 12.4 +/- 0.2 cm. Also, one stone was used for all of the testing in this battery of validation tests. This stone had a mass of 18.9 +/- 0.1 kg.

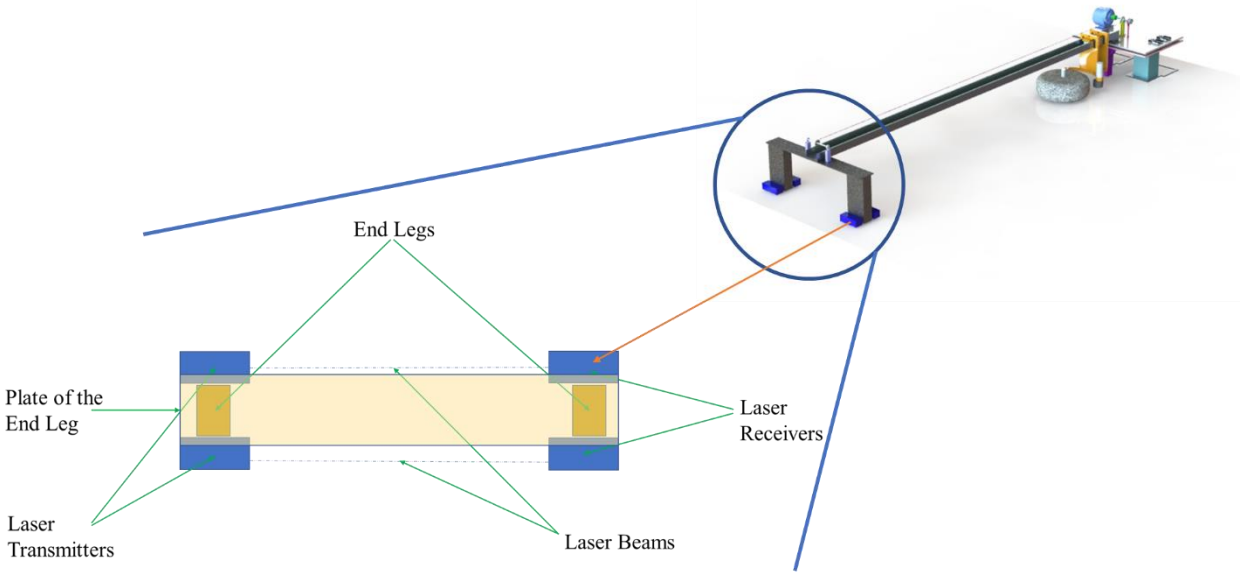

Figure 5.8: Top view of the configuration of the BTS.

In preparation for this set of tests, the ice sheet had been scraped with 5 passes: 3 passes with a straight blade and 2 passes with an angled blade. The pebble preparation was completed in two rounds. In the first one, the pebbles were prepared with a #76 fine pebble head with pebbling water at 56°F (13.3°C), and 46 seconds was the travel time. In the second round, the pebbles were prepared with a #74 medium pebble head with pebbling water at 56°F, and 36 seconds was the travel time. The ice temperature was 22.4°F (-5.3°C) and the air humidity was 55%.

For each trial in this set of tests, the stone was moved into the cradle mount with the handle in the orientation it would have for a real throw. Before each trial, the running band was brushed off in a consistent manner. Once the stone was moved into the cradle mount, the start button was pressed, and the PRL was held in place. After the stone stopped sliding down the ice, the time on the BST, as well as the longitudinal and lateral distance travelled by the stone, were recorded. The longitudinal distance that the stone travelled was read by a laser range finder with +/- 1.5 mm

resolution ("DEWALT Laser Distance Measurer, 165-ft | Canadian Tire," 2020). The datum for this measurement was the back line on the curling rink, with the back end of the range finder lined up with it. When the stone moved laterally, a block of foam aligned with the curling stone's trailing edge was placed on the centerline of the ice sheet to measure the longitudinal distance travelled (see Figure 5.9). The lateral distance travelled by the stone (to +/- 1 cm resolution) was recorded using a ruler or a tape measure to the nearest line located 0.5 cm in from the middle of the centerline (the centerline is a double line that has a 1 cm gap). After each trial, the BTS and the range finder were reset.

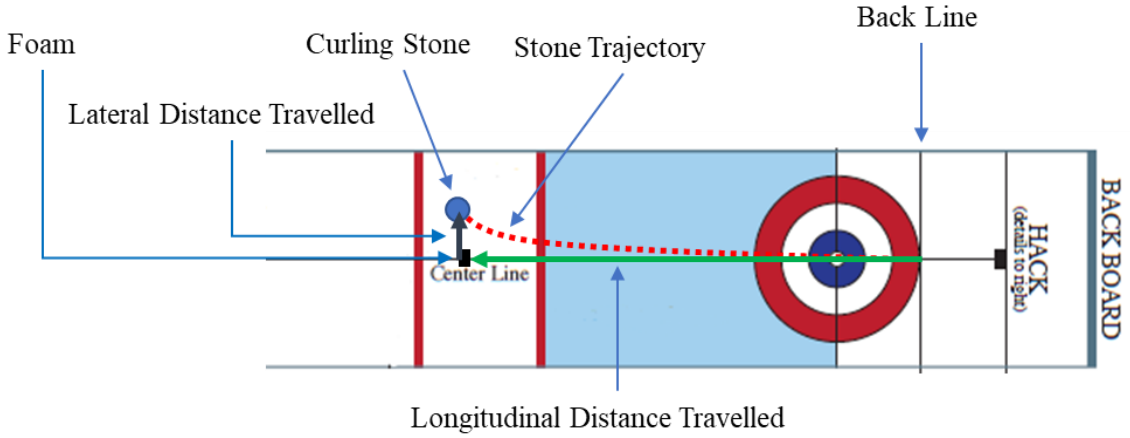

Figure 5.9: The configuration of data collection for longitudinal and lateral distance travelled.

5.3.3. Results and Discussion

The linear velocity validation testing results are shown in Figure 5.10 and Table 5.5. The consistency of the linear velocity provided by the PRL can be characterized by the standard deviations presented in Table 5.5. Figure 5.10 shows the stone's linear speed at release in four sets under different linear speed settings. This graph illustrates that the stone's linear speed at release for each preset linear speed is clearly in a different range. Table 5.5 shows the average and the standard deviation of the stone's linear speed at release. Based on the standard deviations reported here, the linear speed is sufficiently consistent. Previously, in Chapter 3, the objective and the constraint on the stone's linear speed at release were discussed. The respective constraint (discussed in section 3.5.2) explains that the standard deviation of the linear speed must be less than 0.1 m/s. Therefore, the PRL meets this constraint. The difference between the actual linear speed and the target (expected) linear speed is calculated and shown in the error column in this table. Recall that the target linear speed (for 100% linear speed) is the expected linear speed

calculated based on the maximum speed provided by the motor with respect to the required torque. The values of other target speeds were calculated based on the target speed at 100%. The absolute error values validate the design i.e. the actual linear speeds are adequately close to the expected values.

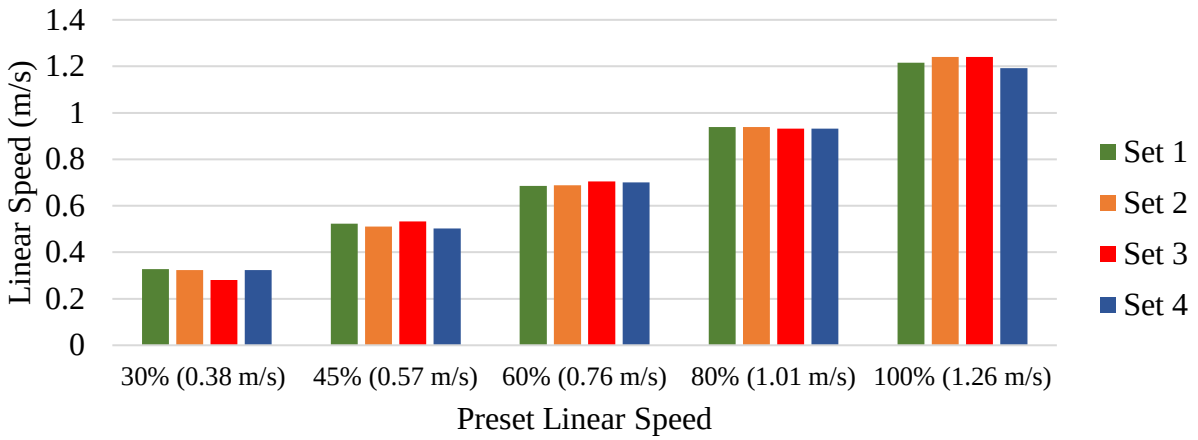

Figure 5.10: The linear speed of the stone at release. Each set refers to a group of trials of 30% (0.38 m/s), 45% (0.57 m/s), 60% (0.76 m/s), 80% (1.01 m/s), and 100% (1.26 m/s) linear speed. Different colors correspond to different sets of trials.

Table 5.5: Analyzed data of linear speed of the stone at release. All the data presented in this table are in m/s.

Preset Linear Speed (Target Linear Speed)	Average	STD	Absolute Error	Error Percentage
30% (0.38 m/s)	0.31	0.022	0.066	18%
45% (0.57 m/s)	0.52	0.013	0.053	9%
60% (0.76 m/s)	0.69	0.009	0.065	9%
80% (1.01 m/s)	0.94	0.004	0.074	7%
100% (1.26 m/s)	1.22	0.023	0.038	3%

A curling stone at a higher linear speed has greater linear momentum as compared to a slower moving stone. In the equation $p = mv$, p is the linear momentum, and m and v are the mass of the curling stone and the linear speed, respectively. The greater momentum of a faster moving stone causes the stone's motion to be proportionately less affected by changes in the friction between the stone's running band and the ice. The linear motion of the curling stone, like its rotational motion, is influenced by changes in friction between the stone's running band and the ice. Since the number of pebbles underneath the stone's running band changes from moment to moment, the friction between the stone and the ice changes too (Maeno, 2014). This can explain

the lower absolute differences between actual and expected speeds of the curling stone at release at the higher linear speeds. The error discussed in Table 5.5 is random error. The random error occurs due to small fluctuations in experimental conditions.

The systematic measurement uncertainty which arises from the limits of measurement precision and the calibration of measurements is also an important factor. The systematic uncertainty in speed measurements for this test is shown in Table 5.6.

Table 5.6: The systematic uncertainty of the linear speed measurement. All the data presented in this table are in m/s.

Linear Speed% (Target Linear Speed)	Average Speed	Systematic Uncertainty at 95% Confidence Level
30% (0.38 m/s)	0.31	±0.02
45% (0.57 m/s)	0.52	±0.03
60% (0.76 m/s)	0.69	±0.05
80% (1.01 m/s)	0.94	±0.07
100% (1.26 m/s)	1.22	±0.09

$$\delta \mathrm{v} = \sqrt{(\frac{1}{t}\delta x)^2 + (xt^{-2}\delta t)^2} \quad \text{.....(5.1)}$$

The uncertainty of the linear speed (δv) was calculated using equation 5.1. In this equation, t is time(s) which is the time that the curling stone takes to travel between two laser beams of the BTS and x is the distance between these laser beams. Also, δt and δx are the uncertainties of the time and distance measurement. The values of uncertainty at a 95% confidence level are presented in Table 5.6. In other words, 95% of the time, the real value will be within the uncertainty bounds for the measurements. The values presented as systematic uncertainty in this table are below 0.1 m/s, which is the consistency constraint. This means that the instruments used to determine the linear velocity were precise enough to investigate the consistency of the PRL.

5.3.4. Conclusion

The consistency of the curling stone's linear speed at release was examined in this validation test. The PRL is able to launch the curling stone at different linear speeds, and the standard deviation of the linear speed of the curling stone at release was as consistent as required i.e. it was below 0.1 m/s.

6. CURLING EXPERIMENTS

In this chapter, two experiments using the PRL are discussed, and their results are analyzed. The first experiment studies the influences of the rotational motion on the longitudinal and lateral distance that the stone travels and the relationships between these longitudinal and lateral distances are explained. The second experiment shows how small changes in the stone's mass may affect the stone's behavior.

6.1. The Effects of the Rotational Motion on the Behavior of the Stone

In the first experiment, the effects of the curling stone's rotational motion on its travelling distance were studied. Later in this section, how the lateral distance travelled by the curling stone correlates with its longitudinal distance travelled is also discussed.

6.1.1. Introduction

Since the investigation of curling stone behavior started almost a century ago, there has been a controversy among sport scientists. A group of them tried to explain that the rotational motion does not affect the stone's travelling distance (Jensen & Shegelski, 2004; Penner, 2001). They expressed that the lateral displacement of the curling stone is almost independent of its rotational speed. Meanwhile, other research showed that the stone's rotational motion influences the stone's travelling distance (Maeno, 2014; Maeno, 2016). Maeno (2014) expressed that a stone has greater lateral displacements at lower translational velocities and higher angular velocities. In the experiment described here, this matter is investigated and discussed. This experiment may help sport scientists better understand the behavior of the stone with different linear and rotational speeds. Furthermore, this experiment could help curling coaches understand which rotational motion can provide a greater lateral displacement of the stone.

6.1.2. Objective

In this test, the issue of whether the rotational motion of the curling stone has any influences on the lateral and longitudinal distances travelled by the curling stone was examined. Afterwards, the relation between the lateral and longitudinal distances travelled will be discussed.

6.1.3. Hypothesis

Based on the literature review, it was hypothesized that the curl of the curling stone is insensitive to the rotational speed of the curling stone. Also, it was hypothesized that the rotational motion does not affect the longitudinal distance travelled by the curling stone.

6.1.4. Methodology

6.1.4.1. Protocol

For this experiment, one stone with a mass of 18.9 +/- 0.1 kg was used for the whole experiment, and the area where the stone slid was "conditioned" by "dragging rocks". This involves passing a series of stones (eight stones) over an area multiple time (six times in this case). Conditioning ice means wearing the tops of the pebbles or "cutting the pebble" and making the tops of the pebbles even or smooth. This is also called making the ice 'mature' (Hritzuk, 2020). In preparation for this set of tests, the ice sheet had been scraped with 5 passes: 3 passes with a straight blade and 2 passes with an angled blade. The pebble preparation was completed in two rounds. In the first one, the pebbles were prepared with a #76 fine pebble head with pebbling water at 56°F (13.3°C), and 46 seconds was the travel time. Travel time is the time that ice technicians travel from one end to another end of the curling ice sheet while spraying water on the sheet (Hritzuk, 2020). In the second round, the pebbles were prepared with a #74 medium pebble head with pebbling water at 56°F, and 36 seconds was the travel time. The ice temperature was 22.4°F (-5.3°C) and the air humidity was 55%.

Before each trial, the running band was brushed off in a consistent manner. In each trial, once the stone was moved into the cradle mount with the handle in the orientation it would have for a real throw, the start button was pressed. Meanwhile, the PRL was held steady in place. After the stone stopped sliding down the ice, the longitudinal and lateral distances travelled by the stone were recorded. Afterwards, the range finder was reset. The testing for this experiment was done in six sets, and each set had nine trials. As such, a total of 54 trials was completed. The linear speed was set at either 30% (0.38 m/s), 60% (0.76 m/s), or 100% (1.26 m/s) for each set, and the rotational speed varied between low (27.7 °/s), mid (55.4 °/s), and high (83.0 °/s) as per the validation testing. The third set of speed profiles (see Figure 5.3) was used to perform this test. The direction of the rotational motion was set clockwise for all throws and all throws were at an angle of 0 degrees to the center line. Also, during this testing the curling stone's release point did not change i.e. the end

leg never moved. The nine combinations of the linear and rotational speeds in each set were randomly ordered. The data points collected in the first set were eliminated from the data analysis since the data collection procedure was not consistent (it was a "training set" for this experiment).

Recall that in the linear validation test of Chapter 5, the curling stone's longitudinal and lateral distances travelled were recorded. The rotational speed for that linear validation test was set to zero. Therefore, to provide an extra rotational speed data point in this experiment, the zero rotation data from the linear validation test was added to the data set collected in the current experimental test. The linear validation testing was done in four sets.

6.1.4.2. Equipment

The longitudinal distance that the stone travelled was read by a laser range finder with +/- 1.5 mm resolution ("DEWALT Laser Distance Measurer, 165-ft | Canadian Tire," 2020). The datum for this measurement was the back line on the curling rink, with the back end of the distance meter lined up with it. A ruler or a measuring tape was used to measure the stone's lateral distance travelled. When the stone moved laterally, a block of foam that was aligned with the curling stone's trailing edge was placed on the centerline of the ice sheet to measure the longitudinal distance travelled (see Figure 5.9). The lateral distance travelled was recorded using a ruler or a tape measure with +/- 1 cm resolution to the nearest line located 0.5 cm in from the middle of the centerline (the centerline is a double line that has a 1 cm gap).

6.1.4.3. Variables and Statistical Methods

In this experimental test, there were two independent variables: the stone's rotational speed at release and its linear speed at release. The stone's longitudinal distance travelled and the stone's lateral distance travelled were analyzed separately as the dependent variables. Since there were two independent variables for each dependent variable, to evaluate whether any differences in the collected data were significant, a factorial ANOVA test was performed and if any interactions were detected, separate one-way ANOVA tests were conducted. The alpha level for this statistical analysis is .05. In these statistical tests, according to the Levene's test results based on median, presented in Appendix A.17, equal variances was assumed and they are done under LSD ("IBM Docs," 2021).

6.1.5. Results and Discussion

Figure 6.1 shows the average of the lateral distance travelled by the stone with 100% (1.26m/s), 60% (0.76 m/s), or 30% (0.38 m/s) linear speeds with zero (0 °/s), low (27.7°/s or 1.92 turns per 25 seconds), mid (55.4 °/s or 3.85 turns per 25 seconds), or high rotational speeds (83.0°/s or 5.75 turns per 25 seconds). The results show that the lateral displacement of the curling stone first slightly grows with the stepping up of the rotational speed from zero to mid and then decreases at the high rotational speed. A spin of 27.7 °/s on the curling stone increases the lateral displacement by around 25 cm compared to the zero rotational speed (for 100% linear speed), and a spin of 83.0 °/s increases the lateral displacement of the curling stone by around 17 cm compared to the zero rotational speed (also for 100% linear speed).

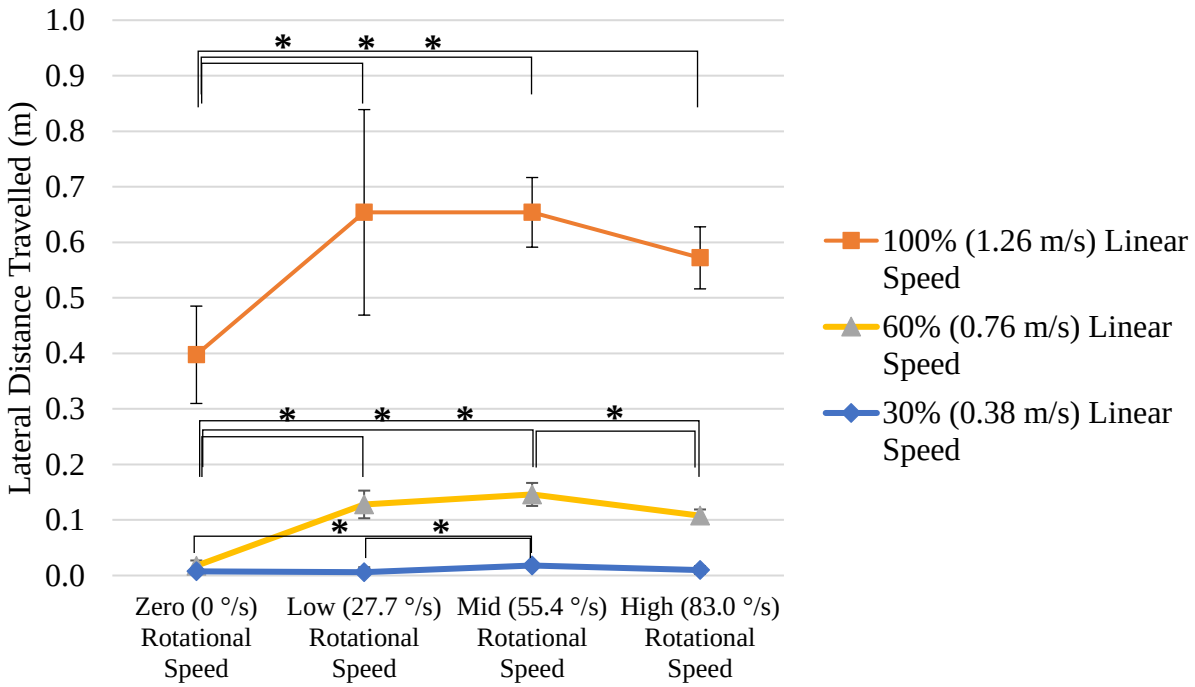

Figure 6.1: Average lateral distance travelled at different linear and rotational release velocities. The vertical lines on the points present the standard deviation of the lateral distance travelled. Asterisks (*) on the graph show the significant differences.

Table 6.1: Table of the values of Figure 6.1.

Linear Speed	Rotational Speed	Average Lateral Distance Travelled (m)
30% (0.38 m/s)	Zero (0 °/s)	0.01
	Low (27.7 °/s)	0.01
	Mid (55.4 °/s)	0.02
	High (83.0 °/s)	0.01
60% (0.76 m/s)	Zero (0 °/s)	0.02
	Low (27.7 °/s)	0.13
	Mid (55.4 °/s)	0.15
	High (83.0 °/s)	0.11
100% (1.26 m/s)	Zero (0 °/s)	0.40
	Low (27.7 °/s)	0.65
	Mid (55.4 °/s)	0.65
	High (83.0 °/s)	0.57

Figure 6.2 presents the average longitudinal distance travelled by the stone with 30% (0.38m/s), 60% (0.76 m/s), or 100% (1.26 m/s) linear speeds with zero (0 °/s), low (27.7 °/s or 1.92 turns per 25 seconds), mid (55.4°/s or 3.85 turns per 25 seconds), or high rotational speeds (83.0°/s or 5.75 turns per 25 seconds). The only noticeable change in the longitudinal distance travelled by the stone is at 100% (1.26 m/s) linear speed. At this linear speed, increasing the stone's rotational speed from zero (0 °/s) to low (27.7 °/s) seems to cause a one-meter increase in the longitudinal distance travelled. Also, a slight increase can be observed at 60% (0.76 m/s) linear speed going from zero (0 °/s) to low (27.7 °/s) rotational speed.

It is important to note that the PRL is only able to launch the curling stone up to a maximum of 9 m which is not the distance that the curling stone travels during typical curling. In typical curling a stone may travel up to 37 m. So, while the results here are valid over the ranges of distances travelled (0-9 m), caution should be exercised in extrapolating them to the 20-40 m range.

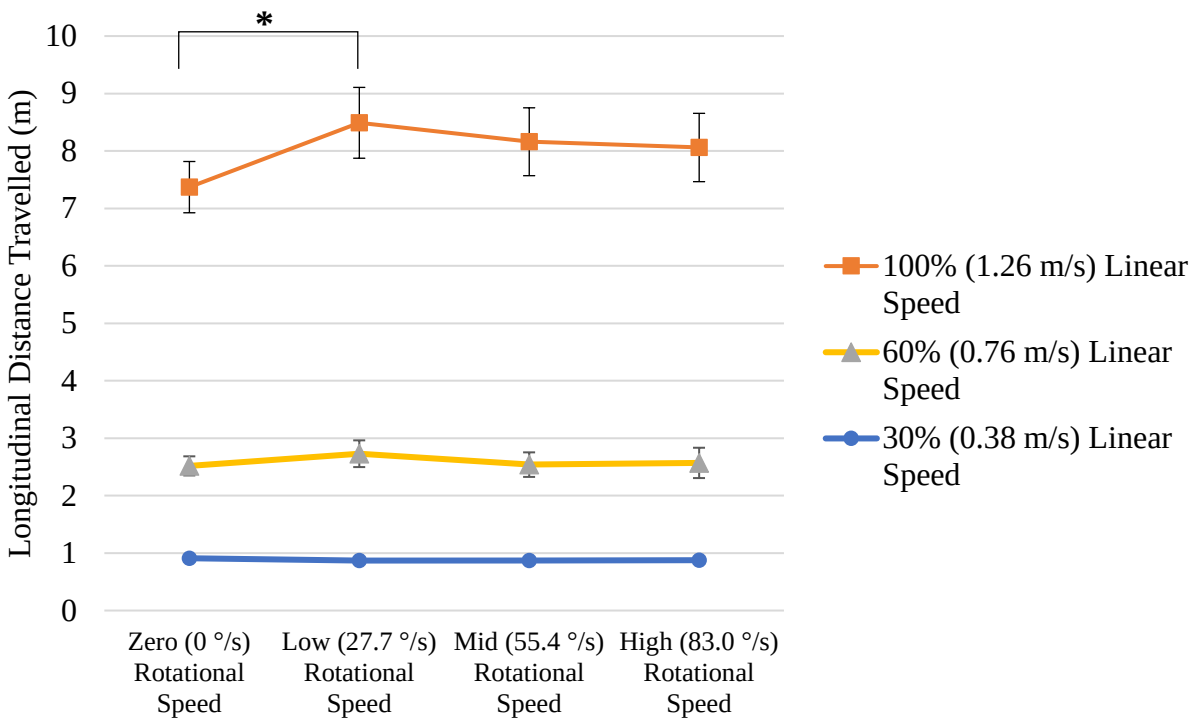

Figure 6.2: Average longitudinal distance travelled at different linear and rotational release velocities. The vertical lines on the points present the standard deviation of the lateral distance travelled. Asterisks (*) on the graph show the significant differences.

Table 6.2: Table of the values of Figure 6.2.

Linear Speed	Rotational Speed	Average Longitudinal Distance Travelled (m)
30% (0.38 m/s)	Zero (0 °/s)	0.91
	Low (27.7 °/s)	0.87
	Mid (55.4 °/s)	0.87
	High (83.0 °/s)	0.88
60% (0.76 m/s)	Zero (0 °/s)	2.52
	Low (27.7 °/s)	2.73
	Mid (55.4 °/s)	2.54
	High (83.0 °/s)	2.57
100% (1.26 m/s)	Zero (0 °/s)	7.37
	Low (27.7 °/s)	8.49
	Mid (55.4 °/s)	8.16
	High (83.0 °/s)	8.06

To evaluate whether the differences presented in Figures 6.1 and 6.2 are statistically significant, a factorial ANOVA test was performed and if any interactions were detected, separate one-way ANOVA tests were conducted.

A factorial ANOVA was performed to compare the main effects of the linear and rotational speed and the interaction effect between the linear and rotational speed on the lateral distance

travelled by the curling stone. The results of the factorial ANOVA test show that the interaction of linear and rotational speed is present ($F(6,45) = 3.55$, $p = 0.006$). So, the one-way ANOVA tests were utilized to find out if there was any significant difference between the average data of each setting. The results of the one-way ANOVA tests illustrate that the differences in the lateral distances travelled at 100% linear speed are only significant between zero and other rotational speeds (zero-low has an F ratio of $F(3,15) = 5.00$, $p = .004$, zero-mid has an F ratio of $F(3,15) = 5.00$, $p = .004$, and zero-high has an F ratio of $F(3,15) = 5.00$, $p = .035$). The means and standard deviations for the 100% linear speed data sets included zero ($M = 0.40$, $SD = 0.09$), low ($M = 0.65$, $SD = 0.19$), mid ($M = 0.65$, $SD = 0.06$), and high ($M = 0.57$, $SD = 0.06$).

The differences between the lateral distances travelled at 60% linear speed are significant between zero and other rotational speeds and between mid and high rotational speed (zero-low has an F ratio of $F(3,15) = 42.09$, $p < .001$, zero-mid has an F ratio of $F(3,15) = 42.09$, $p < .001$, zero-high has an F ratio of $F(3,15) = 42.09$, $p < .001$, and mid-high has an F ratio of $F(3,15) = 42.09$, $p = .005$). The means and standard deviations for the 60% linear speed data sets included zero ($M = 0.02$, $SD = 0.01$), low ($M = 0.13$, $SD = 0.02$), mid ($M = 0.15$, $SD = 0.02$), and high ($M = 0.11$, $SD = 0.01$). The differences between the lateral distances travelled at 30% linear speed are significant between the mid and zero rotational speed and between the mid and low rotational speed (mid-zero has an F ratio of $F(3,15) = 3.11$, $p = 0.034$, and mid-low has an F ratio of $F(3,15) = 3.11$, $p = 0.013$). The means and standard deviations for the 30% linear speed data sets included zero ($M = 0.01$, $SD = 0.01$), low ($M = 0.01$, $SD = 0.01$), and mid ($M = 0.02$, $SD = 0.004$). Therefore, the stone's lateral distance travelled is likely to be insensitive to the stone's rotational speed at 1.26 m/s linear speed and the rotational speed range of 27.7 to 83.0 °/s. Furthermore, the difference of lateral distance travelled between linear speeds at each rotational speed are significant except between 30% ($M = 0.01$, $SD = 0.01$), and 60% ($M = 0.02$, $SD = 0.01$) linear speed at zero rotation which has an F ratio of $F(2,9) = 75.97$, $p = .34$. Identical tests were done on longitudinal distance travelled, and their results discussed in the following paragraph.

A factorial ANOVA was conducted to compare the main effects of the linear and rotational speed and the interaction effect between the linear and rotational speed on longitudinal distance travelled by the curling stone. The factorial ANOVA test for longitudinal distance travelled shows that the interaction between the linear and rotational speed is present ($F(6,45) = 2.35$, $p = 0.047$). So, the next step is the one-way ANOVA tests. Based on the one-way ANOVA tests results, the

differences in the longitudinal distances travelled at 100% is only significant between zero rotational speed (M = 7.37, SD = 0.45) and low rotational speed (M = 8.49, SD = 0.62) which yielded to an F ratio of F (3,15) = 2.93, p = 0.01. Other than that, differences were not significant. The differences in the longitudinal distances travelled at 60% and at 30% linear speed between each rotational speed are not significant. Therefore, the curling stone's initial rotational speed has no significant effects on the longitudinal distance travelled by the curling stone over linear and rotational speed ranges of 0.38 to 1.26 m/s and 28.7 to 83.0 °/s. However, not surprisingly, the differences in longitudinal distances travelled between linear speeds at each rotational speed are significant.

Figure 6.3 shows the lateral vs longitudinal distances travelled by the curling stone in a different format. In each clump of points, all four rotation speeds are represented. This figure clearly shows that the lateral distance travelled correlates with the longitudinal distance travelled by the curling stone. In other words, a stone with higher initial linear speed runs on the ice for a longer duration and therefore has more time to curl. Thus, a curling stone with a higher initial linear speed has a greater lateral displacement.

The R-squared values for each linear regression line (one per rotational speed) are presented in Figure 6.3. However, the linear regression lines presented in this figure are not the best fit regressions for the zero and low rotational speed cases i.e. they seem to be under-fitting. Therefore, to improve the model to better fit the data points, a high order model is used as is shown in Figure 6.4.

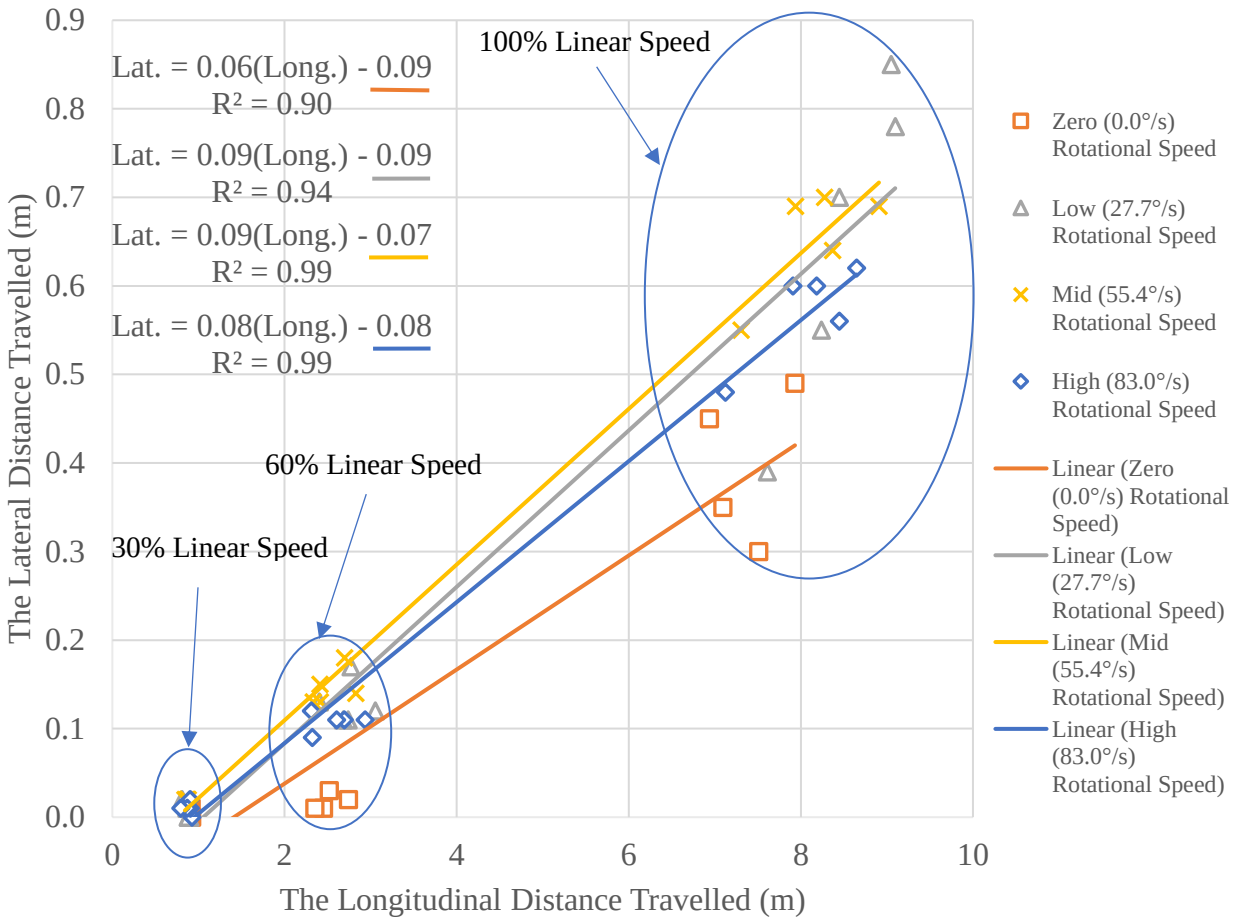

Figure 6.3: The lateral vs the longitudinal distance travelled of the curling stone. The linear regression lines and their equations, as well as the R-squared values, are presented for each rotational speed. The points in each oval have the same linear speed. Different shapes correspond to different rotational speed.

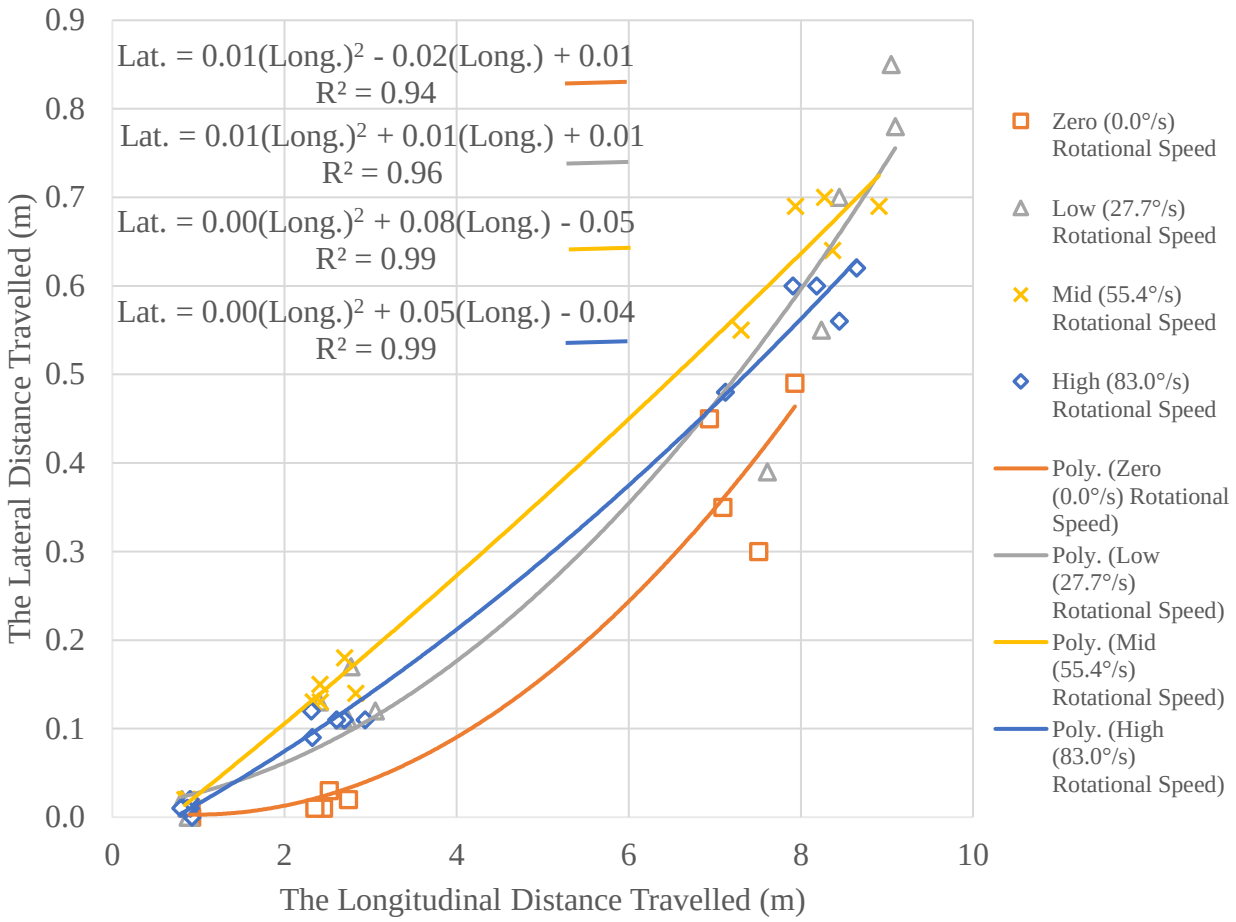

Figure 6.4: The lateral vs the longitudinal distance travelled of the curling stone. The second-order polynomial regression lines and their equations as well as the R-squared values are presented for each rotational speed. Different shapes correspond to different rotational speed.

Figure 6.4 shows that the R-squared values for the zero and low rotational speed improved with the second order polynomial regression. However, the R-squared values of the mid and high rotational speed did not change. Also, although the regression lines for the mid and high rotational speed are polynomial second order in Figure 6.4, these two regression lines are close to linear regression (see yellow and blue lines in Figure 6.4 compared to Figure 6.5). Furthermore, the regression line of the zero rotational speed is curvier compared to the regression line of the low rotational speed. This might be a clue to find the relationship between the lateral and longitudinal distances travelled. It would appear that the relationship between the lateral and longitudinal distances travelled becomes more linear by increasing the rotational speed up to 83.0 °/s rotational speed. Further investigation and more data are required for a more comprehensive conclusion.

In this experiment, the direction of the curling stone's curl was always toward the right side of the centerline. This is because the direction of the rotational motion was set clockwise for the whole experiment. Also, the curl direction of the stone released at zero rotation was still to the right side of the centerline, which might be explained by the scratch-guide mechanism introduced by Nyberg (Nyberg et al., 2013). Since the previous throws had a clockwise rotational motion, the scratches produced by the previous throws may guide the stone to the right side of the centerline, even with an initial zero rotational motion.

Compared to the other discussed results presented by Maeno (2016), Jensen and Shegelski (2004), Denny (2002), and Penner (2001), the data collected using PRL might be more reliable since the PRL launched the curling stone at the same place each time, and it has more consistency in launching the curling stone. However, the range of the linear speeds of the PRL used to perform these experiments in this project was lower than the speeds they used, and extrapolation to their ranges of speeds would be risky.

The summation of the longitudinal distances travelled over all of the trials, at the low (27.7°/s), mid (55.4 °/s), and high (83.0 °/s) rotational speeds, for each linear speed, is illustrated in Figure 6.5. The total longitudinal distance travelled diminishes from set 2 to set 6. As noted, this test was done following the ice conditioning.

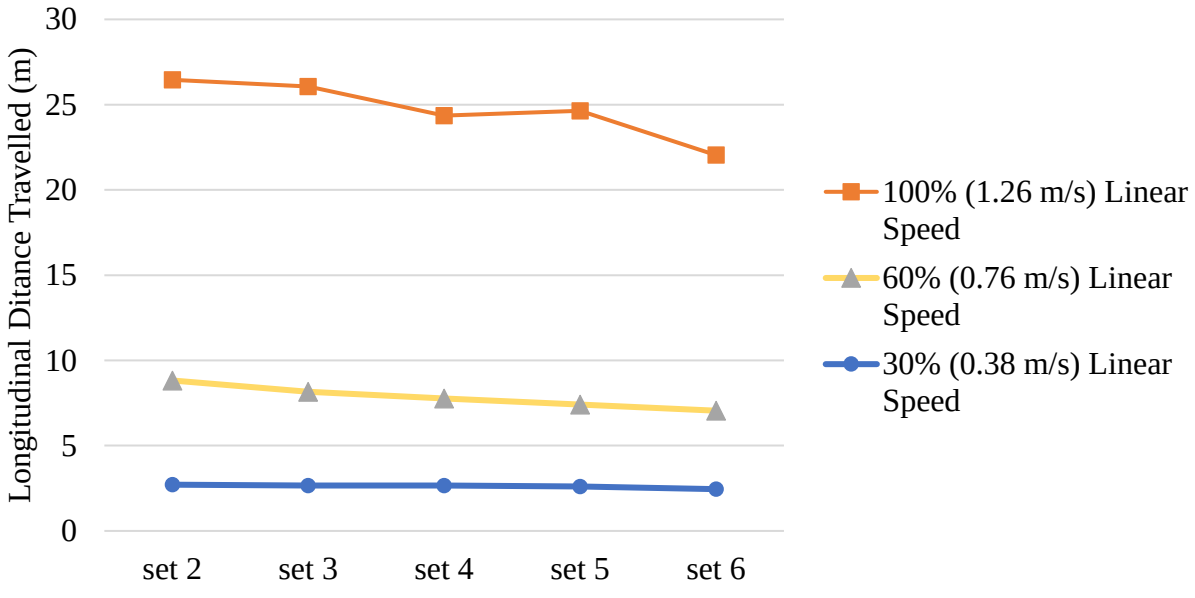

Figure 6.5: Summation of longitudinal distances travelled across low, mid, and high rotational velocities for each linear velocity.

The friction between the curling stone's running band and the top of the pebbles wears the top of the pebbles. Thus, the pebbles are eroded by the curling stone while it is passing over them. Since the pebbles have a conical shape, each time the stone erodes the tops of the pebbles, the stone will contact more surface on its next run (Nyberg et al., 2013, see their Figure 6). Maeno (2014) showed that the higher density (or population density) of pebbles reduces the longitudinal distance travelled by the stone at 2 m/s linear speed and 1.5 rad/s (86 °/s) rotational speed. He explained that since the higher pebble density leads to a higher friction between the running band and the ice, the stone travels less longitudinally on the ice with a greater number of pebbles. Also, he determined the friction coefficient at different linear speeds and at different pebbles densities; the friction coefficient increases with the increasing of the pebble density almost independent of the stone's linear speed (the rotational speed is 1.5 rad/s in his experiment). A higher density of pebbles means that in each instant, the stone's running band area is in contact with more pebbles—the more contact area with ice, the more frictional force on the curling stone. Therefore, a general reduction can be seen in the longitudinal distance travelled by the curling stone after each set in Figure 6.5. A stone with higher speed would run on ice for more time, which increases the time that the frictional force acts on the curling stone. So, more reduction from set 2 to set 6 occurs at a higher initial speed in Figure 6.5. The dependency of the frictional force on the area of contact may show that the friction between the curling stone and ice is not dry friction i.e. it is rejected by Amontons' Second Law in dry friction which explains that the frictional force is independent of the area of contact.

Illustrating just how unclear these issues can be, Lozowski et al. (2015) derived a thermodynamic model to explain the behavior of the curling stone on ice. In this model, the friction coefficient between the stone and the ice decreased with increasing contact area between the stone's running band and the pebbles.

Curlers believe that the longitudinal distance travelled by a stone first increases in the early ends of a game, then stabilizes for a few ends of play, and then decreases as the game progresses (Hritzuk, 2020). Hritzuk (2020) explained that after the first stone is thrown in the game and smooths off the pebbles, the succeeding curling stones travel more longitudinally, but only to a certain point. This point depends on different variables such as the ice temperature, the air temperature, the humidity level, the size of pebbles, the density of pebbles, etc. After reaching this point, the stone's longitudinal distance travelled remains constant for a few ends. Then, in the latter

part of the game, the pebbles wear down. Due to the higher contact area between the stone's running band and the ice, and consequently higher frictional forces, the stone's longitudinal distance travelled decreases (Hritzuk, 2020). Figure 6.5 clearly shows that the curling stone travels less far longitudinally after each set of the experiment. In the experiments performed using the PRL, before the testing began the ice was conditioned (see Section 6.1.2.1). In other words, the ice was mature in these experiments. Therefore, one could argue that the initial increment followed by the plateau of the stone's longitudinal travel evolution was eliminated.

6.1.6. Conclusion

The rotational motion of the curling stone has effects on its lateral distance travelled, comparing zero rotation to other rotational speeds. However, once the stone has rotational speed over the range of 27.7 °/s to 83.0 °/s, the change in rotational motion does not affect the stone's Longitudinal distance travelled. Also, the stone's rotational motion has virtually no effect on the curl at 1.26 m/s over the range of 27.7 °/s to 83.0 °/s. Moreover, there is a correlation between the longitudinal and lateral distance travelled. This correlation becomes more linear by increasing the rotational speed over a range of 0.38 to 1.26 m/s linear speed and 0 to 83 °/s rotational speed. Furthermore, the analyzed data showed that the curling stone travels less longitudinally after each throw following ice conditioning.

6.2. Effect of Stone Mass on Its Longitudinal Distance Travelled

The second experiment studied the influences of small changes in the curling stone's mass on its sliding behavior.

6.2.1. Introduction

In each curling ice sheet, 16 stones are using for curling. These curling stones have slightly different masses. Based on the literature, the mass of the curling stones varies between 17 and 20 kg (Lozowski et al., 2015). The mass of the curling stone is one of the contributing factors in friction. However, no researchers have investigated the effects of small changes in a curling stone's mass on its behavior. In this experiment, the effects of a minor variation of the mass of a curling stone on its longitudinal distance travelled were investigated. Characterizing this situation would help scientists have a better understanding of the behavior of a curling stone.

6.2.2. Objective

The effects of a slight change in a curling stone's mass on its longitudinal distance travelled was examined.

6.2.3. Hypothesis

Based on the fact that higher momentum can cause the curling stone to travel further, it was hypothesized that the longitudinal distance travelled by the curling stone will increase if the curling stone's mass is increased.

6.2.4. Methodology

6.2.4.1. Protocol and Equipment

For this experiment, one stone was used for all of the testing. It was the same stone as the one used in the first experiment. This stone had a mass of 18.9 +/- 0.1 kg. Since the mass of a curling stone varies between 17 and 20 kg, a 360 +/- 1 g weight was utilized to make a weight difference. The mass was chosen for its appropriate value and for its convenient installation on the stone. This test had four sets, and each set had five trials. The rotational speed was set at zero, and for each trial in a set, the linear speed was ordered randomly among 30% (0.38 m/s), 45% (0.57m/s), 60% (0.76 m/s), 80% (1.01 m/s), and 100% (1.26 m/s). All throws were at an angle of 0 degrees to the center line and during this experiment the curling stone's release point did not change i.e. the end leg never moved. The 360 g weight was centered on the center of gravity of the stone in every other set. So, two sets were conducted with the weight, and two were conducted without. Before the experiment, the ice sheet area where the stones would slide was conditioned with 10 passes of a series of rocks (eight rocks).

As in the previous tests, the ice sheet had been scraped with 5 passes: 3 passes with a straight blade and 2 passes with an angled blade. The pebble preparation was completed in two rounds. In the first one, the pebbles were prepared with a #76 fine pebble head with pebbling water at 56°F, and 46 seconds was the travel time. Travel time is the time that ice technicians travel from one end to another end of the curling ice sheet while spraying water on the sheet (Hritzuk, 2020). In the second round, the pebbles were prepared with a #74 medium pebble head with pebbling water at 56°F, and 36 seconds was the travel time. The ice temperature was 22.4°F and the air humidity was 55%.In each trial, the stone's running band was brushed off, and then the stone was moved into the cradle mount with the handle in the orientation for a real throw. The start button

was pushed, and the PRL was held steady in place. The linear speed of the stone upon release was read using the BTS, as was done in Chapter 5. The distance between the BTS' two laser beams was 12.4 +/- 0.2 cm. After the stone stopped sliding down the ice, the time on the BTS, as well as the longitudinal and lateral distances travelled by the stone, were recorded. The longitudinal distance that the stone travelled was read by a laser range finder with +/- 1.5 mm accuracy ("DEWALT Laser Distance Measurer, 165-ft | Canadian Tire," 2020). The datum for this measurement was the back line on the curling rink, with the back end of the range finder lined up with it. Afterwards, the BTS and the range finder were reset.

In this experiment, the stone's linear speed with and without the weight was measured to ensure that the device was able to launch both at the same linear speed each time. Figure 6.6 shows the comparison of the stone's linear release speed with and without the weight. This figure clearly shows that the linear speed of the stone, with and without the weight, for each preset linear speed, varied randomly in a small range. Table 6.3 illustrates the average linear speed with and without the weight. Based on the presented data, the device was sufficiently consistent in launching the stone with and without the weight to assume that the presence of the weight made no systematic difference in release speed.

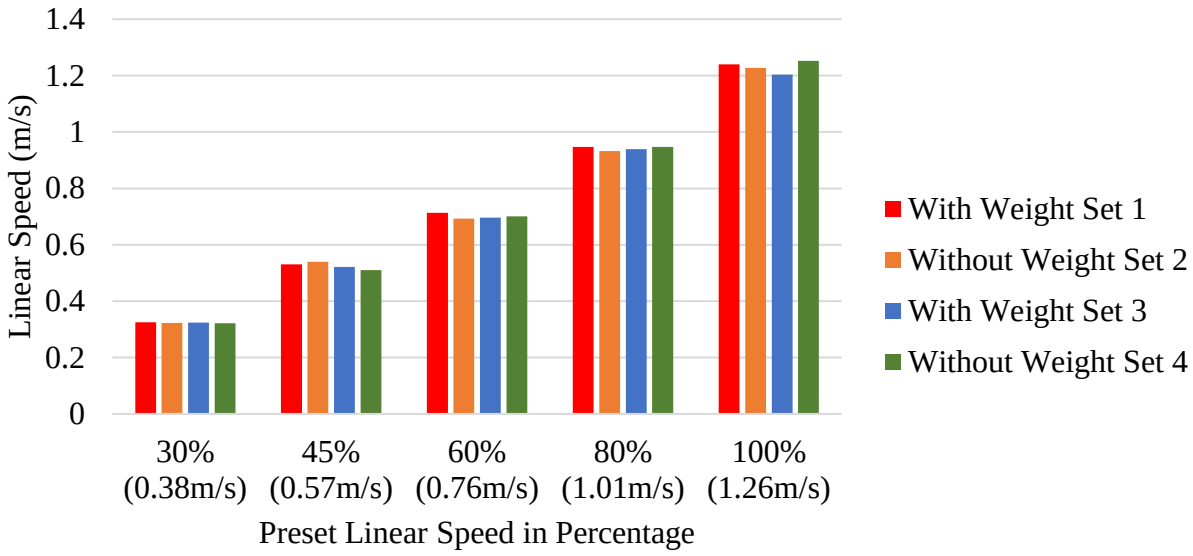

Figure 6.6: Linear speed of the stone with and without weight at release. Each set refers to a group of trials of 30% (0.38 m/s), 45% (0.57 m/s), 60% (0.76 m/s), 80% (1.01 m/s), and 100% (1.26 m/s) linear speed. Different colors correspond to different sets.

Table 6.3: The analyzed data of the stone's initial linear speed with and without weight.

Preset Linear Speed (%)	W/Wo Weight	Average of Linear Speed(m/s)	Standard Deviation(m/s)
30	With	0.32	0.00
	Without	0.32	0.00
45	With	0.52	0.02
	Without	0.53	0.01
60	With	0.70	0.01
	Without	0.70	0.01
80	With	0.94	0.01
	Without	0.94	0.01
100	With	1.24	0.02
	Without	1.22	0.03

6.2.4.2. Variables

The variables in this experiment were the initial linear speed of the curling stone as an independent variable, and the longitudinal distance travelled by the stone as a dependent variable.

6.2.5. Results and Discussion

Since the stone's linear speed with and without the weight at release was sufficiently consistent, the behavior of the stone when it was launched with and without the extra weight mounted on it could be reliably compared. Figure 6.7 presents the results of this testing.

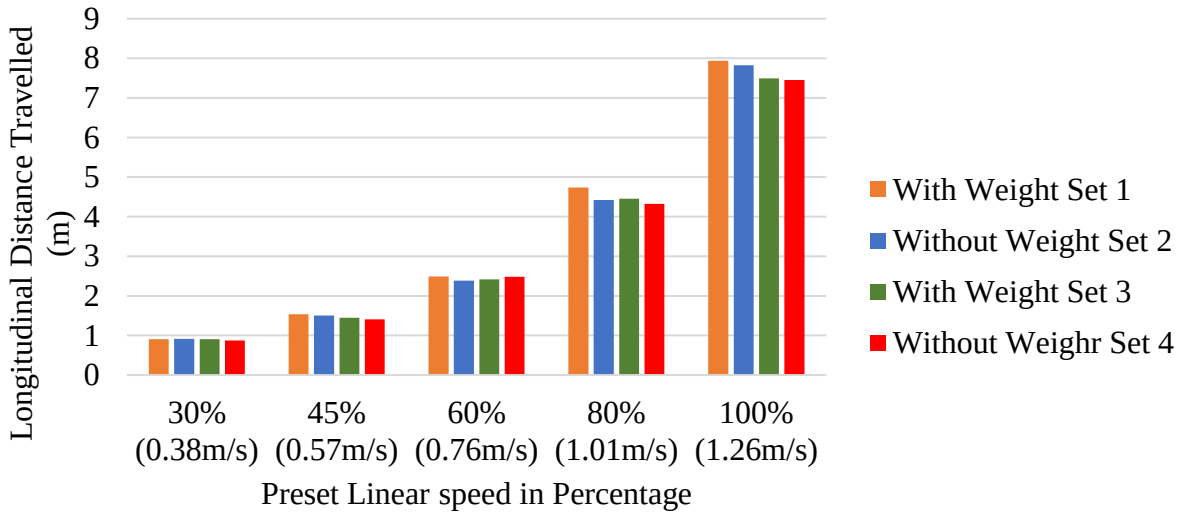

Figure 6.7: Longitudinal distance travelled with and without the weight. Each set refers to a group of trials of 30% (0.38 m/s), 45% (0.57 m/s), 60% (0.76 m/s), 80% (1.01 m/s), and 100% (1.26 m/s) linear speed Different colors correspond to different sets.

The difference in travelling distance is a factor that curlers need to understand. Before a match, curlers typically release the stone a few times to distinguish the stones in terms of their travelling distance under identical linear and rotational speeds. Higher mass causes higher momentum and kinetic energy for a given release speed, which may cause the stone to travel further. The situation is not this simple, though. Note that the longitudinal distance travelled shown in Figure 6.7 from set 1 to set 4 generally decreases, which can be also partly explained by the effect of increasing the frictional force between the stone and the ice (the erosion of the pebbles after each throw).

In this experiment (Figure 6.7), the order of the sets was mistakenly arranged so that it was not possible to determine which of the discussed factors (the extra weight, the erosion of the pebbles after each throw, or both) caused the stone to travel less far, longitudinally. For example, at 100% linear speed from set 1 to set 2, a reduction in the stone's longitudinal distance travelled can be seen. This reduction might be caused by travelling without extra weight or it might be caused by the increasing friction between the stone and the ice surface. This experiment needs to be redone, and the variables should be arranged randomly so it will be possible to examine the effects of the extra weight and the erosion of the pebbles after each throw on the stone's behavior distinctly.

6.2.6. Conclusion

Since the effects of the erosion of the pebbles after each throw and the extra weight were combined, the data collected was confounded. This experiment should be redone with a more randomized protocol.

6.3. Summary of Conclusions

The results presented in this chapter show that over the range of 0.38 to 1.26 m/s linear speed and 0 to 83 °/s rotational speed for a stone at release, the lateral distance travelled correlates with the longitudinal distance travelled. The analysis of the data also shows that the relation between the lateral and longitudinal distance travelled becomes more linear by increasing the rotational speed in this range. Moreover, the stone travels less longitudinally after each throw following ice conditioning. The data collected in the second experiment that looked at the effects of small changes in the mass of a stone, was confounded. This second experiment should be redone with a more appropriate protocol now that the two confounding factors of stone mass and ice condition have been recognized.

7. CONCLUSIONS AND RECOMMENDATIONS

7.1. Conclusions

In the presented dissertation, a device was designed to launch a curling stone at preset linear and rotational velocities at a preset angle to the long axis of the ice sheet. A prototype of the designed device was fabricated, and four sets of tests were performed using it. These tests include validation tests and experimental tests.

The prototype of the designed device illustrated whether the designs of different components of the device were acceptable. The open-loop control system that controls two motors worked well for an open-loop system. It can control the starts and stops of the main motor and rotational motor. Also, it is able to carry out the different acceleration profiles on the linear motion of the curling stone. The control system can read the signals from the switches and accordingly control the motor drivers. It also runs the motors at the preset speeds.

In the prototype, the power of the main motor and the power transmission system was designed to linearly accelerate the curling stone to 50% of the curling stone's speed in typical curling, and the prototype successfully did that. The prototype's rotational system can also rotate a curling stone up to 50% of the stone's maximum rotational speed in typical curling.

The main platform was able to support the weight of the components, and it was stable. The bridge could support the linear bearing, the chain, and the cradle mount. The end leg also has a solid design. The power transmission system has sufficient strength to support the motion of the cradle mount. The cradle mount can move the curling stone linearly down the ice. However, in terms of the rotational motion, the cradle mount needs some modifications since it could not meet the performance constraints. The rotational motor on the cradle mount should be relocated in order to have more normal force between the curling stone and the rotational motor's wheel to have more traction.

The test results showed that the prototype has an acceptable consistency in accelerating the curling stone linearly. The prototype also was able to accelerate the curling stone rotationally. However, the angular motion's consistency that the device produced could not meet the constraints and objectives of the angular speed.

The prototype of the device was used to do experimental tests as well. These tests illustrated that the curl on the curling stone correlated with the stone's longitudinal distance travelled up to nine meters. The correlation between the lateral and longitudinal distance travelled becomes more linear by increasing the rotational speed within the range of 0.0 to 83.0 °/s. Also, the results show that the rotational speed has no significant effect on the longitudinal distance travelled by the stone at 1.26m/s over the rotational speed range of 27.7 to 83.0 °/s.

Furthermore, the data collected in the experimental tests confirmed that the curling stone travelled less far after each throw, after suitable ice conditioning. This testing indicates that the curling stone travelled roughly 17% less at an initial speed of 1.26 m/s after five sets of throwing the stone down the ice, where three trials were done in each set.

Additionally, a test was performed to show the effects of changing the curling stone's mass on its behavior while travelling down the ice. However, the data collected in this test was confounded. Therefore, the effects of changing the curling stone's mass on its longitudinal distance travelled was not distinctive from the effects of the erosion of the pebbles after each throw on the stone's behavior.

The prototype has the ability to perform several tests in curling. The prototype was built to show whether the designed device can accelerate the stone linearly and rotationally to preset velocities and throw the curling stone at a preset angle to the centerline of the ice sheet. The test results are promising, and they show the opportunities this device would provide for sport scientists, physicists, engineers, ice technicians, curlers, and curling coaches. These opportunities include performing more scientific tests on the curling stone to investigate the reason behind its unusual behavior, matching the curling stones, and investigating the effects of sweeping on curling stone behavior. Also, as a mechanical engineering student, this project was a chance to experience all the previous studies and learn how to convert the theory into reality and understand their differences.

7.2. Recommendations and Future Work

The current prototype shows some shortcomings, which need to be fixed in the next design iteration. The prototype should be modified to perform its tasks with higher consistency and with greater similarity to typical curling. In the following paragraphs these modifications will be discussed. These modifications are stepping-stones to get to the final design.

Although the rotational motor has the ability to accelerate the curling stone up to 50% of the required rotational speeds, the consistency of the rotational speed of the curling stone at release was not acceptable. Some modifications should be carried out on the rotational motor's wheel and the structure of the cradle mount. The outer layer of the wheels should be replaced with a material that has more traction with the curling stone. The cradle mount's structure should be modified to better support the curling stone i.e. to cover more of the curling stone's circumference. In this modification, the rotational motor should be relocated to increase the traction between the rotational motor's wheel and the curling stone by increasing the normal force between the curling stone and the wheel. Another potential modification is to use two rotational motors instead of one. Two rotational motors should make the stone's rotational speed more consistent.

The open-loop control system of the device should be replaced with a closed-loop control system. For this purpose, encoders should be utilized to provide feedback signals on the motors' speeds for the control system. The closed-loop control system increases the consistency of the linear and rotational motion that the prototype provides to the stone. Also, a sensor (perhaps ultrasonic) should be added to the control system to slow down the cradle mount before its stop at the end of the bridge. This sensor will help prevent damage on the end legs. Also, it will reduce the shock vibration on the system, which may cause loose wiring.

A gearbox should be added to the power transmission system to increase the cradle mount's linear speed. This increment in the cradle mount's linear speed will make it possible to launch the curling stone at speeds up to the target described in the constraints, i.e. 3 m/s. Also, a wheel with a greater diameter should be utilized on the rotational motor in order to spin the curling stone up to the target described in the constraints i.e. 2.09 rad/s.

A box of plexiglass or other transparent plastic should be used to cover the electrical components as well as the moving parts like the chain and the sprockets. Using this box increases the safety of the prototype and protects the electrical components from any accidental damage.

A longer bridge should be used in order to have a smoother acceleration profile for the linear motion. Also, to increase the prototype's portability, a hinge should be installed in the bridge's midpoint to make it foldable.

To prevent the main platform from slipping on the ice while launching a curling stone, a pair of plastic blocks should be added to the bottom part (legs) of the main platform to fill in the gaps between the hack's blocks and the legs.

Based on the informal experiment performed on the static friction (discussed in Appendix A.7), the assumption in this project on the value of the static friction (discussed in Appendix A.1.1) is poor. Further investigations are required to determine accurate values of the static friction between the stone and the ice using a winch and a force sensor.

Using the current prototype (the PRL), research on curling can be continued in a variety of areas. The effectiveness of sweeping techniques can be investigated using the PRL. Also, the theories explaining the behavior of the curling stone can be examined using the PRL. After the modifications discussed in this section, the tests accomplished using the PRL can be repeated with higher linear and rotational velocities at a greater consistency.

Furthermore, the current PRL is able to launch the curling stone at a preset angle to the centerline. This ability of the PRL should be validated in future. Also, throwing stones at different angles to the centerline will show whether the quality of the curling ice changes by the distance from the centerline.

The last experiment presented here (dealing with the mass of a stone) should be redone, and the variables should be arranged so that the effects of changing the curling stone's weight can be distinguished from the effects of the erosion of the pebbles after each throw on the stone's behavior. The results would be clearer if the order of the sets was altered so that set 1 was performed by a stone without extra weight and set 2 was performed by a stone with extra weight, or if all trials were randomized for the presence of the incremental weight. With these new procedures, it should be possible to see those effects distinctly.

Finally, the PRL can also be used to measure how changes in ice temperature, air temperature, humidity level, size of pebbles, and density of pebbles (discussed in the second last paragraph of Section 4.2.2.) will affect the stone's longitudinal distance travelled as Hritzuk (2020) suggested. He explained that the ice makers try to minimize the variance of the stone's longitudinal distance travelled from the start to the finish of a curling game. The PRL can be utilized to find the best combination of the effective variables to minimize the change in longitudinal distance travelled change during a curling game.

REFERENCES

12V, 118RPM 958.2oz-in HD Premium Planetary Gearmotor w/ Encoder. (2016). Retrieved January 20, 2021, from Robotshop.com website: https://www.robotshop.com/ca/en/12v-118rpm-9582oz-in-hd-premium-planetary-gearmotor-encoder.html

24V 350W DC Motor Gear Reduction Motor MY1016Z3, for E-Bike, E-scooter: Amazon.ca: Tools & Home Improvement. (2021). Retrieved January 20, 2021, from Amazon.ca website: https://www.amazon.ca/Motor-Reduction-MY1016Z3-Bike-scooter/dp/B08SJLWQBD/ref=sr_1_1?dchild=1&keywords=DC+Motor%2C+MY1016Z3+24V%2C+and+350W+Gear+Reduction+Electric+Motor+for+E-Bike+Scooter&qid=1611167411&s=hi&sr=1-1

Brower Timing Systems. (2020). Brower Timing Systems. Retrieved January 20, 2021, from Brower Timing Systems website: https://browertiming.com/

Curling Canada | Curling Sheet: The playing surface. (2020). Retrieved January 20, 2021, from Curling.ca website: https://www.curling.ca/about-curling/getting-started-in-curling/curling-sheet-the-playing-surface/#:~:text=The%20playing%20surface%20or%20curling,sheet%20are%20called%20the%20backboards.

Curling Terminology. (2020). Retrieved December 30, 2020, from Srcc.ca website: http://www.srcc.ca/en-us/aboutcurling/curlingterminology.aspx.

Curling Tips - Garrison Golf and Curling Club. (2016, November 9). Retrieved January 20, 2021, from Garrison Golf and Curling Club website: https://ggcc.on.ca/curling/curling-rules/curling-tips

Denny, M. (2002). Curling rock dynamics: Towards a realistic model. Canadian Journal of Physics, 80(9), 1005–1014. https://doi.org/10.1139/p02-072

DEWALT Laser Distance Measurer, 165-ft | Canadian Tire. (2020). Retrieved January 7, 2021, from Canadiantire.ca website: https://www.canadiantire.ca/en/pdp/dewalt-laser-distance-measurer-165-ft-0574605p.html

Digitize graphs and plots - GetData Graph Digitizer - graph digitizing software. (2021). Retrieved January 6, 2021, from Getdata-graph-digitizer.com website: http://getdata-graph-digitizer.com/.

Hacks. (2014). Retrieved January 20, 2021, from Dakota Curling Supplies website: https://dakotacurling.supplies/collections/hacks

Harrington, L. E. (1924). An experimental study of the motion of curling stones. Proc. and Trans. Roy. Soc. Canada, 18(3), 247-258.

Hatfield, J. (2016, January 25). How Much Does It Cost To Repair An Electric Motor? Retrieved December 31, 2020, from Hecoinc.com website: https://www.hecoinc.com/blog/how-much-does-it-cost-to-repair-an-electric-motor.

Hritzuk, E. (2019, May 24). Former World Senior men's champion skip, Saskatoon, Canada (Interview)

Hritzuk, E. (2020, Nov 9). Former World Senior men's champion skip, Saskatoon, Canada (Interview)

IBM Docs. (2021). Retrieved April 21, 2021, from Ibm.com website: https://www.ibm.com/docs/en/spss-statistics/26.0.0?topic=anova-one-way-post-hoc-tests

Jensen, E. T., & Shegelski, M. R. (2004). The motion of curling rocks: Experimental investigation and semi-phenomenological description. Canadian Journal of Physics, 82(10), 791–809. https://doi.org/10.1139/p04-020

Kasberg, J. (2015, July). The Fundamentals of Ball Screws. Retrieved April 19, 2021, from Machine Design website: https://www.machinedesign.com/mechanical-motion-systems/linear-motion/article/21834347/the-fundamentals-of-ball-screws

Kucheran, L. (2019, May 24). Ice technician at the Nutana club, Saskatoon, Canada (Interview)

Lahayne, O., Pichler, B., Reihsner, R., Eberhardsteiner, J., Suh, J., Kim, D., … Persson, B. N. J. (2016). Rubber Friction on Ice: Experiments and Modeling. Tribology Letters, 62(2). https://doi.org/10.1007/s11249-016-0665-z

Levene's Test | Real Statistics Using Excel. (2021, February 3). Retrieved April 23, 2021, from Real-statistics.com website: https://www.real-statistics.com/one-way-analysis-of-variance-anova/homogeneity-variances/levenes-test/

Linear Motion Primer - Phidgets Legacy Support. (2020). Retrieved January 18, 2021, from Phidgets.com website: https://www.phidgets.com/docs21/Linear_Motion_Primer.

Lozowski, E. P., Szilder, K., Maw, S., Morris, A., Poirier, L., & Kleiner, B. (2015, July). Towards a first principles model of curling ice friction and curling stone dynamics. In The Twenty-fifth International Ocean and Polar Engineering Conference. International Society of Offshore and Polar Engineers.

Macaulay, W. H., & Smith, G. E. (1930). Curling. Nature, 125(3150), 408-409.

Maeno, N. (2009). Mechanism of curling stone to curl-Evaporation-abrasion model. In Proceedings of JSSI and JSSE Joint Conference, 219.

Maeno, N. (2014). Dynamics and curl ratio of a curling stone. Sports Engineering, 17(1), 33-41.

Maeno, N. (2016). Curling. The Engineering Approach to Winter Sports, 327–347. https://doi.org/10.1007/978-1-4939-3020-3_10

Martignano, A. (2011). RPM Speed & Wow. Retrieved January 6, 2021, from Google.com website: https://play.google.com/store/apps/details?id=com.AM.AM.RPMSpeed&hl=en_CA&gl=US.

Mccahan, S., Weiss, P. E., Anderson, P., & Kortschot. (2015). Introduction to Engineering Design. Retrieved from https://www.wiley.com/en-ca/Designing+Engineers%3A+An+Introductory+Text-p-9780470939499

Merriam-Webster Dictionary. (2021). Retrieved February 10, 2021, from Merriam-webster.com website: https://www.merriam-webster.com/dictionary/backlash

Moog Inc. (2021). Actuators. Retrieved January 18, 2021, from Animatics.com website: https://www.animatics.com/products/actuators.models.html.

Nyberg, H., Alfredson, S., Hogmark, S., & Jacobson, S. (2013). The asymmetrical friction mechanism that puts the curl in the curling stone. Wear, 301(1-2), 583-589.

Nyberg, H., Alfredson, S., Hogmark, S., & Jacobson, S. (2013). The asymmetrical friction mechanism that puts the curl in the curling stone. Wear, 301(1-2), 583-589.

Ohman, J. M. (2004). Curling Ice Explained. World Curling Federation, Perth

Ovchinnikov, E. L., & Ivanov, V. V. (2011). Theoretical basis of comfortable, tolerable and destructive effects of sounds and noise. Journal of Physics: Conference Series, 305, 012128. https://doi.org/10.1088/1742-6596/305/1/012128

Park, R. (2014). Retrieved from light guide systems: http://www.lightguidesystems.com/index.php/curling-technology/sweeptracker

Penner, A. R. (2001). The physics of sliding cylinders and curling rocks. American Journal of Physics, 69(3), 332–339. https://doi.org/10.1119/1.1309519

Rosset, M. (2017, October 20). Manitoba curling club builds world's first rock throwing machine. Retrieved January 15, 2021, from Global News website: https://globalnews.ca/news/3816318/manitoba-curling-club-builds-worlds-first-rock-throwing-machine/

Rules of Curling for Officiated Play. (2018). CURLING CANADA.

Ruptly. (2018). "Curly" the curling-playing robot loses game to humans [YouTube Video]. Retrieved from https://www.youtube.com/watch/4WmXmoc88wA

Shegelski, M. R. (2016). Pivot–slide model of the motion of a curling rock. Canadian Journal of Physics, 94(12), 1305-1309.

Shegelski, M. R. A., & Lozowski, E. (2018). First principles pivot-slide model of the motion of a curling rock: Qualitative and quantitative predictions. Cold Regions Science and Technology, 146, 182–186. https://doi.org/10.1016/j.coldregions.2017.10.021

Shegelski, M. R., & Lozowski, E. (2019). Null effect of scratches made by curling rocks. Proceedings of the Institution of Mechanical Engineers, Part P: Journal of Sports Engineering and Technology, 233(3), 370-374.

Shegelski, M. R., Niebergall, R., & Walton, M. A. (1996). The motion of a curling rock. Canadian Journal of Physics, 74(9-10), 663-670.

Soccer MachineTM. (2018). Retrieved January 18, 2021, from Jugs Sports website: https://jugssports.com/products/soccer-machine.html.

Super User. (2021). SweepTracker. Retrieved January 15, 2021, from Lightguidesystems.com website: http://www.lightguidesystems.com/index.php/curling-technology/sweeptracker

TRANSIENT BEHAVIOUR – CURRENT SURGES (Motors And Drives). (2021). Retrieved April 21, 2021, from What-when-how.com website: http://what-when-how.com/motors-and-drives/transient-behaviour-current-surges-motors-and-drives/

Tschirhart, B (2020, November 3). Matching Stones 101. Retrieved November 3, 2020, from Blogspot.com website: http://truenorthbill.blogspot.com/2014/02/matching-stones-101.html

Won, D. O., Kim, B. D., Kim, H. J., Eom, T. S., Müller, K. R., & Lee, S. W. (2018, July). Curly: An AI based Curling Robot Successfully Competing in the Olympic Discipline of Curling. In IJCAI, 5883-5885.

APPENDIX

A.1. Derivation of the Equations of Motion

A.1.1. Linear Motion

To calculate the force required to accelerate the stone from stationary to a preset speed, we need the stone's acceleration. The maximum velocity is known, and its value is 3 m/s. Also, the length of the bridge available to accelerate the stone is 2 m. About 10 cm of its actual 2.2 m length is needed at each end for attachment to the main platform and the end leg. It is assumed that the stone has a constant acceleration. To determine this acceleration, the time of action and displacement are required.

$$s = \frac{1}{2}at^2 + v_0 t + s_0 \quad \text{(A.1)}$$

$$v = at \quad \text{(A.2)}$$

In equation A.1, s is the displacement, a is the acceleration of the stone, t is the time of action, and v_0 and s_0 are the initial values of speed and displacement, respectively. The stone starts from stationary so, v_0 is equal to zero. Also, the stone always starts from the datum so, s_0 is equal to zero as well. In equation A.2, v is velocity.

The acceleration is assumed constant during the process of launching the stone. This assumption was made to simplify the derivation of the equation of motion. The value of acceleration and time of action are calculated using equation A.1 and equation A.2 and the maximum speed value. The stone's constant acceleration is equal to 2.25 m/s^2 and the time of action is equal to 1.33 s.

$$F = ma \quad \text{(A.3)}$$

In equation A.3, F is the force required to accelerate the stone, and m is the mass of the curling stone. To design the system conservatively, the maximum value reported for the stone's mass, which is 20 kg, is used. Also, the kinematic friction between the stone and the ice has been determined by Nyberg (2013). It is assumed that the static friction is as much as twice of the kinematic friction. The maximum value for the kinematic friction reported by Nyberg (2013) is 4.40 N (the maximum kinetic friction coefficient reported is 0.022379), so, based on the assumption made earlier, the static friction is 8.80 N.

Knowing the mass and the acceleration of the curling stone, the force required to accelerate the stone can be determined as 49.4 N. This force has to be transferred through a 73.5mm diameter sprocket, a 4 m chain, and the cradle mount, to the stone. The mass of the cradle mount and the chain are 2.5 kg and 0.15 kg/m, respectively. In accelerating the stone, the cradle mount has to be accelerated as well as the chain. Consequently, the total force required to accelerate the chain, cradle mount and the curling stone is equal to 56.375 N.

$$\tau = Fd \quad \text{(A.4)}$$

In equation A.4, τ is the torque and d is the length of the lever which the force is acting on. In this case, the calculated force is exerted to a sprocket. So, the lever of the force is the radius of the sprocket (Figure A.1). The required torque to accelerate the stone to the maximum linear speed is 2.07 N·m. Also, a 0.323 N·m torque on the sprocket is required to move the stone from stationary. As noted, the force of the static friction is 8.80 N, and the radius of the sprocket is 0.03675 m. A safety factor of 1.5 would be applied on the calculated torques. Consequently, a 3.11 N·m torque is required to accelerate the curling stone to its maximum linear speed and a 0.485 N·m torque is required to initiate the linear motion on the curling stone.

Since the selection of motors is based on two parameters, torque and speed, the motor's maximum required speed must be determined. The maximum speed of the stone is 3 m/s. Since the stone, cradle mount, and the chain are attached together, they move at the same speed. Therefore, the chain must be moved at 3 m/s.

$$v = \omega r \quad \text{(A.5)}$$

In equation A.5, ω is the angular velocity, and *r* is the radius of the sprocket. Therefore, ω of the sprocket should be 81.6 rad/s.

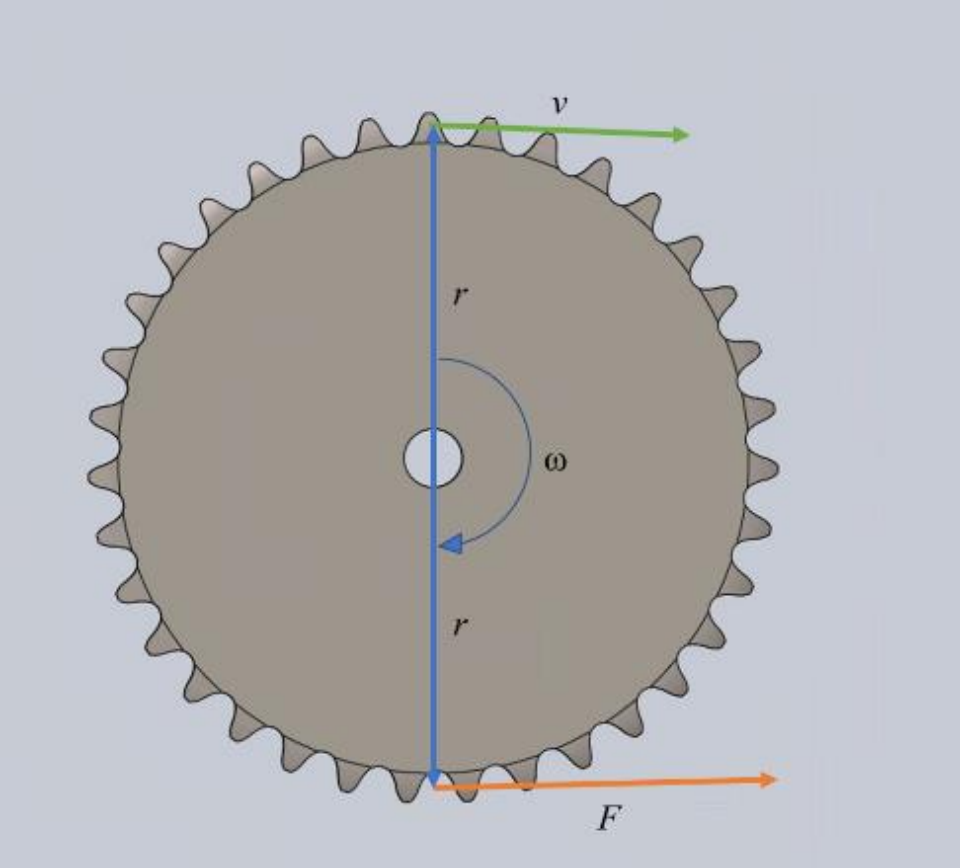

Figure A.1: The sprocket, the linear velocity of a point on its circumstance, and the force exerted on it by the chain.

A.1.2. Rotational Motion

In this section, the rotational motion of the stone is analyzed. The maximum rotational speed is 20 rpm or 2.09 rad/s. Also, the running band's diameter is 13 cm, and the radius of the stone is 14.5 cm. For the equation of rotational motion of the curling stone, it is assumed that the kinetic friction determined by Nyberg (2013) can be applied on the rotational motion as well. Therefore, the friction acts as a concentrated force, and it is located on a point in the middle of the running band. The direction of the friction is opposite to the direction of the point's velocity. As mentioned before, this machine is conservatively designed based on the maximum values.

To determine the torque required to accelerate the stone to the maximum rotational speed, the angular acceleration is required.

$$\omega = \dot{\omega} t \quad \text{(A.6)}$$

In equation A.6, $\dot{\omega}$ is the angular acceleration. From the linear motion, it is calculated that the time of action for accelerating the stone to its maximum linear speed is 1.33 seconds. Therefore, the rotational motor has 1.33 seconds to accelerate the stone to the maximum angular speed. Consequently, the angular acceleration is 1.5714 rad/s^2.

$$\tau_{rot.} = I\dot{\omega} \quad \text{(A.7)}$$

In equation A.7, $\tau_{rot.}$ is the required torque to rotate the stone with $\dot{\omega}$ acceleration. *I* in this equation is the moment of inertia of the curling stone. To determine *I* of the curling stone, a curling stone is modelled in SolidWorks (Figure A.2). Value of *I* is equal to $10.96 \cdot 10^{-2}$ kg m^2 as noted in Appendix A.3. Consequently, $\tau_{rot.}$ is equal to 0.17223 N·m. From the previous section, the kinetic friction is 4.40 N, and the radius of the running band is 0.065 m so, using the equation A.4, the torque required to overcome the force of the kinetic friction can be determined ($\tau_{Kinetic\ Friction}$ = 0.286 N·m). Therefore, the total torque required to accelerate the stone rotationally up to the maximum angular speed is 0.45823 N·m. The torque required to accelerate the wheel rotationally is negligible since the wheel's moment of inertia is negligibly low.

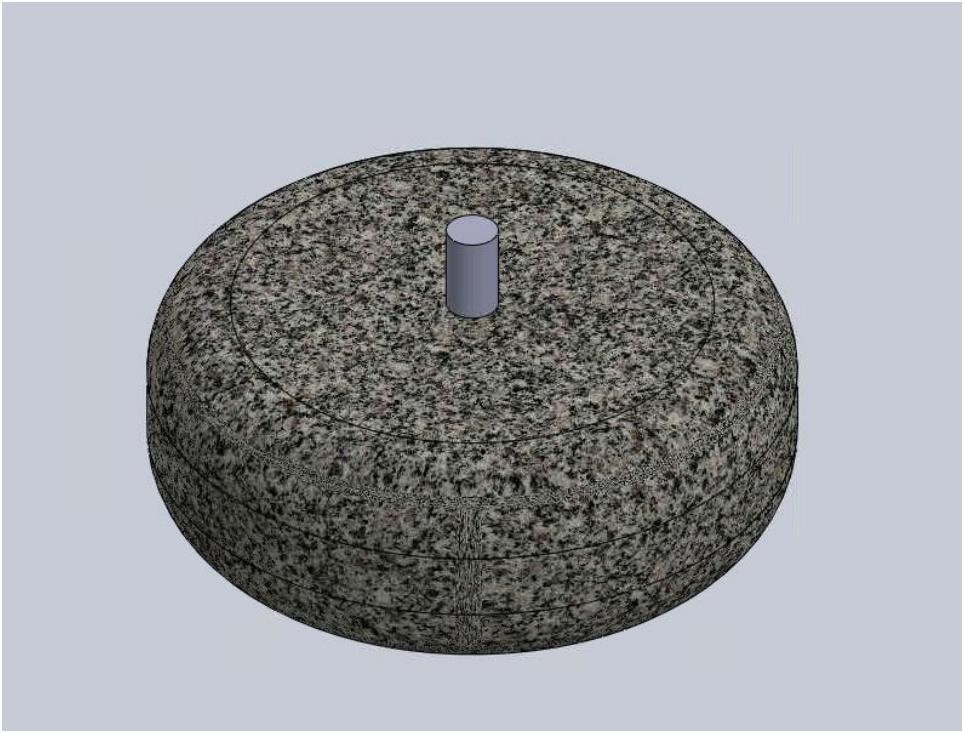

Figure A.2: The simulated curling stone.

The motor rotates the stone with a wheel attached to the motor's shaft. Figure A.3 shows how the wheel interacts with the stone.

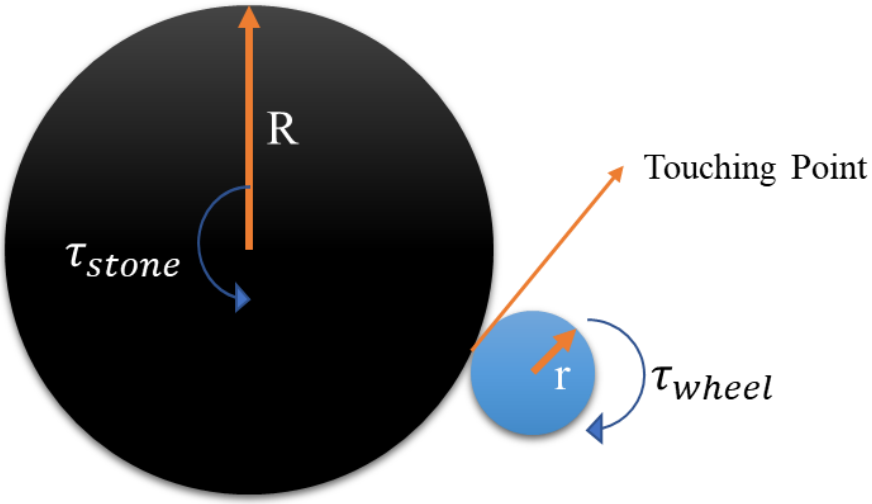

Figure A.3: The top view of the stone and the wheel of the rotational motor. It is assumed that the engagement of the stone and the wheel is perfect.

The forces acting on each circle at the touching point are equal. So, from equation A.4, it can be derived that:

$$\tau_{stone}/R = \tau_{wheel}/r \quad \text{(A.8)}$$

In equation A.8, τ_{stone} is the torque required on the stone to accelerate it to the maximum angular speed. τ_{wheel} is the torque required on the wheel in order to have τ_{stone} on the stone. R is the radius of the stone, and r is the radius of the wheel. The radius of the wheel is 3.60 cm. Therefore, the torque required on the wheel in order to rotate the stone at its maximum rotational speed is 0.114 N·m. A safety factor of 1.5 would be applied on the calculated torque calculated in this section. Consequently, a 0.171 N·m torque is required to accelerate the curling stone to its maximum rotational speed.

To produce the maximum rotational speed of the stone, the speed of the motor needs to be calculated as well. The maximum rotational speed is 2.09 rad/s. According to Figure A.3, the linear speeds of the touching point of circles are equal. So, based on equation A.5:

$$\omega_{stone}R = \omega_{wheel}r \quad \text{(A.9)}$$

In equation A.9, ω_{stone} and ω_{wheel} are the angular speeds of the stone and the wheel, respectively. Therefore, the angular speed required on the wheel in order to rotate the stone at its maximum rotational speed is 8.42 rad/s.

A.2. Software Architecture

The Rock Launcher's control system is divided into two main systems: a control system for linear motion, and a control system for rotational motion. The codes for controlling the linear and rotational motion are presented here.

A.2.1. Software for the Rotational Motion Control System

The control system of the rotational motor has two inputs: a rotary switch controlling the motor's speed, and a toggle switch controlling the direction of the rotation motion. The rotary switch has 4 positions for zero, low, mid, and high rotational speed. The Arduino controlling the rotational motor receives a binary signal from the rotary switch and translates it to PWM signals on the motor driver's pin. The toggle switch is located between the motor driver and the rotaitonal motor in the circuit.

A.2.1.1. Codes of the Rotational Motion Control System

```
int s1=10;   // Pin for detecting the min velocity
int s2=11;   // Pin for detecting the med velocity
int s3=12;   // Pin for detecting the max velocity
int S1;      // Value for the pin of min velocity
int S2;      // Value for the pin of med velocity
int S3;      // Value for the pin of max velocity
int in1=3;   // Pin of input of motor driver
const int chA=2;  // Pin for encoder channel A
const int chB=3;  // Pin for encoder channel B
unsigned long time0; // Time at the start for encoder
unsigned long timeF; // Time at the current moment for encoder
unsigned long pulses; // Number of pulses for encoder
float encoderSpeed;   // Speed detected by the encoder
int c;              // Counter
long pulse1;        // Pulses value to check if the motor is moving or not
unsigned long CurrentTime = millis();  // Current time for running time
unsigned long StartTime = millis();   // Starting time for running time
unsigned long Timelapce;            // Time-lapse of running
int speed1;                    // Pot value
float t;                      // Running time
int I1=A4;                     // Starting switch
int i1;                       // Value of the starting switch
float V;                       // Velocity we put on motor

void setup() {
  pinMode(s1,INPUT_PULLUP);      // Define pin min velocity
```

```
  pinMode(s2,INPUT_PULLUP);      // Define pin med velocity
  pinMode(s3,INPUT_PULLUP);      // Define pin max velocity
  pinMode(in1,OUTPUT);            // Motor driver pin
  pinMode(chA,INPUT);             // Encoder pin channel A
  pinMode(chB,INPUT);             // Encoder pin channel B
  pinMode(I1,INPUT);              // Starting pin
  Serial.begin(9600);             // Activating the display
}

void loop() {
  // Put your main code here, to run repeatedly:
S1=digitalRead(s1); // Read the pin and value for the rotational speed

S2=digitalRead(s2); // Read the pin and value for the rotational speed

S3=digitalRead(s3); // Read the pin and value for the rotational speed

    // Low speed //
    while ( S1 == LOW)       //Low speed
         {
          if (i1>=700)             // Starting switch
            {
             analogWrite(in1,0);       // Motor off
             CurrentTime = millis();   // Running time
             Timelapce=0;              // Running time
             c=1;                      // Counter
             pulses=0;                 // Encoder pulses
             time0=millis();           // Encoder starting time
             StartTime=CurrentTime;    // Starting time for running


             while ( Timelapce <= t) // Loop of running
                  {
                   V=255/3;              // Value for min velocity
                   action();             // Function of running the motor
                  }

             c++;                 // Counter
             CurrentTime = millis();   // Running time
             Timelapce=CurrentTime-StartTime;  // Time-lapse of running

            }

           analogWrite(in1,0);               // Motor off
           S1=digitalRead(s1);               // Read the pin and value for the rotational speed
           break;
          }
    ////
    // Mid speed //
    // Comments are the same for the next sections and will comment the new codes //
    while ( S2 ==LOW)         // Med speed
         {
          if (i1>=700)
            {
             analogWrite(in1,0);
             CurrentTime = millis();
```

```
            Timelapce=0;
            c=1;
            pulses=0;
            time0=millis();
            StartTime=CurrentTime;

            while ( Timelapce <= t)
                 {
                  V=255*2/3;
                  action();

                 }
            c++;
            CurrentTime = millis();
            Timelapce=CurrentTime-StartTime;
           }
       analogWrite(in1,0);
       S2=digitalRead(s2);
       break;
     }
    ////
    // Max speed //
    while ( S3 ==LOW)          // Max speed
         {
          if (i1>=700)
            {


             analogWrite(in1,0);
             CurrentTime = millis();
             Timelapce=0;
             c=1;
             pulses=0;
             time0=millis();
             StartTime=CurrentTime;
             while ( Timelapce <= t)
                  {
                   V=255;
                   action();
                  }
             c++;
             CurrentTime = millis();
             Timelapce=CurrentTime-StartTime;
            }

          analogWrite(in1,0);
          S1=digitalRead(s1);
          break;
        }
    ////
analogWrite(in1,0);

}

// Function for running the motor //
void action()
```

```
        {
         pulse1=pulses;      // To check if the motor is running or not
         if (c==1)     //for the first round
            {
             time0=millis();
            }
         analogWrite(in1,V);     // Putting the voltage on pin of the motor driver
         attachInterrupt(digitalPinToInterrupt(chA), encoder, RISING);       // Calculating the velocity of the motor
         timeF=millis();
         rpm();      // Function for calculating the speed of the encoder and display it
         if (c>=3)
            {
             if (pulse1==pulses)
                {
                 pulses=0;
                 Serial.println("Motor stopped");
                 c=1;
                 }
            }
        }
////
// Function of calculating the speed //
void rpm()
{
  Serial.print("RPM:");
  encoderSpeed=((float)pulses/853.98)/((float)(timeF-time0)/(60000.0));
  Serial.println(encoderSpeed);
}
////
// Function of the encoder //
{
  if (digitalRead(chA)==HIGH)
     {
      pulses++;
     }
}
////
```

A.2.2. Software for the Linear Motion Control System

The main motor control system has two inputs: a potentiometer, and a toggle switch. The Arduino detects a binary signal from the toggle switch. This signal starts the process of launching the stone. The signals from the potentiometer are continuous variable voltage signals. The Arduino receives these signals and maps them into PWM signals and sends them to the main motor driver. Also, a signal is sent to the rotational motor's Arduino to start the rotational motor.

A.2.2.1. Codes of the Linear Motion Control System

```
int PotVol;                    //Output Voltage of potentiometer
int StartSwitch=A5;            //Start switch
int ValueStartSwitch;          //Value of the starting switch
int StopSwitchB=A4;            //Stop Switch for backward motion
```

```
int ValueStopSwitchB;          //Value of the stopping switch for backward motion
double SpeedTest;              //Value of speed in percentage
float t;                       //Calculated running time
int RotArduino=4;              //sending signal to rotational Arduino
int SpeedPin=5;                //Speed Pin of motor driver
int Dir=6;                     //Direction pin of motor driver
int Sp;                        //Speed of linear motor
int StopSwitchF=A2;            //Stop Switch for forward motion
int ValueStopSwitchF;          //value of stop switch for forward motion
int Sp1;                       //Initial speed
float m;                       //Coefficient of second profile
int y=0;                       //Counter for profile selection
int u=1;                       //Counter of first acceleration profile

int profile_selector=10;       //Profile selecting parameter
int CounterPulse=1;            //Counter of profile selecting
int profile_LED1=11;           //Pin of the first acceleration profile
int profile_LED2=12;           //Pin of the second acceleration profile
int profile_LED3=13;           //Pin of the third acceleration profile


unsigned long CurrentTime = millis();     // Current time
unsigned long StartTime = millis();       // Start time
unsigned long StartTime1 = millis();      // Parameter for second acceleration profile
unsigned long Timelapce;                  // Time-lapse
unsigned long Timelapce1;                 // Time-lapse


void setup() {
// Define each pin for Arduino //
pinMode(A0,INPUT);                    //Pot output (PotVol)
pinMode(StartSwitch,INPUT);
pinMode(StopSwitchB,INPUT_PULLUP);
pinMode(RotArduino,OUTPUT);
digitalWrite(RotArduino,HIGH);
pinMode(SpeedPin,OUTPUT);
pinMode(Dir,OUTPUT);
pinMode(StopSwitchF,INPUT_PULLUP);
pinMode(profile_selector, INPUT_PULLUP);
pinMode(profile_LED1, OUTPUT);
digitalWrite(profile_LED1,LOW);
pinMode(profile_LED2, OUTPUT);
digitalWrite(profile_LED2,LOW);
pinMode(profile_LED3, OUTPUT);
digitalWrite(profile_LED3,LOW);
StartTime = millis();
Serial.begin(9600);                   // starting the display
////
}

void loop()
      {
       ValueStartSwitch=analogRead(StartSwitch);
       ValueStopSwitchF=analogRead(StopSwitchF);
       // Selecting between acceleration profiles //
       if(digitalRead(profile_selector)==0)
```

```
  {
   y=1;
  }

if(digitalRead(profile_selector)==1 && y==1)
  {
   CounterPulse=CounterPulse+1;
   Serial.println(CounterPulse);
   y=0;
  }

if (CounterPulse>3)
   {
    CounterPulse=1;
   }

if (CounterPulse==1)
   {
    digitalWrite(profile_LED1,LOW);
    digitalWrite(profile_LED2,LOW);
    digitalWrite(profile_LED3,HIGH);
   }

 if (CounterPulse==2)
    {
     digitalWrite(profile_LED2,LOW);
     digitalWrite(profile_LED1,HIGH);
     digitalWrite(profile_LED3,LOW);
    }

 if (CounterPulse==3)
    {
     digitalWrite(profile_LED3,LOW);
     digitalWrite(profile_LED1,LOW);
     digitalWrite(profile_LED2,HIGH);
    }
  ////

  // Forward running //
if (ValueStartSwitch>=700)      //running switch
   {
    PotVol=analogRead(A0);
    Serial.print("Pot voltage:");
    Serial.println(PotVol);
    PotVol=PotVol*1;
    SpeedTest= float(PotVol) / 1023 ;
    if (SpeedTest != 0)      //check if we have voltage on pot
       {
        // First Profile //
        if(CounterPulse==1)
          {
           Timelapce=0;
           CurrentTime = millis();
           StartTime=CurrentTime;
           ValueStopSwitchF=analogRead(StopSwitchF);
           delay(10000);
```

```
      PotVol=analogRead(A0);      //pot value
      Sp1=1;
      Sp=map(PotVol,0,1023,0,255);
      u=1;

      while (ValueStopSwitchF<500)
           {
            ValueStopSwitchF=analogRead(StopSwitchF);
            digitalWrite(RotArduino,LOW);      //sending signals to rotational Arduino
            if (u==1)
              {
               digitalWrite(Dir,LOW);
               analogWrite(SpeedPin,26);
               delay(2000);
               u=2;
              }
           // Active forward on motor driver //
           digitalWrite(Dir,LOW);
           Serial.println(Sp);
           analogWrite(SpeedPin,Sp);
           CurrentTime = millis();
           digitalWrite(RotArduino,LOW);      //sending signals to rotational Arduino
           CurrentTime = millis();
           Timelapce=CurrentTime-StartTime;
           Serial.print("timer:");
           Serial.println(Timelapce);
           ValueStopSwitchF=analogRead(StopSwitchF);
          }
    }
////

 // Second Profile //
if(CounterPulse==2)
  {
   Timelapce=0;
   CurrentTime = millis();
   StartTime=CurrentTime;
   ValueStopSwitchF=analogRead(StopSwitchF);
   delay(10000);
   //while ( Timelapce <= t)
   t=1800.3*(pow(PotVol,-1.018));
   t=t*1000;
   Sp1=18;
   PotVol=analogRead(A0);      //pot value
   Sp=map(PotVol,0,1023,0,255);
   m=(Sp-Sp1)/(t);
   StartTime1=millis();
   while (ValueStopSwitchF<500)
        {
         ValueStopSwitchF=analogRead(StopSwitchF);
         // Active forward on motor driver //
         digitalWrite(Dir,LOW);
         analogWrite(SpeedPin,Sp1);
         CurrentTime = millis();
         Timelapce1=CurrentTime-StartTime1;
```

```
            if (Timelapce1%100==0 && Sp1<Sp)
              {
               Sp1=(m*(Timelapce1))+18; //18 is Sp1
               Serial.println(Sp1);
              }

            if (Sp1>Sp)
              {
               Sp1=Sp;
               Serial.println(Sp1);
              }

             if (Sp1>255)
               {
                Sp1=255;
               }
             digitalWrite(RotArduino,LOW);      //sending signals to rotational Arduino
             CurrentTime = millis();
             Timelapce=CurrentTime-StartTime;
             ValueStopSwitchF=analogRead(StopSwitchF);
           }
      }
   ////
   // Third profile //
   if(CounterPulse==3)
     {
      Timelapce=0;
      CurrentTime = millis();
      StartTime=CurrentTime;
      ValueStopSwitchF=analogRead(StopSwitchF);
      delay(10000);
      Sp1=18;
      PotVol=analogRead(A0);      //pot value
      Sp=map(PotVol,0,1023,0,255);
      while (ValueStopSwitchF<500)
           {
            digitalWrite(RotArduino,LOW);      //sending signals to rotational Arduino
            ValueStopSwitchF=analogRead(StopSwitchF);
            // Active forward on motor driver //
            digitalWrite(Dir,LOW);
            analogWrite(SpeedPin,Sp1);
            CurrentTime = millis();
            if ((CurrentTime-StartTime)%100==0 && Sp1<Sp)
              {
               Sp1= Sp1+3;
              }
            digitalWrite(RotArduino,LOW);      //sending signals to rotational Arduino
            ValueStopSwitchF=analogRead(StopSwitchF);
           }
     }
  ////
  // Stop both rotational and linear motors //
    digitalWrite(Dir,LOW);
    analogWrite(SpeedPin,0);
    digitalWrite(RotArduino,HIGH);      //sending signals   to rotational Arduino
    delay(2000);
```

```
    // Avtive backward on motor driver //
    ValueStopSwitchB=analogRead(StopSwitchB);
    while (ValueStopSwitchB>=500)
         {
          //////////active motor backward//////////
          digitalWrite(Dir,HIGH);
          analogWrite(SpeedPin,30);
          ValueStopSwitchB=analogRead(StopSwitchB);
          ////////////////////////////////////////
          }
    ////////motor off//////////
    digitalWrite(Dir,LOW);
    analogWrite(SpeedPin,0);
    /////////////////////////
       }
    }
}
```

A.2.2.2. The Second Acceleration Profile

To program this set of speed profiles, the times of action for 10 speeds (10%, 20%, 30%…100%), under the set of constant speed profiles, were recorded. Time of action is the time that the cradle mount without stone needs to reach the end of the bridge. Next, an equation was derived using the collected data that explained the relationship between the motor's speed and the time of action. Using the derived equation and the dynamic equations (Eq.1 and Eq.2) used in Appendix A.1.1, the Arduino was programmed to calculate each speed's acceleration.

A.3. Specification of Simulated Stone

A curling stone has been simulated in SolidWorks to determine its moment of inertia. In the following, the report obtained using SolidWorks is presented. The simulated curling stone has 14.5 cm radius. Also, the granite was chosen for the material of the stone. A schematic of the simulated stone presented in Figure A.2.

Mass properties of stone

Configuration: Default

Coordinate system: -- default --

Density = 2.75 grams per cubic centimeter

Mass = 18766.70 grams

Volume = 6824.26 cubic centimeters

Surface area = 203926.88 square millimeters

Center of mass: (millimeters)

X = 0.00

Y = -2.54

Z = 0.00

Principal axes of inertia and principal moments of inertia: (grams × square millimeters)

Taken at the center of mass.

Ix = (1.00, 0.00, 0.00) Px = 109457226.16

Iy = (0.00, 0.00, -1.00) Py = 109457226.16

Iz = (0.00, 1.00, 0.00) Pz = 183386688.23

Moments of inertia: (grams * square millimeters)

Taken at the center of mass and aligned with the output coordinate system.

Lxx = 109457226.16 Lxy = 0.00Lxz = 0.00

Lyx = 0.00 Lyy = 183386688.23 Lyz = 22.11

Lzx = 0.00Lzy = 22.11Lzz = 109457226.16

Moments of inertia: (grams * square millimeters)

Taken at the output coordinate system.

Ixx = 109577915.48 Ixy = 0.00 Ixz = 0.00

Iyx = 0.00 Iyy = 183386688.23 Iyz = 22.51

Izx = 0.00 Izy = 22.51 Izz = 109577915.48

A.4. The Available Area of the Ice Sheet for the Device

The device must be set up in a 41.62 m^2 area, and it must be able to throw the curling stone in this area. Figure A.4 shows the dimensions of the curling ice sheet. The length of the area available is 10.059 m (tee line to hog line 6.401 m+ back line to tee line 1.829 m+ hack to back line 1.829 m), and the width of the ice sheet is 4.318 m. Therefore, the area available is 41.62 m^2.

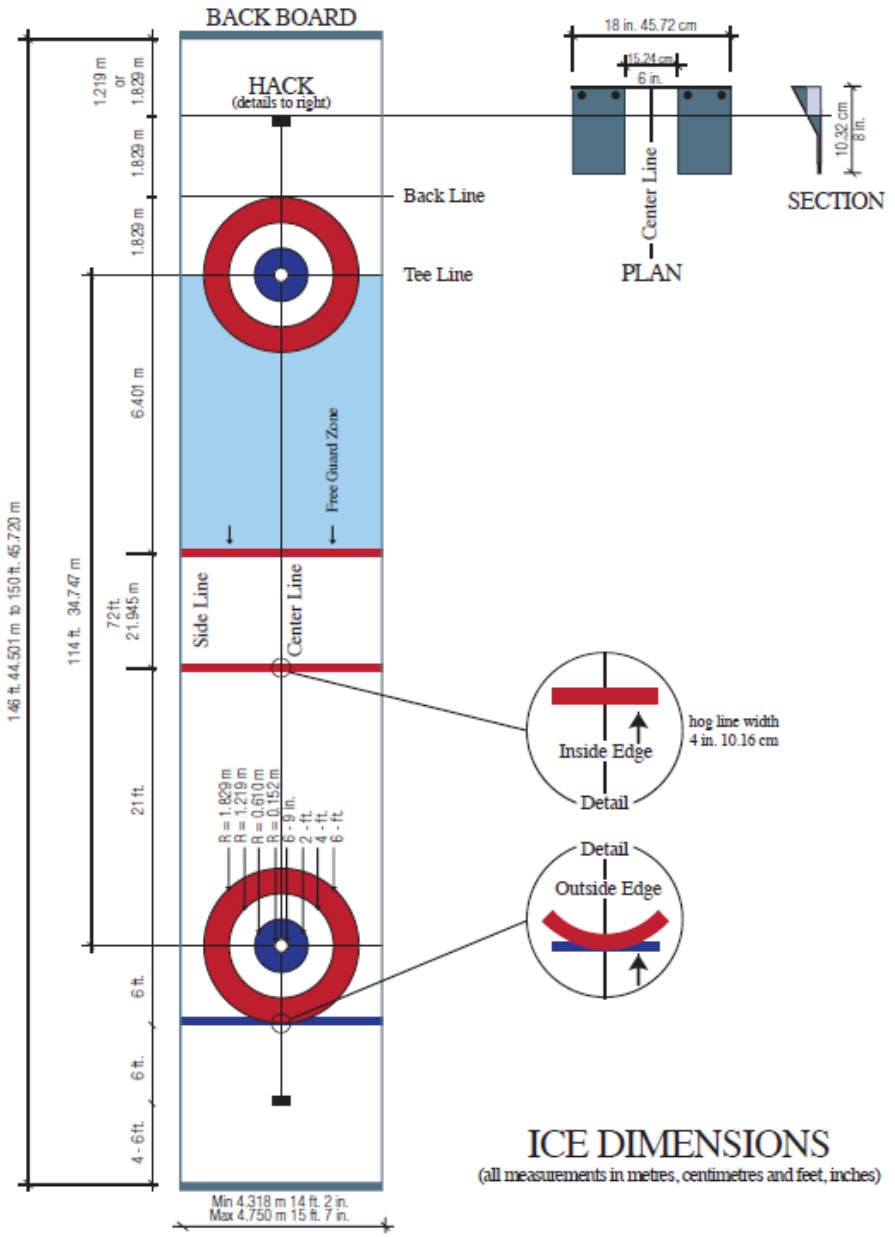

Figure A.4: The dimensions of the curling ice sheet ("Curling Canada | Curling Sheet: The playing surface," 2020).

A.5. Maintenance Cost

The maintenance cost has been estimated to be $600 for one year. This cost includes the lubrication of the device and any part that might need to be changed after one year. It is anticipated that the linear bearing of the device needs to be lubricated each time before use. Also, the screws of the device need to be checked and tight before each use. The linear motor gearbox and the rotational motor need to be serviced occasionally. Due to the curling rink's low temperature, the wires might be more fragile and require to be replaced more frequently.

The service of each motor would cost $200 in one year based on the available information on the internet. The cost of service of the motors is divided into years that the motors can work without service. It is anticipated that the motors can work 5 years without service. This service is hourly, and the cost is $50/hour (Hatfield, 2016). Each motor requires approximately 25 hours to be serviced based on the information available in the Hatfield website. The additional $200 of the maintenance cost is for the lubrication and electrical components' maintenance.

Moreover, based on the interview with potential customers, this expense is acceptable for the Rock Launcher's maintenance cost.

A.6. Release Angle

The release angle is the angle between the centerline of the ice sheet and the direction in which the stone is released. Based on the interviews with curling coaches, the maximum release angle aims the stone to the side edge of the biggest circle of the house. Figure A.5 displays the maximum angle on the curling ice sheet (the curling stone moves from the right to the left of this figure). The maximum angle based on the dimensions provided on this figure is tan(1.8 m/38.4 m) = 2.7°. So, the constraint on the release angle is rounded to +/- 3° from the centerline.

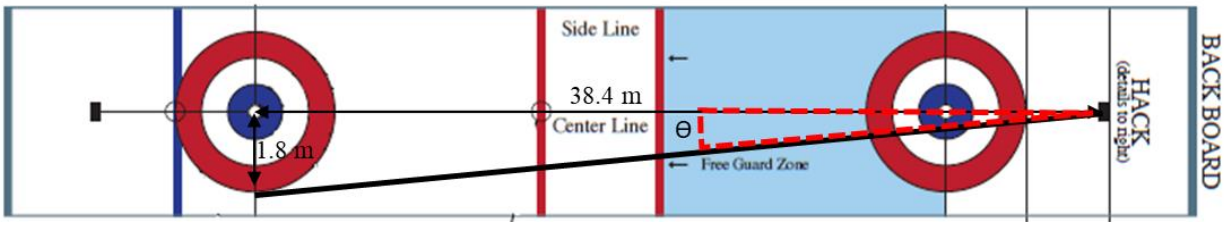

Figure A.5: The maximum release angle ("Curling Canada | Curling Sheet: The playing surface," 2020).

A.7. Static and Kinetic Friction

An informal experiment was done to find the static and kinetic friction between the curling stone and the ice surface using a luggage gauge. The stone was pulled from stationary on the ice and read the luggage gauge's values once the stone wants to start moving. The values of the static friction collected using the luggage gauge are between 8 and 14lbs (35.5 to 62.3 N). Afterwards, the stone was moved at an approximately constant speed with the luggage gauge. The values collected for the kinetic friction are between 0.5 and 1.5lbs (2.2 to 6.7 N).

A.8. Speed-Load Graph of the Rotational Motor

Figure A.6 presents the rotational speed-load graph of the rotational motor. The unit of the speed in this graph is rpm and the unit for the load is oz·in.

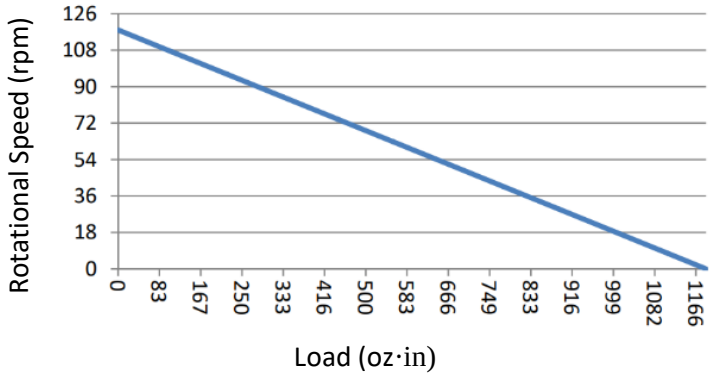

Figure A.6: Speed-Load graph of the rotational motor. This motor is 118 RPM heavy duty premium planetary gear motor, its part number is 638324 (w/encoder) ("12V, 118RPM 958.2oz-in HD Premium Planetary Gearmotor w/ Encoder," 2016).

A.9. Data Collected for the Validation of the Rotational Motion of the Curling Stone at Release

The raw data of the validation test of the curling stone's rotational motion at release is presented in Table A.1. The data presented in Table A.1 includes four sets performed at 85% (1.07 m/s) linear speed.

Table A-1: Raw data of the rotational motion validation test.

Rotational Speed	Rotational Speed at 2.6s (rpm)	Rotational Speed at 2.6 s (°/s)
Zero (0 °/s)	0.230114	1.380684
Low (27.7 °/s)	3.41753	20.50518
Mid (55.4 °/s)	7.38462	44.30772
High (83.0 °/s)	10.6967	64.1802
Zero (0 °/s)	0.0652921	0.3917526
Low (27.7 °/s)	3.03088	18.18528
Mid (55.4 °/s)	7.55837	45.35022
High (83.0 °/s)	11.4261	68.5566
Zero (0 °/s)	0.0827586	0.4965516
Low (27.7 °/s)	3.42202	20.53212
Mid (55.4 °/s)	7.8593	47.1558
High (83.0 °/s)	12.1962	73.1772
Zero (0 °/s)	0.247347	1.484082
Low (27.7 °/s)	3.02673	18.16038
Mid (55.4 °/s)	7.29293	43.75758
High (83.0 °/s)	11.7348	70.4088

A.10. Data Collected for the Validation of the Linear Motion of the Curling Stone at Release

The raw data of the validation test of the curling stone's linear motion at release is presented in Table A.2. The data presented in Table A.2 includes four sets performed at Zero (0°/s) rotational speed. The BTS used to record the time that stone passes between two laser beams. The distance between two laser beams is 12.4 +/- 0.2 cm.

Table A-2: Raw data of the rotational motion validation test.

Linear Speed (Target Speed)	Brower time (s)	Linear Speed (m/s)
30% (0.38 m/s)	0.379	0.33
45% (0.57 m/s)	0.237	0.52
60% (0.76 m/s)	0.181	0.69
80% (1.01 m/s)	0.132	0.94
100% (1.26 m/s)	0.102	1.22
30% (0.38 m/s)	0.384	0.32
45% (0.57 m/s)	0.243	0.51
60% (0.76 m/s)	0.180	0.69
80% (1.01 m/s)	0.132	0.94
100% (1.26 m/s)	0.100	1.24
30% (0.38 m/s)	0.441	0.28
45% (0.57 m/s)	0.233	0.53
60% (0.76 m/s)	0.176	0.70
80% (1.01 m/s)	0.133	0.93
100% (1.26 m/s)	0.100	1.24
30% (0.38 m/s)	0.384	0.32
45% (0.57 m/s)	0.247	0.50
60% (0.76 m/s)	0.177	0.70
80% (1.01 m/s)	0.133	0.93
100% (1.26 m/s)	0.104	1.19

A.11. Data Collected for the Experiment of Section 6.1

The raw data of the experiment on the effects of rotational motion of the curling stone on its trajectory are presented in Table A.3. The data presented in Table A.3 includes five sets. In this table, “L” refers to the low rotational speed, “M” refers to the mid rotational speed, and “H” refers to the high rotational speed.

Table A-3: The raw data of the experiment on the effects of the rotational motion on stone’s trajectory.

Linear Speed	Rotational Speed	Longitudinal Distance	Lateral Distance
%	Setting	m +/- .01	cm +/- 1
30	L	0.886	0
30	L	0.898	0
30	L	0.879	0
30	L	0.867	1
30	L	0.812	2
30	M	0.899	1
30	M	0.869	2
30	M	0.880	2
30	M	0.871	2
30	M	0.843	2
30	H	0.927	0
30	H	0.905	1
30	H	0.903	2
30	H	0.870	1
30	H	0.796	1
60	L	3.056	12
60	L	2.773	17
60	L	2.739	11
60	L	2.683	11
60	L	2.405	13
60	M	2.831	14
60	M	2.699	18
60	M	2.418	13
60	M	2.413	15
60	M	2.336	13
60	H	2.936	11
60	H	2.696	11
60	H	2.607	11
60	H	2.324	9
60	H	2.311	12
100	L	9.097	78
100	L	9.051	85
100	L	8.240	55
100	L	8.449	70
100	L	7.611	39
100	M	8.908	69
100	M	8.370	64
100	M	7.940	69
100	M	8.277	70
100	M	7.306	55
100	H	8.449	56
100	H	8.648	62
100	H	8.185	60
100	H	7.907	60
100	H	7.123	48

A.12. Data Collected for the Experiment of Section 6.2

The raw data of the validation of the curling stone's linear speed without/with extra weight are presented in Table A.4. The data presented in Table A.4 includes four sets. Also, the raw data of the experiment on the effects of change in curling stone's weight on its longitudinal distance travelled are presented in Table A.5. The data presented in Table A.5 includes four sets.

Table A.4: The raw data of validation of the linear speed of a curling stone without/with extra weight.

Linear Speed (%)	Brower time (s)
30%	0.384
45%	0.230
60%	0.179
80%	0.133
100%	0.101
30%	0.383
45%	0.238
60%	0.178
80%	0.132
100%	0.103
30%	0.385
45%	0.243
60%	0.177
80%	0.131
100%	0.099
30%	0.382
45%	0.234
60%	0.174
80%	0.131
100%	0.100

Table A.5: The raw data of the experiment on the effects of change in curling stone's weight on its longitudinal distance travelled.

Linear Speed (%)	Longitudinal distance travelled (m)
30%	0.910
45%	1.534
60%	2.490
80%	4.737
100%	7.941
30%	0.911
45%	1.503
60%	2.387
80%	4.423
100%	7.828
30%	0.904
45%	1.448
60%	2.419
80%	4.454
100%	7.491
30%	0.872
45%	1.409
60%	2.479
80%	4.328
100%	7.453

A.13. Stress Analysis of the End Leg

In the following images, the stress analysis of the end leg is presented. Based on this stress analysis, the material of the end leg can be oak wood. The force is exerted to a square-shaped area of the top plate of the end leg. The square-shaped area is where the bridge attaches to the end leg. This force includes the weight of the bridge, the cradle mount, and the chain. The weight of the bridge is divided into two supports, as well as the weight of the chain. It was assumed that the cradle mount stays at the end of the bridge, so the total weight of the cradle mount must be tolerated by the end leg. The mass of the bridge is 4.18 Kg. The mass of the cradle mount is 2.5 kg and the mass of the chain is 0.6 kg. The g (gravitational constant) was assumed 9.81m/s^2.

Material Properties

Model Reference	Properties		Components
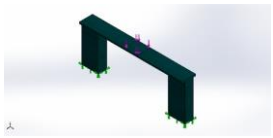	Name:	**wood oak**	**SolidBody 1(Split Line1)(Part1)**
	Model type:	**Linear Elastic Isotropic**	
	Default failure criterion:	**Unknown**	
	Yield strength:	**8.6e+06 N/m^2**	
	Tensile strength:	**5.5 N/m^2**	
	Compressive strength:	**4.6e+07 N/m^2**	
	Elastic modulus:	**9.3e+09 N/m^2**	
	Poisson's ratio:	**0.03**	
	Mass density:	**600 kg/m^3**	
	Shear modulus:	**1.23e+07 N/m^2**	

Figure A.7: The properties of the material used for the stress analysis.

Name	Type	Min	Max
Stress1	VON: von Mises Stress	8.368e+02N/m^2 Node: 920	2.854e+06N/m^2 Node: 12942

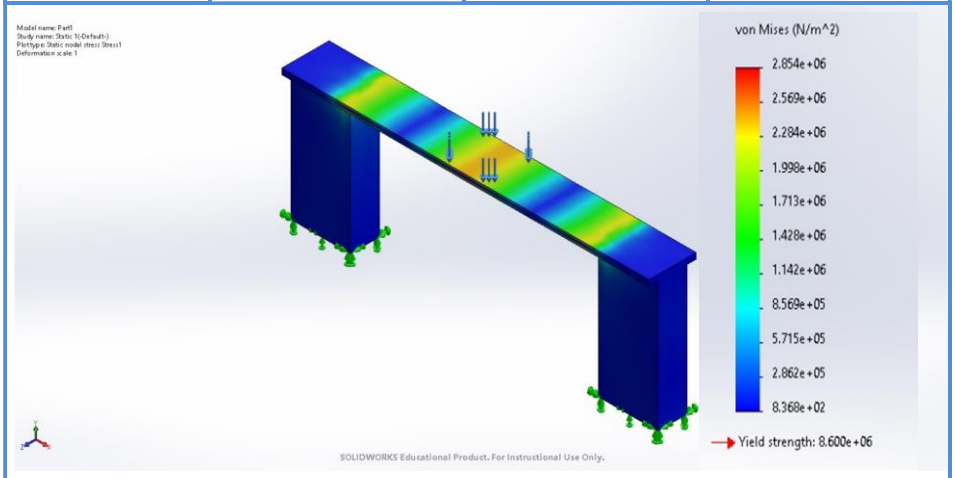

Part1-Static 1-Stress-Stress1

Figure A.8: The stress analysis of the end leg. The results of the von Mises Stress.

Name	Type	Min	Max
Displacement1	URES: Resultant Displacement	0.000e+00mm Node: 751	4.966e-01mm Node: 11218

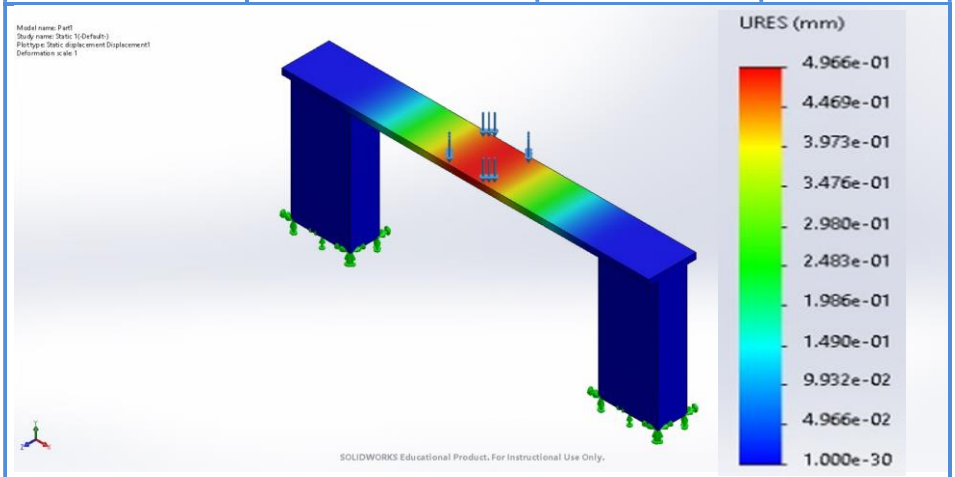

Part1-Static 1-Displacement-Displacement1

Figure A.9: The stress analysis of the end leg. The results of the displacement.

A.14. Permissions

The permission for using Figure A.4 and A.5 is granted by Danny Lamoureux on April 4th, 2021.

The permission for using Figure 4.7 is granted by Kevin Bates on Feb 18th, 2021.

The permission for using Figure 2.1 granted by Springer Nature is presented below.

SPRINGER NATURE LICENSE
TERMS AND CONDITIONS
Apr 08, 2021

This Agreement between University of Saskatchewan -- Amirhossein Ravanbod ("You") and Springer Nature ("Springer Nature") consists of your license details and the terms and conditions provided by Springer Nature and Copyright Clearance Center.

License Number	5011610190545
License date	Feb 17, 2021
Licensed Content Publisher	Springer Nature
Licensed Content Publication	Springer eBook
Licensed Content Title	Curling
Licensed Content Author	Norikazu Maeno
Licensed Content Date	Jan 1, 2016
Type of Use	Thesis/Dissertation
Requestor type	non-commercial (non-profit)
Format	electronic
Portion	figures/tables/illustrations
Number of figures/tables/illustrations	1
Will you be translating?	no
Circulation/distribution	1 - 29
Author of this Springer Nature content	no
Title	The Rock Launcher
Institution name	University of Saskatchewan
Expected presentation date	Feb 2021
Portions	Figure 10.14
Requestor Location	University of Saskatchewan 1325 10TH ST E, Saskatoon SASKATOON Saskatoon, SK S7H 0J2 Canada Attn: University of Saskatchewan
Total	0.00 CAD

The permission for using Figure 2.2 is granted under NRC 2004. Also, the permission for using Figure 4.5 is granted in https://creativecommons.org/licenses/by-nc-nd/3.0/.

A.15. Summary of Interviews

In this section, a brief transcript of the interviews done for this project is presented. The interviewers were Dr. Sean Maw and the author, and the interviewees were Mr. Eugene Hritzuk, Mr. Don Greer, Mr. Lawrence Kucheran, and Mr. Mark Horechka. Each interviewee was interviewed once and individually. Since these interviews were not official, the notes of the interviews are in form of drafts written by the author. In the following, the notes from these interviews are provided in the form of bullet points.

-How would this machine help curlers and curling coaches?

- Teaching new curlers, match the rocks for new clubs, conditioning the rocks after manufacturing, reconditioned used rocks.
- Teaching new ice makers
- Rocks need to be sharpened. Most club do it twice a year. This device helps match stones after sharpening.
- Sweep training for curlers
- Ice makers- check the quality of the ice
- A curler cannot have 15 shots subsequently the same as the first one
- It is an interesting device that might be used for disabled players

-What is the maximum speed of the curling stone during curling?

- It travels hog to hog 7 to 9 seconds for a fast shot (Take out shot)
- 3 to 2.5 rotations hog to hog
- More rotation for a straighter shot

-What is the maximum angle from the centerline for throwing the curling stone?

- It is good to be able to shoot for the edge of the circles of the house

-How does the speed of the curling stone vary during curling?

- It is a sense that curlers learn it by time and experience, from 14 seconds hog to hog to 7 to 9 seconds hog to hog

-Where do curlers mostly release the curling stone?

- It happens before hog line.
- Launching early is better
- Before hog line, no matter where (2 ft before hog line)

-What would be a reasonable cost for this machine?

- It depends on the performance, 2000 to 5000 CAD
- 9000 CAD every 10 years for ice calibration
- If it costs 1000 to 2000 CAD, each club might want to have one
- Less than $800 for the maintenance cost per year

-What are the other factors that are important for this project?

- It should be portable.
- Should be able to throw a stone on the left and right side of the centerline to check the consistency of the ice.
- It can be fixed on either hacks or backboard (keep in mind that the backboards are adjustable)
- The dimensions of the hacks are standard in all curling rinks

A.16. Ball Screw

A sample of screw in ball screw mechanism and its cost is presented in Figure A.10.

Specification Sheet Online:
https://www.thomsonlinear.com/en/product/RM6320-2000.00-XXX-XX-XX

Thomson Customer Support:
https://www.thomsonlinear.com/en/support/global-customer-service-call

THOMSON
Linear Motion. Optimized.™

RM6320-2000.00-XXX-XX-XX

Ball Screws - Screw Only

Ball Screw, Precision, 63mm X 20mm, RH, 23 µm/300mm, 2000.00 mm Long

Lead Time: 3 Days

$3236.24 each+

- Screw only, No Ball nut
- Screws must be machined to fit into end support bearings. Screws can be ordered with ends machined, assembled with ball nuts and/or support bearings.
- Please submit a drawing or description for a quotation on a machined screw or screw and nut assembly.

+The price shown here is the North American List Price for general reference only. Please Contact Thomson for actual net price and current delivery schedule which will vary with geographic region, quantity ordered and distribution channel. Estimated costs for shipping, packaging and import taxes/duty are not included in this list price. Please contact Thomson Customer Support for more information.

Figure A.10: A quote for a ball screw mechanism.

A.17. Results of Levene's Test

A Levene's test was conducted to check whether the variances of each rotational speed at different linear speed is equal. This test was performed based on the median (Brown and Frosythe) since it provides good robustness against many types of non-normal data while retaining good power ("Levene's Test | Real Statistics Using Excel," 2021). The result of this test in form a chart is presented in Table A.6.

Groups	F	df1	df2	Sig.
100% Lateral	2.13	3	15	0.14
60% Lateral	0.61	3	15	0.62
30% Lateral	0.40	3	15	0.76
100% Longitudinal	0.07	3	15	0.98
60% Longitudinal	0.23	3	15	0.87
30% Longitudinal	0.75	3	15	0.54